Distribution Agreement

In presenting this thesis or dissertation as a partial fulfillment of the requirements for an advanced degree from Emory University, I hereby grant to Emory University and its agents the non-exclusive license to archive, make accessible, and display my thesis or dissertation in whole or in part in all forms of media, now or hereafter known, including display on the world wide web. I understand that I may select some access restrictions as part of the online submission of this thesis or dissertation. I retain all ownership rights to the copyright of the thesis or dissertation. I also retain the right to use in future works (such as articles or books) all or part of this thesis or dissertation.

Signature:

_____ _____

Andrew Ephron Date

Synthesis of Septanose glycals and progress towards *endo*-mode cyclizations of polyepoxides

By

Andrew Ephron
Masters of science

Chemistry

Frank McDonald
Advisor

Simon Blakey
Committee Member

Nathan Jui
Committee Member

Accepted:

Lisa A. Tedesco, Ph.D.
Dean of the James T. Laney School of Graduate Studies

Date

Synthesis of Septanose glycals and progress towards *endo*-mode cyclizations of polyepoxides

By

Andrew Ephron
B.S., University of West Florida, 2015

Advisor: Frank McDonald, PhD

An abstract of
A thesis submitted to the Faculty of the
James T. Laney School of Graduate Studies of Emory University
in partial fulfillment of the requirements for the degree of
Master of Science in Chemistry
2018

Abstract

Synthesis of Septanose glycals and progress towards *endo*-mode cyclizations of polyepoxides

By Andrew Ephron

Septanose glycals have successfully been synthesized starting from both lyxose and ribose. These structures were accessed in 4 steps from pentose starting materials yielding 3,4 benzylidene septanose glycals. X-ray crystallography shows an unanticipated epimerization of the *cis*-benzylidene to the more stable *trans*-benzylidene. This has been shown to occur during the Bestmann-Ohira homologation. Glycosylations using various sources of electrophilic iodine and Brønsted acid activators of ribose and lyxose based septanose glycals are described.

Attempts to synthesize a tetraene precursor of the DE ring sector of brevenal via a series of Grignard and Claisen rearrangement reactions were made. However, due to E/Z selectivity difficulties, other methods were explored. Julia coupling of two sulfone/aldehyde pairs were eventually successful in forming the desired tetraene product. Oxidations of the tetraenes were then explored. Lewis acid catalyzed epoxide cascades were also attempted on model systems.

Synthesis of Septanose glycals and progress towards *endo*-mode cyclizations of polyepoxides

By

Andrew Ephron
B.S., University of West Florida, 2015

Advisor: Frank McDonald, PhD

A thesis submitted to the Faculty of the
James T. Laney School of Graduate Studies of Emory University
in partial fulfillment of the requirements for the degree of
Master of Science in Chemistry
2018

Acknowledgements

I would like to thank Dr. McDonald as well as my committee members Dr. Simon Blakey and Dr. Nathan Jui for their continued support of me throughout the graduate program. Thank you to Dr. John Bacsa and Tom Pickle for help with crystal structure analysis especially important to chapter 1. Thank you to the chemistry staff, Dr. Wu, Dr. Bing and Dr. Strobel for their support in the NMR and Mass Spectroscopy facilities. To Claire Scott and Steve Krebs in the stock room for their friendly hellos in the morning and unending patience with order forms. Thank you to Dr. Jessica Hurtak and Dr. Noah Setterholm for their support of me in lab. A special thanks to Dian Ding for collecting some key characterization data present in this work as well as always being a great undergraduate researcher.

Table of contents

List of figures

Chapter 1

Chapter 2

Abbreviations

Ac_2O	acetic anhydride
Aq	aqueous
BF_3•THF	boron trifluoride tetrahydrofuran complex
Bn	benzyl
BnOH	benzyl alcohol
BnBr	benzyl bromide
Bpy	2,2'-bipyridyl
$CDCl_3$	deuterated chloroform
COPD	chronic obstructive pulmonary disease
COSY	^{1}H-^{1}H correlated spectroscopy
d	doublet
DCM	dichloromethane
dd	doublet of doublets
ddd	doublet of doublets of doublets
dddd	doublet of doublets of doublets of doublets
d.r	diastereomeric ratio
ddt	doublet of doublets of triplets
DET	diethyl tartrate
DIBAL	diisobutylaluminum hydride
DIAD	diisopropyl azodicarboxylate
DMAP	4-dimethylaminopyridine
DMDO	dimethyldioxirane
DME	dimethoxyethane
DMF	dimethylformamide
e.r	enantiomeric ratio
Et_2O	diethyl ether
Et_3N	triethylamine
EtOAc	ethyl acetate
EtOH	ethanol
FT-IR	Fourier transform infrared spectroscopy
H	hour
hex	hexanes
HMBC	heteronuclear multiple bond correlation spectroscopy
HRMS	high resolution mass spectroscopy
hv	light
Hz	hertz

IDCP	iodine dicollidine perchlorate
*i*Pr	isopropyl
K. *brevis*	Karenia brevis
KHMDS	Potassium bis(trimethylsilyl)amide
M	molar
m	multiplet
m-CPBA	meta-chloroperoxybenzoic acid
MeCN	acetonitrile
MeOH	methanol
MeMgBr	methyl magnesiumbromide
Mg	milligrams
mL	milliliters
mmol	millimols
MS	molecular sieves
n-BuLi	butyl lithium
NIS	N-iodosuccinimide
NOE	nuclear Overhauser effect
NMI	*N*-methylimidazole
NMR	nuclear magnetic resonance
OLEC	olefinic ester cyclization
Tf	triflate
Ph	phenyl
PT	phenyl tetrazole
PTSH	1-Phenyl-1*H*-tetrazole-5-thiol
pyr	pyridine
q	quartet
quin	quintet
RBF	round bottom flask
r.t	room temperature
s	singlet
t	triplet
td	triplet of doublets
tt	triplet of triplets
t-BuOOH	tert-butyl hydroperoxide
TBAF	tertbutylammonium fluoride
TBS	tert-butyldimethylsilyl
TBSCl	tert-butyldimethylsilyl chloride
TBDPS	tert-butyldiphenylylsilyl chloride
TBDPSCl	tert-butyldiphenylylsilyl chloride
TEMPO	(2,2,6,6-Tetramethylpiperidin-1-yl)oxyl
TFA	trifluoroacetic acid
THF	tetrahydrofuran
THP	tetrahydropyran
TLC	thin layer chromatography
TMS	trimethylsilyl

Chapter 1: Synthesis of Septanose glycals

Introduction

The study of non-natural biomolecules is an exciting area of active research with non-natural peptides and nucleotides having potential as therapeutic agents and informing biological reactivity in vivo. Peptides composed of mixtures of α- and β-amino acids adopt a similar conformation to their natural α-helices allowing α/β-peptides to mimic the natural functionality.[1] These α/β-peptides have been found to be more resistant to proteolytic degradation and have found applications in probing the roles of therapeutic targets and protein-protein interactions.[1] In the same way that non-natural peptides can inform reactivity, homologs of nucleotides have been used to address the question "why did natural selection prefer furanose nucleotides over pyranose?"[2] Recently it has been proposed that pyran and oxepane based nucleotides have potential as therapeutic agents.[3] Naturally occurring oligo- and polysaccharide carbohydrates and their glycoconjugates have been used in targeted drug delivery systems and tissue engineering applications.[4-6] Septanose monomers, seven-membered homologs of the naturally occurring six-membered pyranose sugars, have been shown to bind lectins.[7] Because of this, it is plausible that septanose oligo- and polysaccharide carbohydrates may have similar uses to their pyranose counterparts. However, there is a lack of studies of septanose oligosaccharides and their glycoconjugates due to the absence of synthetic methods.

Due to their stability, five and six membered ring carbohydrates (furanose and pyranose respectively) dominate the structures of natural carbohydrates and their glycoconjugates. The only sugar to have a naturally occurring seven membered ring

(septanose) form is D-Idose **1**, which, at equilibrium in aqueous solution at 37 °C, only contains 1.6% of the septanose form **2** (Figure 1). [8]

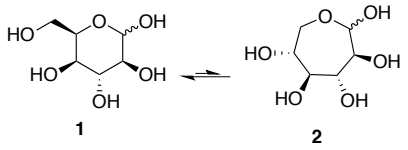

Figure 1: Equilibrium between pyranose and septanose forms of D-idose

Even though these structures are generally unavailable from nature, they have been made synthetically. One synthetic route to septanose sugars involves a ring expansion of a cyclopropanated pyranose. The current state of the art for this type of chemistry is described by Sridhar *et al*. (Figure 2).[9] This method involves a stereoselective Luche reduction followed by a Simmons-Smith cyclopropanation and a Swern oxidation of pyranose **3** to yield the cyclopropanated sugar **4**. Compound **4** is then treated with a Lewis acid to catalyze the ring expansion to form intermediate oxocarbenium ion **5** *via* cleavage of the cyclopropane ring. In the presence of a variety of alcohol nucleophiles, glycosides in the form of **6** were synthesized. Using this method, Sridhar's group was able to synthesize a variety of septanose based 2,3-deoxy di and trisaccharides such as **7** and **8**.[10] While this method is useful for forming up to trisaccharides of septanose carbohydrates, forming larger oligosaccharides is difficult due to the iterative build up of monomer units.

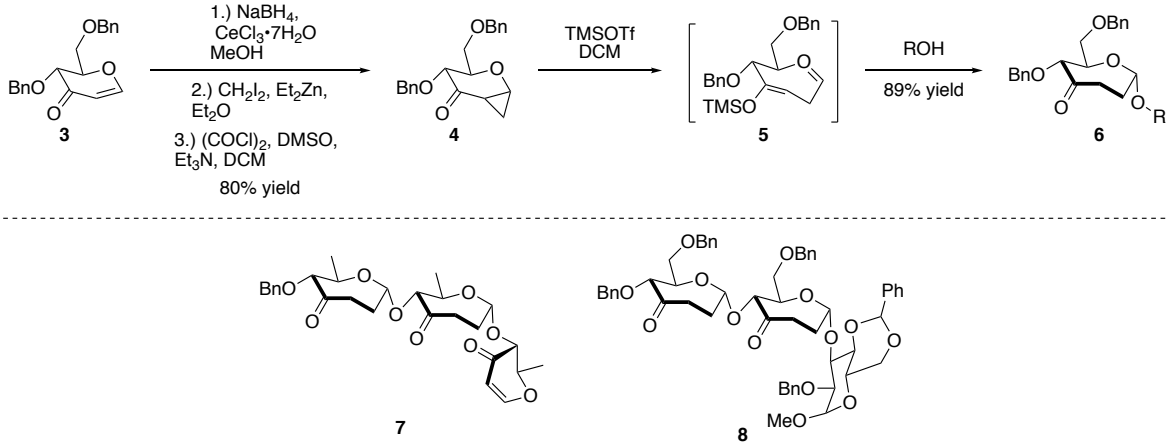

Figure 2: Sridhar's approach to ring expansion and glycosylation to form septanose glycosides

The Peczuh laboratory has recently reported a scaleable approach to septanose sugars and septanose glycals (Figure 3).[11] In this method, a per-benzylated hexose sugar is first opened at the anomeric carbon with vinyl magnesium bromide. The resultant alkene **9** is then exposed to ozone yielding the corresponding aldehyde **10**. Aldehyde **10** is reported in a previous paper to exist as the 7-membered ring hemiacetal. Acetylation of the hemiacetal yields septanose **11**. Compound **11** is then debenzylated and acetylated to yield the peracetyl septanose **12**. Using this method the Peczuh group accessed a wide variety of peracetylated septanoses. These septanoses could then be reacted under Fischer-Zach conditions[12] to yield peracetyl septanose glycals. This methodology allows for the synthesis of a variety of different septanoses and septanose glycals. However the limited protecting group scope makes these glycals problematic for controlled oligosaccharide synthesis.

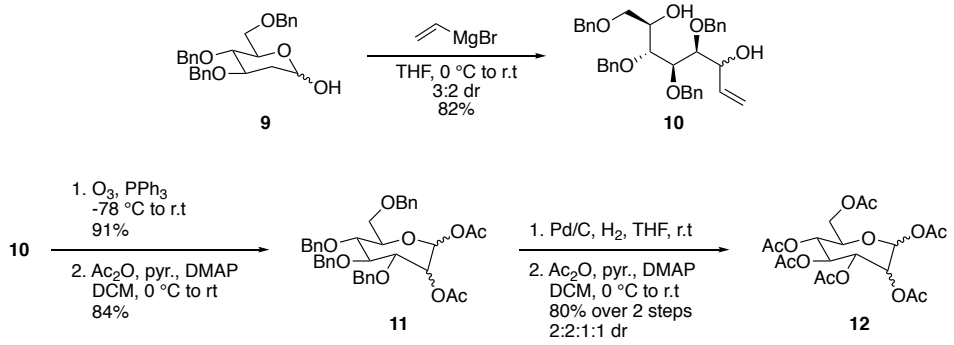

Figure 3: Peczuh laboratories synthesis of septanose sugars.

Previous work in the McDonald laboratory has focused primarily on the synthesis of septanose glycals that may mimic the reactivity of their hexose counterparts for glycosylation.[9] The first work done in this area by our laboratory initially started as an attempt to make hexose glycals *via* tungsten catalyzed cyclization of alkyne **15**. During this investigation, it was found that the reaction exclusively cyclized at the primary alcohol to yield the endocyclic septanose enol ether **16**, instead of the expected exocyclic hexose product (Figure 4).[13] This was demonstrated with both the acetonide protected ribose **13** and acetonide protected lyxose.[9] This allowed for the efficient synthesis of septanose glycals with cis substitution at C3 and C4.

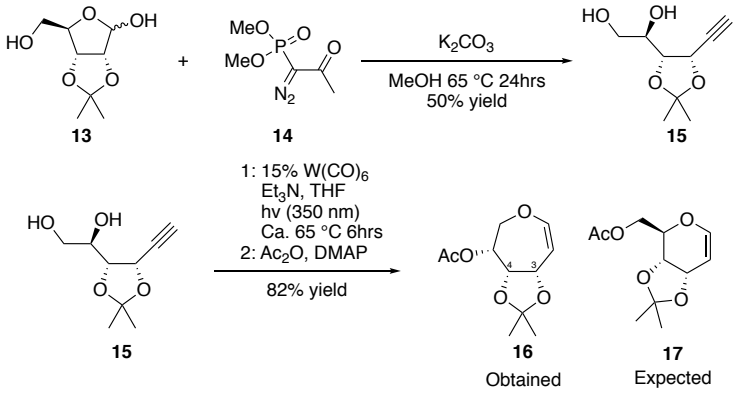

Figure 4: Synthesis of a septanose glycal from ribose starting material

To access the trans C3 C4 septanose glycal analogues of glucose and mannose **19**, alkynyl diol **18** was synthesized from 1,4-but-2-ene diol over 12 steps. Alkynyl diol **18**

could not be made directly from arabinofuranose because the benzylidene protection favors the 3,5-benzylidene over the 2,3-benzylidene . Alkynyl diol **18** was then photocyclized using tungsten hexacarbonyl and 350 nm light from a photo reactor yielding septanose glycal **19**. Epoxide **21** was then formed in 3 steps from septanose glycal **19** via deprotection/ protection of the C3/C4 diol followed by epoxidation of the C1/C2 alkene. Compound **21** was converted into glycal acceptor **22** in 3 steps and into glycal donor **23** in 4 steps. Acceptor **22** and donor **23** were then glycosylated using N-iodosuccinimide and silver triflate as activators yielding dimer **24** in 20 steps (Figure 5). Deprotection of **24** and glycosylation with donor **23** again yielded a septanose trimer in a total of 22 steps.[14] While septanose dimers and trimers can be accessed via this method, this route is not ideal for polymer/oligomer synthesis due to its high step count and step-wise addition of monomer units. Furthermore, the cyclic benzylidene protecting group, while needed for the cyclization of **18**, was not suitable for later transformations and had to be removed and replaced before glycosylation could be performed.

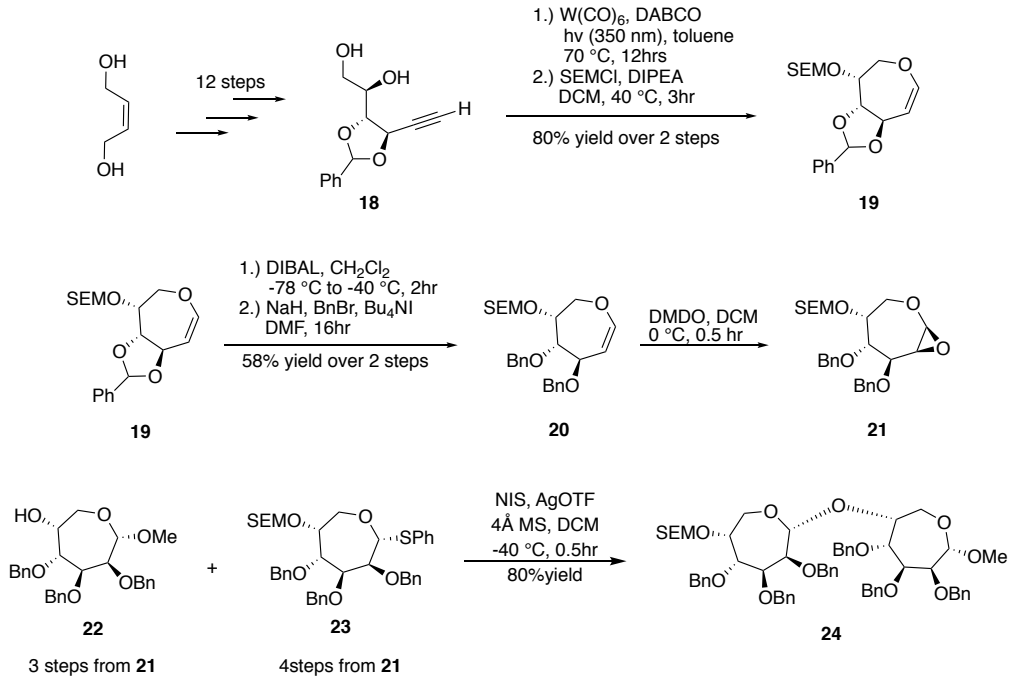

Figure 5: Synthesis of septanose dimer **24** from 1,4-but-2-ene diol

The overall goal of my research was the development of a septanose based polymer such as **25** with possible uses as targeted drug delivery systems and tissue engineering applications.[4-6] We hypothesized these materials would be accessed through activation of an endocyclic enol ether followed by nucleophilic addition of another septanose unit such as **26**. Glycal **26** would be synthesized *via* photocyclization of alkyne **27**. Alkyne **27** could be made from a simple furanose sugar such as lyxose **28** *via* Seyferth-Gilbert Homologation (Figure 6).

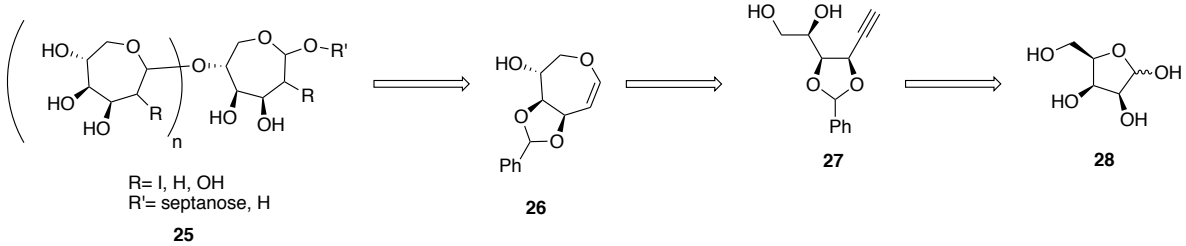

Figure 6: Retrosynthetic analysis of septanose polymer

There are various examples of glycosylation of glycals using different iodine sources via iodonium ions. These 3 membered rings are then opened selectively at the

anomeric position by an alcohol nucleophile.[15] More recently there have been a few examples of glycosylation of glycals through hydrogen bonding catalysis with the glycosyl acceptor using weakly acidic thiourea catalysts.[16-17]

Results and Discussion

Initially, we aimed to make septanose glycal **26** from D-lyxose **28**. This glycal was expected to be the septanose analogue of galactose. This was done through protection of the 2,3-diol of D-lyxose with benzaldehyde followed by a Bestmann-Ohira modified Seyferth-Gilbert homologation. The sequence commenced with a tungsten catalyzed photochemically-induced cyclization developed in the McDonald laboratory (Figure 7A).[13] The selective protection of **28** was first achieved by George Just using anhydrous $CuSO_4$.[18] During optimization it was found that $CuSO_4$ was not needed in the reaction to produce comparable yields.

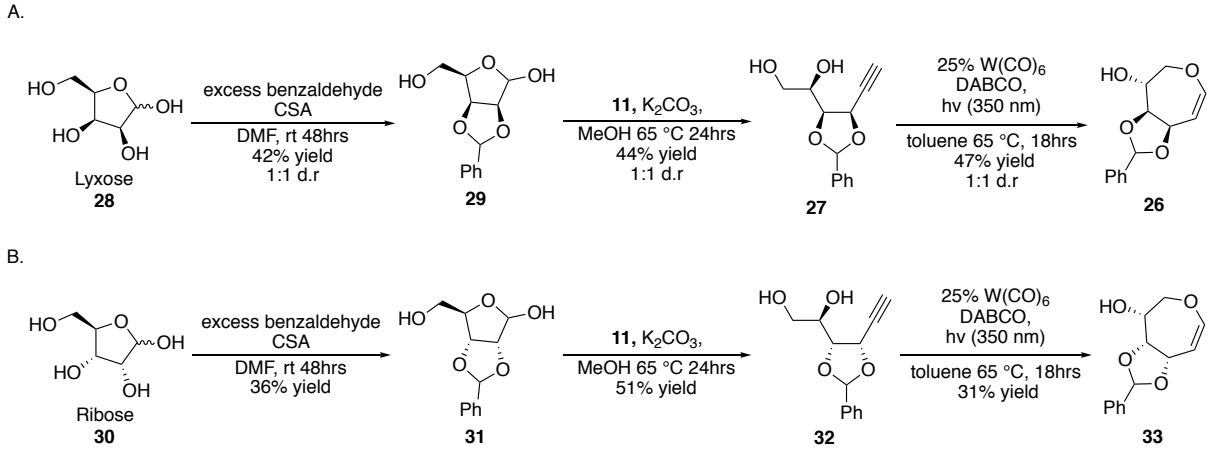

Figure 7: Synthesis of A) lyxose based septanose glycal **26** and B) ribose based septanose glycal **33**. Structures **27-26** and **32-33** depict the stereochemistry that was originally assigned, prior to the discovery of the epimerization.

While Bestmann-Ohira modified Seyferth-Gilbert homologations are typically run at room temperature, with the furanose hemiacetal, **29**, the reaction required elevated

temperature to shift the equilibrium toward the aldehyde form of **29**. Although low to modest yields typical for this procedure were obtained, the reaction was successful in forming the alkynyl diol product. Photocyclization of **27** was successful in constructing the septanose glycal product **26**. Interestingly, X-ray crystallography of septanose glycal **26** showed the product epimerized to the *trans* (*S, S)* stereochemistry at the C3 and C4 positions resulting in septanose glycal **34** instead of the expected *cis*, (*R*, *S)* stereochemistry of the septanose glycal (Figure 8A). Because of this, we decided to study the septanose glycal derived from ribose to see if this unanticipated result would occur with other compounds. The D-ribose derived septanose glycal **33** was synthesized in the same fashion as **26** (Figure 7B). X-ray crystallography showed the *trans* (*R*, *R)* stereochemistry glycal **35** instead of the expected *cis* (*S*, *R)* stereochemistry at C3 and C4 respectively, revealing that it too had epimerized at C3 (Figure 8B).

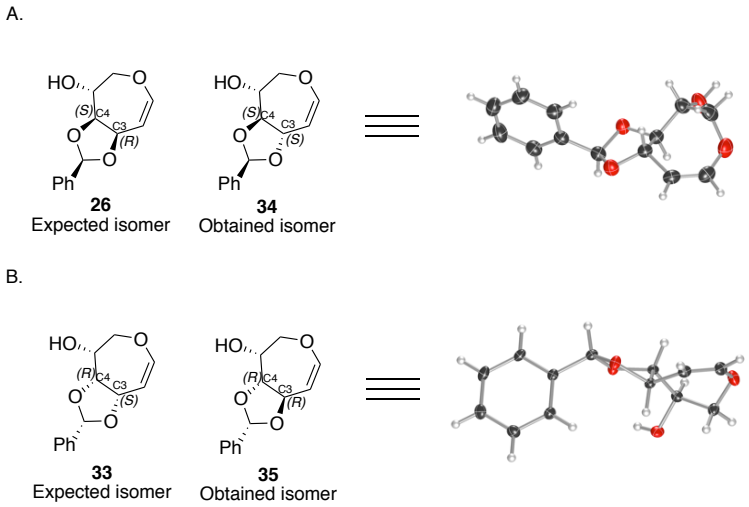

Figure 8: Expected and obtained stereoisomers and X-ray crystal structures of septanose glycals from A) Lyxose and B) Ribose.

This unexpected result can be explained by epimerization of the benzylidene in the aldehyde form of the sugar to the thermodynamically favored *trans* benzylidene under strongly basic conditions and elevated temperature needed for the Bestmann-Ohira

reaction. This was confirmed by closer examination of the ^{1}H NMR spectra and 1D NOE experiments of alkyne **27**. The ^{1}H NMR shows that the coupling constant between C3 and C4 is ~6Hz which is consistent with a dihedral angle of about 140°, however this is also similar to what would be expected from the *cis* isomer. The NOE of the benzylidene hydrogen showed an interaction with only one hydrogen on the 5 membered ring which supports a *trans* fused ring. If the benzylidene were *cis* we would expect NOE signals from both or neither of these hydrogens (Figure 9). This epimerization allows for the access of the mannose/glucose septanose isomer precursor starting from commercially available ribose. This stereoisomer was thought to be unobtainable through this route because 2,3 *trans* furanose rings could not be selectively protected at the 2,3 position and instead favored protection of the 3,5 diol.

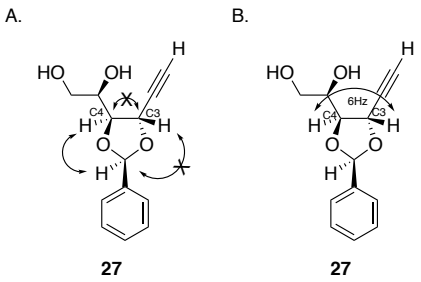

Figure 9: A) observed NOEs of **27** B) coupling constant between C3 and C4 of **27**

Having prepared and characterized septanose glycals from lyxose and ribose different glycosylation methods were explored. The first methods explored were by acid catalysis with Schreiner's thiourea acid catalyst or triphenylphosphine hydrobromic acid (PPh_3•HBr).[19-20] Schreiner's acid catalyst, **37**, is a thiourea Bronsted acid catalyst that has, under very mild conditions, promoted glycosylation with various primary and secondary alcohol nucleophiles on hexose glycal materials.[16] Schreiner's acid catalyst is proposed to work by forming an alcohol-thiourea complex through hydrogen bonding. This complex delivers a proton followed by nucleophilic attack of the

alcohol anion. When used in an attempted glycosylation of acetate protected septanose glycal **36** with benzyl alcohol no reaction was observed over three days. Beyond three days the only notable reaction was minor deprotection of the benzylidene acetal (Figure 10).

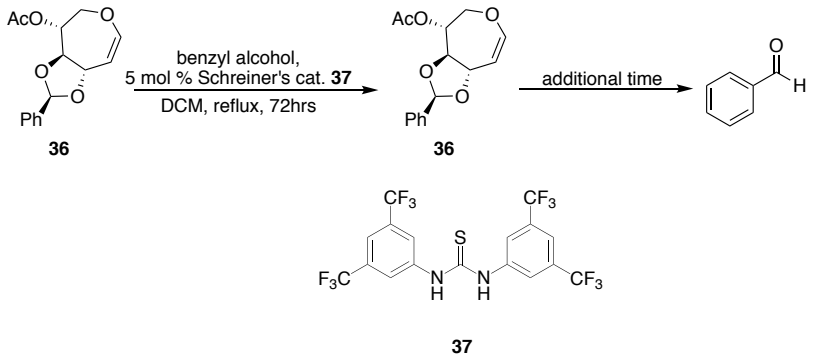

Figure 10: Attempted glycosylation using Schreiner's catalyst

When PPh_3.HBr (5 mol %) was used as the acid catalyst in DCM at room temperature, it proved to be too strong of an acid. The benzylidene was almost immediately deprotected, and upon longer reaction times the alkene was no longer present by ^{1}H NMR spectroscopy. The products were a complex mixture, possibly due to the acetate group migrating between alcohols under the strongly acidic conditions.

With both negative results by acid catalysis the focus turned toward halogen activation. Electrophilic iodine sources such as iodine dicollidine perchlorate (IDCP) and *N*-iodosuccinimide (NIS) are commonly used in glycosylation chemistry.[21-22] IDCP was initially tried over *N*-Iodosuccinimide (NIS) or other electrophilic iodine sources because neither the collidine substituent nor the perchlorate anion has significant nucleophilic properties, unlike succinimide in NIS. Initially septanose glycal **34** was reacted with IDCP in methanol as the solvent to yield the 1-methoxy, 2-iodoseptanoside **38**. Stereochemical assignments were determined by coupling constants between C1 and C2, as well as between C2 and C3 in the ^{1}H NMR spectra. Septanose glycal **35** was also

glycosylated with methanol to yield 1-methoxy, 2-iodoseptanoside **40** (Figure 11). The stereoselectivity of this process favors the iodonium complex forming on the top face for both lyxose and ribose. Due to difficulty in formation of a dimer product and difficulty in the production of IDCP, NIS was explored.

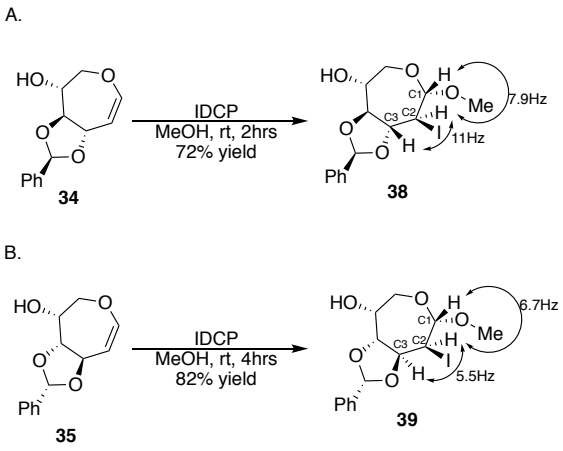

Figure 11: Glycosylation of A) septanose glycal **34** and B) septanose glycal **35** with IDCP as an activator and stereochemical assignment of products

When the glycosylation was attempted using benzyl alcohol with ribose derived glycal **35** activated by NIS the reaction was successful and yielded a single diastereomer of the glycoside **40** (Figure 12). The stereochemistry of the product was determined by ^{1}H NMR. The iodine was determined to be *cis* to the C3 benzylidine because of a 5.4 Hz coupling constant between the two protons. The 7 Hz coupling constant between the protons on C1 and C2 supports *trans* stereochemistry between the iodine and benzyl ether. Attempts at the dimerization under similar conditions have yielded only starting material. The lack of reactivity during the dimerization could be due to steric effects of the iodonium complex of **35**, or due to constrained conformation because of the cyclic benzylidene protecting group.

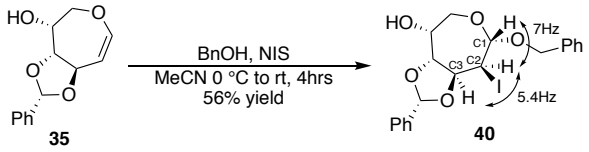

Figure 12: Glycosylation of **35** using NIS as an electrophilic iodine source.

Conclusions

Septanose glycals were successfully synthesized from D-ribose and D-lyxose. From X-ray crystal structure, it was determined that these septanose glycals had undergone an unexpected epimerization at the C3 position. From carful examination of the ^{1}H NMR spectra as well as 1D NOE data, it was determined that the epimerization occurred during the Bestmann-Ohira reaction, likely due to the harsh basic reaction conditions. These septanose glycals have successfully been glycosylated with simple alcohols by IDCP and NIS mediated glycosylation.

Future work on this project will focus on different methods to form the *cis* benzylidene protected alkyne such as **27**. The McDonald laboratory is interested in exploring this to determine if the *cis* protected benzylidene alkyne would still form septanose glycals through an *endo*-mode cyclization, or if the preferred hexose glycal would be favored from *exo*-mode cyclization. The *cis* benzylidene may be able to be formed from the same benzylidene protected D-lyxose or D-ribose starting materials, but utilizing a Colvin rearrangement. The milder conditions typical of this reaction may allow for conversion to the *cis* protected alkyne **27**.

Chapter 2: Progress towards *endo*-mode cyclizations of polyepoxides

Introduction

Red tide events off the coasts of the Gulf of Mexico are caused by large algal blooms of the marine dinoflagellate *Karenia brevis* (*K. brevis*) and result in devastating effects on the ecosystem. Dense concentrations of these dinoflagellate results in discoloration of the water to a reddish-brown color, hence the name red tide. *K. brevis* blooms produce a neurotoxin that can kill marine fish and animals, including dolphins and manatees. Other animals that eat infected marine life, such as birds, humans, and other animals can also be affected by these toxins causing devastating effects on the ecosystem. In 1981, Nakanishi identified the toxin responsible for these effects as brevetoxin B.[23]

Brevetoxin B was the first to be characterized of a family of natural products known as marine polycyclic ethers. These natural products are characterized by their ladder shape, made up of fused 5-9 membered ring polycyclic ethers. Substitutions on polycyclic ether natural products are limited to occasional methyl or hydroxyl substitution. These natural products range in size from the smallest, hemibrevetoxin B, having only 4 rings to the largest, maitotoxin, having 32 rings.[24-25] Maitotoxin is also the largest natural product characterized to date other than biopolymers. Members of this family are also characterized by their *trans*-*syn*-*trans*-fusions among the rings. A few examples of these natural products include brevetoxin B[23], hemibrevetoxin B[25], and brevenal[26], and are summarized in figure 13.

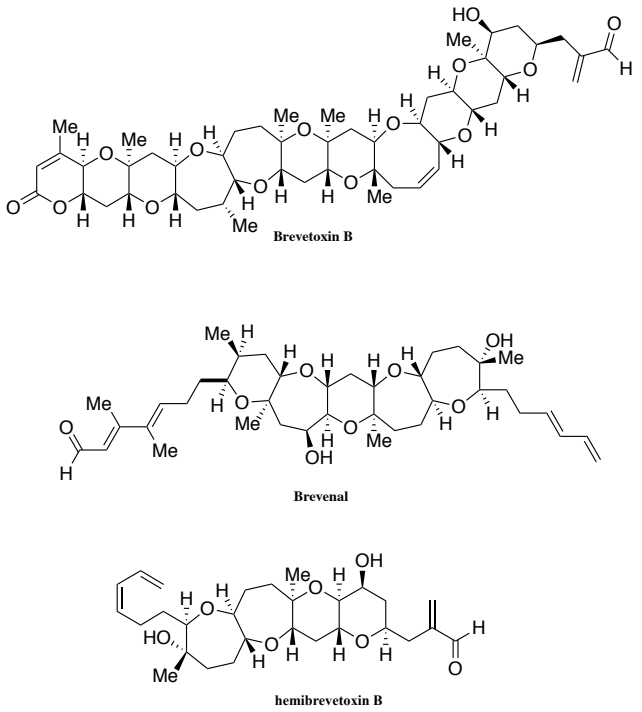

Figure 13: Select marine polycyclic natural products.

Of these, brevenal has received considerable attention, due to its ability to act as a antagonist of brevetoxin B as well as a sodium channel blocking agent for treatment of cystic fibrosis and chronic obstructive pulmonary disease (COPD), as well as being non toxic.[27] Despite this, limited availability of the pure compound has slowed biological evaluation. Because of this, chemical synthesis may play an important role in providing viable quantities of pure compound for complete biological evaluation. To date five total syntheses of brevenal from three laboratories have been completed. In 2006 Sasaki completed the first synthesis of brevenal.[28]This strategy was refined over three generations and in 2011 was able to access gram-scale quantities of the pentacyclic core.[29-30] Total syntheses of brevenal have also been completed by Yamamoto and Kadota in 2009[31], and Rainier in 2011.[32]

Sasaki's retrosynthetic analysis of the core of brevenal from his 3rd generation synthesis is shown in figure 14.[29] The side chains of brevenal in this synthesis, and all other syntheses of brevenal, were added after the completion of the pentacyclic core via Wittig olefination and Stille coupling. The pentacyclic core **41** was formed *via* a Suzuki-Miyaura coupling of the exocyclic alkene AB ring precursor **42** and the enol phosphate DE ring precursor **43** followed by a mixed thioacetalization to close the C ring. The AB ring system **42** was produced from a similar sequence on the B ring enol phosphate **44**, which was subsequently synthesized by oxidative lactonization of diol **45**. The DE ring system **43** was synthesized via Suzuki coupling of the E ring enol phosphate **46** followed by oxidative lactonization. The E ring enol phosphate **46** was prepared through oxidative lactonization on diol **47**. Overall the pentacyclic core of brevenal was obtained in a longest linear sequence of 34 steps. Furthermore, using this sequence the group accessed the pentacyclic core in gram quantities.

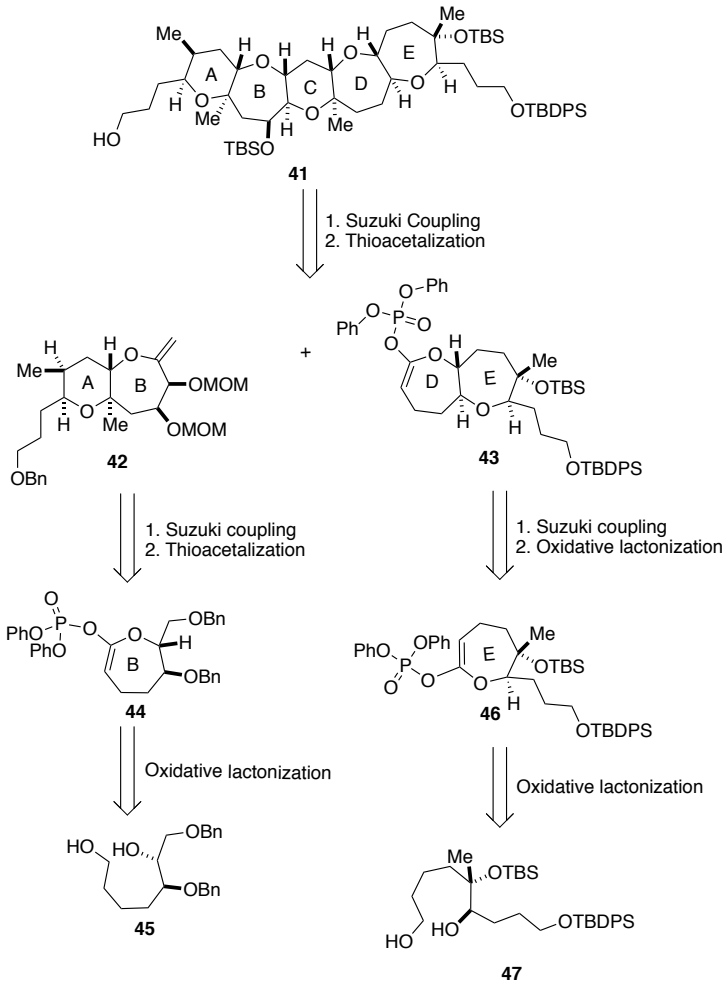

Figure 14: Sasaki's retrosynthesis of brevenal.

Yamamoto and Kadota reported a total synthesis of brevenal in 2009 (Figure 15).[31] The pentacyclic core **48** was synthesized via an intramolecular allylation reaction of the α -chloroacetoxy ether **49** to close the D ring, followed by a Grubbs ring closing metathesis reaction on the resulting diene to close the E ring. α-chloroacetoxy ether **49** was formed by Yamaguchi esterification of the ABC tricyclic acid **50** and the linear E ring alcohol precursor **51**. The ABC tricyclic acid **49** was synthesized via a series of monocyclizations building onto the C ring starting material **52**. Overall Yamamoto and Kadota accessed the pentacyclic core of brevenal in 40 steps longest linear sequence.

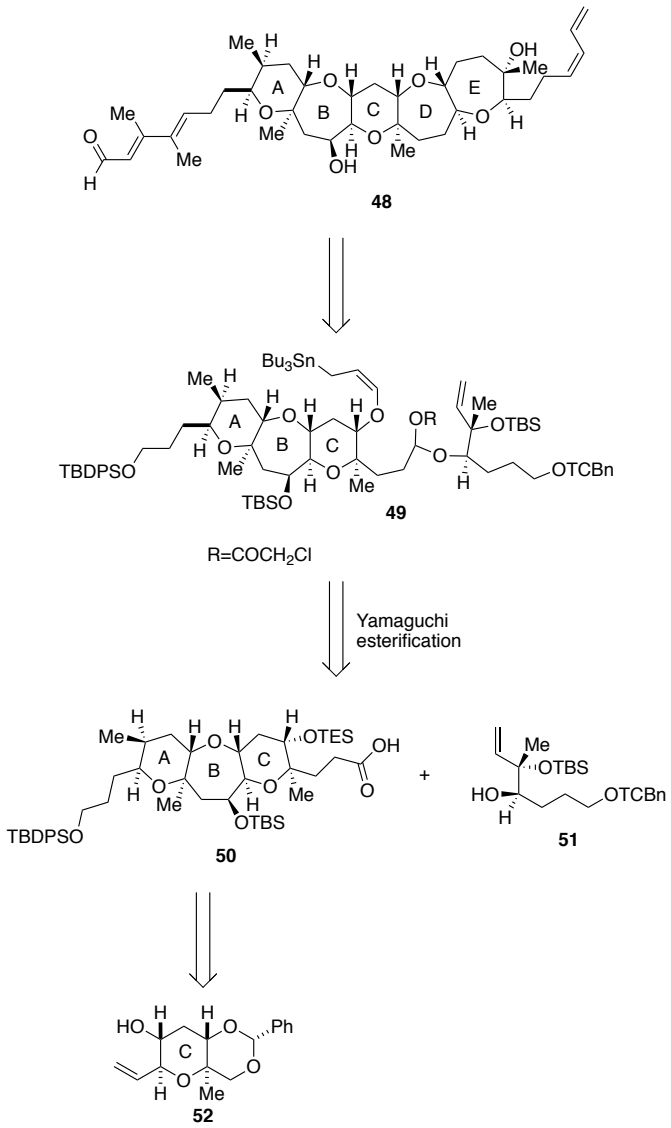

Figure 15: Yamamoto and Kadota's retrosynthetic analysis of Brevenal

The 2011 synthesis from the Rainier laboratory accessed the pentacyclic core **53** via a reductive cyclization of the hydroxy ketone made from cyclic enol ether **54** (Figure 16).[32] This enol ether was formed by titanium mediated olefinic ester cyclization (OLEC) of ester **55**. Ester **55** was synthesized via esterification of AB ring acid **56** and E ring alcohol **57**. Both the AB and E ring segments were produced by OLEC cyclization procedure from the olefin ester starting materials **58** and **59**. Overall this method was used to access brevenal's pentacyclic core in a longest linear sequence of 26 steps.

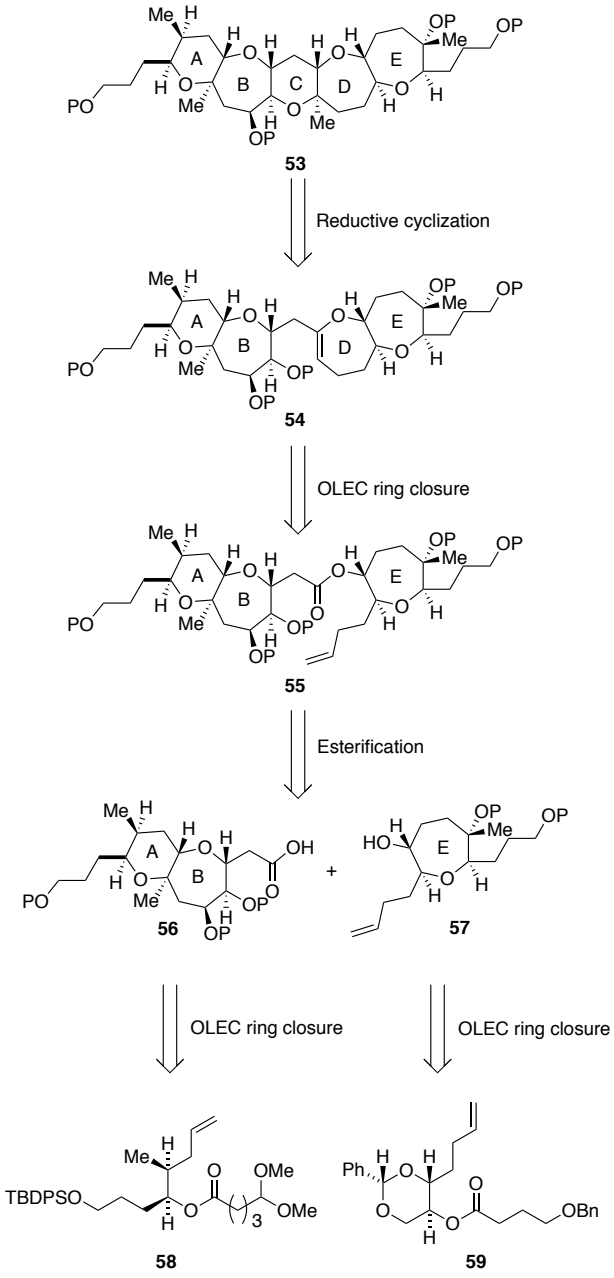

Figure 16: Rainier's retrosynthetic analysis of brevenal.

The Nakanishi hypothesis for the biogenesis of polycyclic ether natural products has inspired biomimetic synthesis *via* polyepoxide cascades.[33] Many laboratories have undertaken the task of searching for chemical evidence for this hypothesis through development of *endo*-regioselective polyepoxide cascade reactions, which are step economical and atom-efficient ways to rapidly build complexity.[34-38] Of these

laboratories, the McDonald laboratory[37] and the Jamison laboratory[38] have made particularly important contributions to the development of *endo*-selective polyepoxide cascades resulting in polypyran and polyoxepane structures.

In the proposed biosynthesis of polycyclic ether natural products, a completely *endo*-selective oxacyclization cascade must occur on a polyepoxide precursor to obtain the polycyclic ether cores.[33] Synthetically, intramolecular epoxide opening reactions may occur either through *endo* or *exo* pathways (Figure 17). For simple alcohol substrates, *exo*-mode cyclization are favored due to the kinetically favored spiro transition state.[39] Because of this, synthetic chemists have aimed to overcome this preference by either stabilizing positive charge on the *endo* carbon, or destabilizing positive charge on the *exo* carbon.

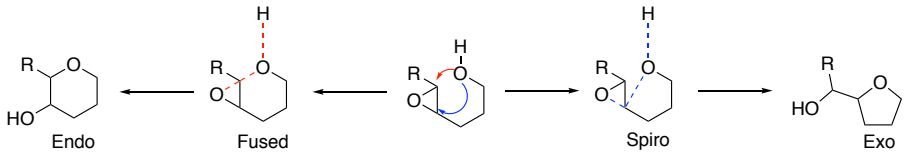

Figure 17: Intramolecular *endo* and *exo* mode epoxide opening with alcohols

The Jamison laboratory's approach to favoring the fused transition state was by attaching the polyepoxide to a tetrahydropyran template.[40-41] In water, Jamison effected the *endo*-selective polyepoxide cascade of triepoxide **60** in neutral pH water to afford the HIJK ring sector of gymnocin A, **61**, in a single step and moderate yields (Figure 6).[40] The THP template pre-organizes the substrate in a conformation that favors the fused transition state over the usually favored spiro transition state leading to the *endo* product. The proposed rationale for this selectivity is that two water molecules coordinate to both the hydroxyl nucleophile and the epoxide electrophile activating and orienting these components for *endo*-cyclization (Figure 18).[41] While this methodology can be very

powerful in building fused tetrahydropyrans it has two major limitations. This methodology is not suitable if there are substituents on the polyepoxide chain. Many polycyclic ether natural products have several methyl substituents. Furthermore, oxepanes are inaccessible from this methodology.

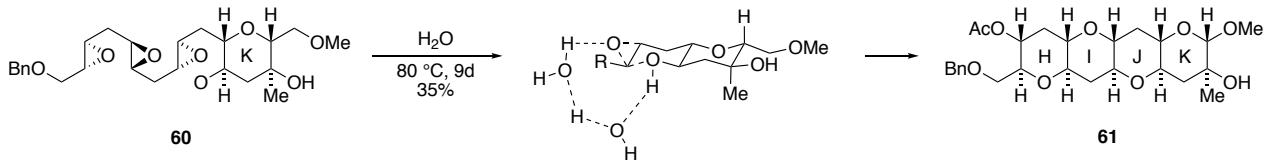

Figure 18: Jamison's water promoted *endo*-selective polyepoxide cascade.

Recently Jamison has reported a Rh(I) catalyzed *endo*-selective epoxide opening cascade capable of forming both pyrans and oxepanes.[42] This methodology was demonstrated in the formal synthesis of brevisin (Figure 19).[42] Utilizing site-specific rhodium coordination of the alkenyl epoxides **62** and **63**, the ABC ring sector **64** and EF ring sector **65** of brevisin were each constructed from a monocyclic diepoxide in a single step. Both cyclization pathways proceeded via a tandem 7-*endo*, 6-*endo* modes.

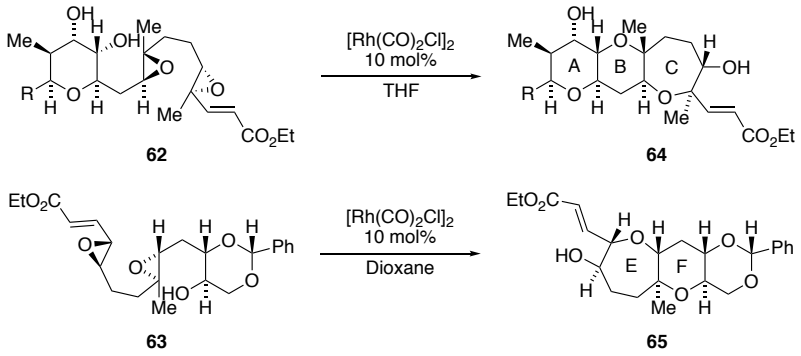

Figure 19: Jamison's rhodium catalyzed epoxide cascade to form the ABC and EF rings of brevisin

The McDonald laboratory aimed to build polycyclic ethers via a Lewis acid catalyzed *endo*-mode polyepoxide cascade. This methodology was demonstrated in the

formation of the dioxepane **68** (Figure 20).[43] From the triepoxide **67**, a Lewis acid coordinates to the terminal epoxide leading to attack by the closest epoxide forming the proposed bicyclic epoxonium ion **67**. This process then repeats with a third epoxide, and the sequence is completed by attack of the final epoxonium ion by the carbonate nucleophile yielding dioxepane **68**. Having a tertiary *endo* carbon on the terminating epoxide was crucial to favor the *endo*-mode cyclization by stabilizing positive charge on the *endo* carbon. However, attempts to extend this methodology to pyrans were challenging.[44] In these cases, when using a carbonate terminating nucleophile, the *exo*-mode product was favored. By using a more nucleophilic carbamate terminating nucleophile the desired endo-mode cyclization was possible, however this was substrate specific and produced in low yield.

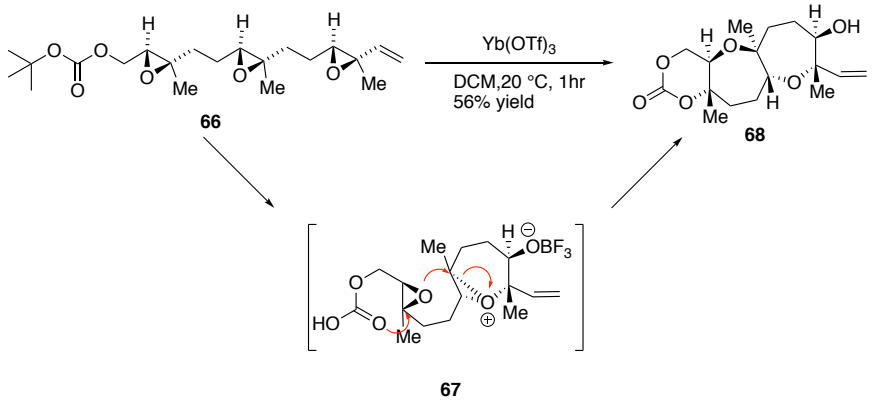

Figure 20: McDonald's *endo*-mode Lewis acid catalyzed polyepoxide cascade

The McDonald laboratory has also explored *exo*-mode cyclization strategies for the synthesis of polycyclic ether natural products. This methodology was utilized in the synthesis of the ABC ring sector of brevenal **72** by Dr. Jessica Hurtak (Figure 21).[45] The sequential build up of the ABC ring sector began with a diasterioselective iodocyclization on the linear precursor **69** to form the A ring **70**. Next the B ring was formed via a base promoted conjugate addition reaction. The resulting ketone was then reduced to the

alcohol via Luche reduction followed by the hydrolysis of the acetonide protected diol with trifluoroacetic acid/ water to afford the alkenyl triol AB ring substrate **71**. Finally the C ring was synthesized by mercuric trifluoroacetate promoted oxacyclization to yield **72**. Attempted iodocyclizations on **71** led only to decomposition. The authors speculate that this is due to a pseudoaxial orientation of the reactive alcohol and carbon chain on the B ring.

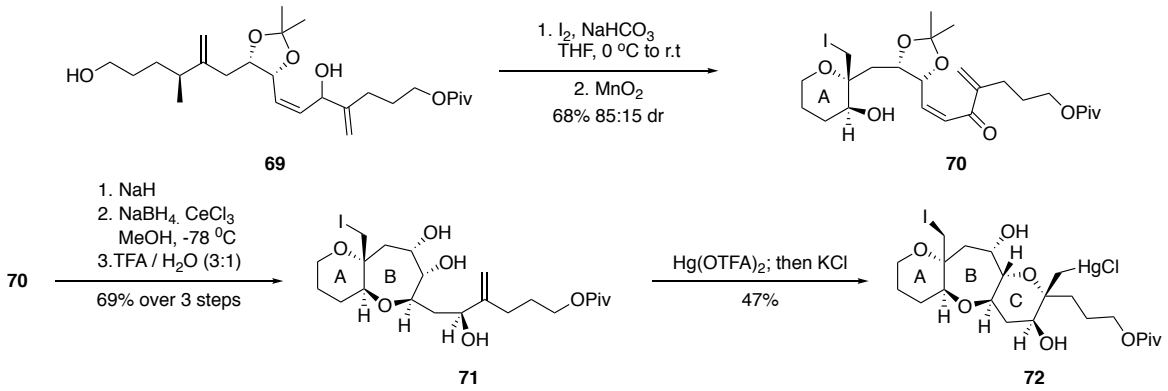

Figure 21: McDonald's laboratory sequential *exo*-mode cyclizations to form the ABC ring segment of Brevenal

The goal of my research is to explore the scope of the Lewis acid catalyzed *endo*-mode polyepoxide cyclizations in application to brevenal. In particular we expect that Lewis acid catalyzed *endo*-mode polyepoxide cyclizations will form the DE ring of brevenal **73** from triepoxide **74** (Figure 22). Triepoxide **74** would be synthesized by Shi epoxidation of tetraene **75**.[46] The tetraene would be formed via Stille coupling of vinyl iodide **76** and tributylvinyl tin. **76** could be made via a carboalumination iodination of alkyne **77**. Finally **78** would be made via a series of Grignard and Claisen reactions starting from TMS protected 4-pentyn-1-al.

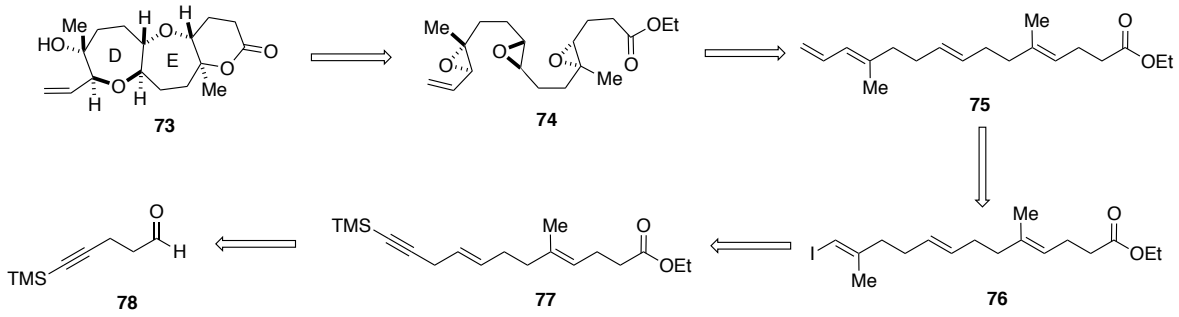

Figure 22: Retrosynthetic analysis of the DE ring sector of brevenal

The major difference between the proposed cyclization cascade, and the cascades previously described by the McDonald group is that the methyl and vinyl groups are no longer both on the *endo* carbon (Figure 23).[43] We propose that the electronic stabilization from the allylic group may be stable enough to favor the *endo*-mode cyclization over the *exo*-mode.

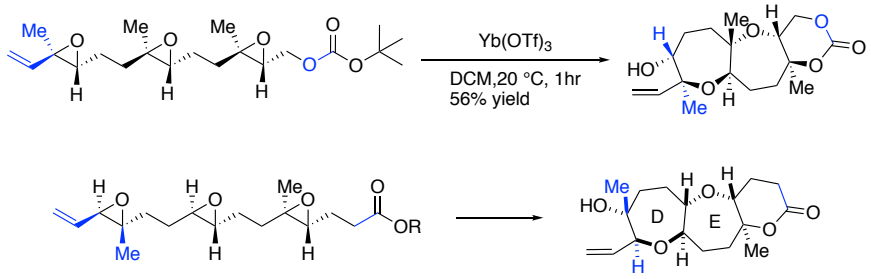

Figure 23: Differences between previous Lewis acid catalyzed *endo*-mode polyepoxide cascades and proposed Lewis acid catalyzed polyepoxide cascade.

Results and Discussion:

The first attempted synthesis of 7**3** began with Stahl oxidation of TMS protected 4-pentyn-1-ol **79** in good yield (Figure 24). The resulting aldehyde **78** was then reacted with vinyl magnesium bromide to yield allylic alcohol **80**. From ^{1}H NMR data, the major byproduct appeared to be deprotection of the TMS protected alkyne, possibly arising from the basic reaction conditions. Next **80** was reacted under Claisen rearrangement

conditions with 2-methoxy propene to yield ketone **81**. The major byproduct was once again observed to be the TMS deprotected starting material. Ketone **81** was then reacted with vinyl magnesium bromide to yield allylic alcohol **82**. Allylic alcohol **82** was exposed to Johnson-Claisen rearrangement conditions in an attempt to form ester **83**. However, ester **83** was not observed and only TMS deprotected starting material and unidentified side products were isolated.

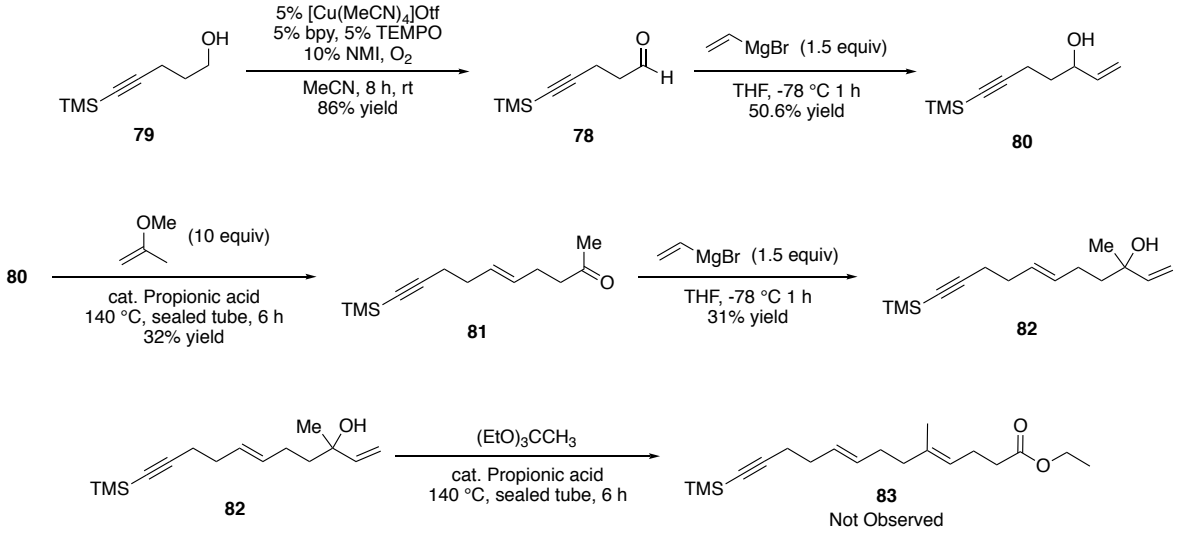

Figure 24: First generation synthesis

Because of the significant difficulties caused by the TMS alkyne, we decided to study alternate routes to obtain DE core **83** as described in figure 25. We still planned to do the polyepoxide cascade from tetraene **85**. However, tetraene **85** would now be synthesized via carboalumination/iodination of 4-pentyn-1-ol **84** to yield vinyl iodide **85**. Aldehyde **86** would then be made via Kumada coupling of **85** with vinyl magnesium bromide followed by Stahl oxidation of the resultant diene. Diene **86** would then be reacted through a series of Grignard and Claisen reactions to form tetraene **75**. This synthesis allows us to avoid the difficulties resulting from the TMS protected alkyne, as well as reducing the step count by avoiding a TMS protection/deprotection.

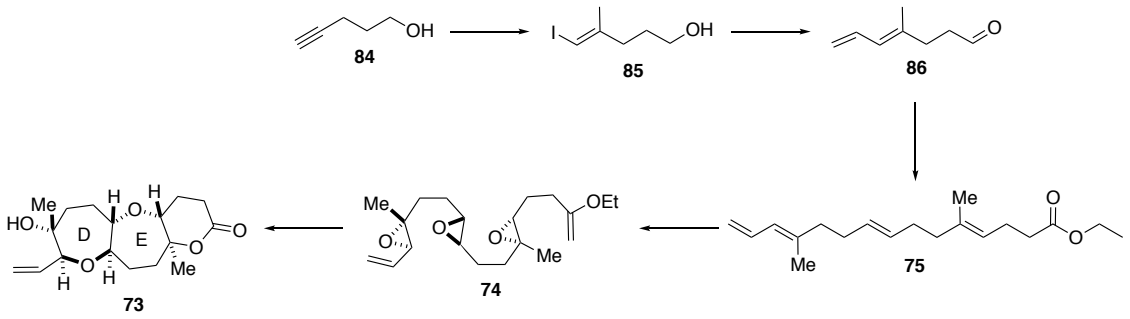

Figure 25: Planned second-generation synthesis of the DE sector of Brevenal.

The carboalumination/iodination of **84** proceeded in high yield to vinyl iodide **85**. Kumada coupling of **85** proceeded in modest yield to diene-ol **87 (**Figure 26). Compound **87** Was then oxidized to aldehyde **86** via Stahl oxidation without the need for purification. However aldehyde **86** was very volatile and because of this was kept as a solution in ether. Grignard reaction of aldehyde **86** with vinyl magnesium bromide proceeded to allylic alcohol **88** in modest yield. The remainder of the mass appeared to be decomposition products. Claisen rearrangement of **88** with 2-methoxypropene was then performed yielding ketone **89** in modest yields. During optimization of this reaction, it was found that longer reaction times (6hrs to overnight) resulted in lower yields of desired ketone **89**, and an increase in decomposition products. Shorter reaction times of 1-2hrs resulted in the intermediate ether as the primary product with only trace amounts of product formed. Grignard reaction of **89** resulted in tertiary alcohol **90** in modest yields.

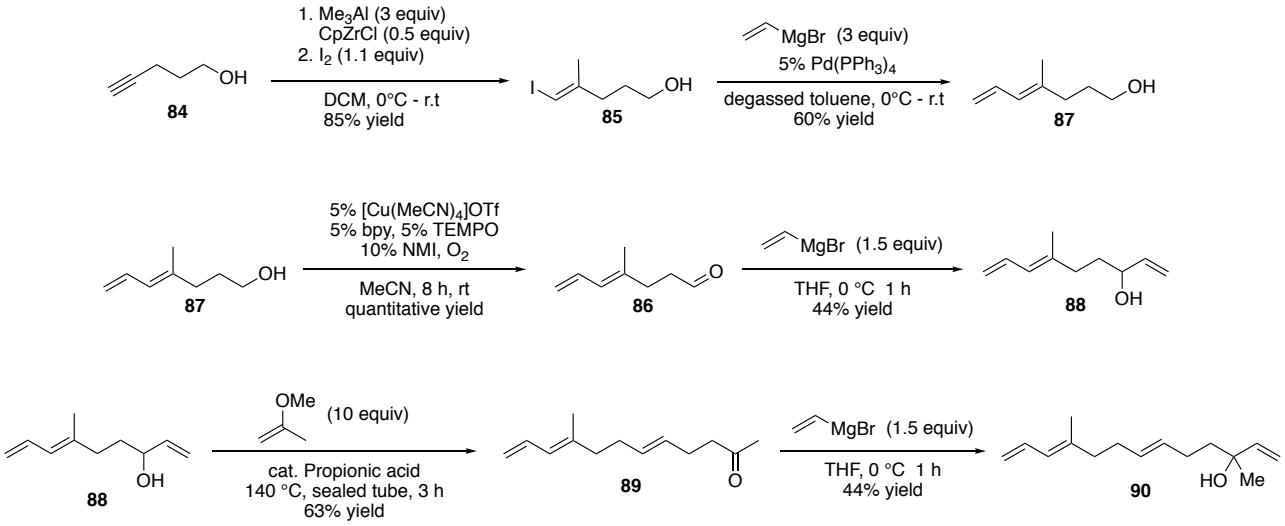

Figure 26: 2nd generation synthesis

Because of the difficulties of the Johnson-Claisen reaction in the first generation synthesis as well as challenges in the earlier Claisen rearrangement, we decided to explore the Johnson-Claisen on a model system before attempts with the valuable tertiary alcohol **90**. To make the model system, ketone **91** was reacted with vinyl magnesium bromide to yield tertiary alcohol **92** (Figure 27A). Alcohol **92** under Johnson-Claisen conditions only led to decomposition products after two days. Shorter reaction times led to either decomposition or recovery of starting material. After looking through the literature I found a paper by Gaydou *et al*. described the same Johnson-Claisen reaction. They found that under similar conditions, after 8 days reaction time a 55:45 mixture of E:Z alkenes **93** and **94** was formed (Figure 27B). The lack of stereoselectivity is likely due to the similar relative size of the methyl and vinyl groups in the chair transition state of the reaction.

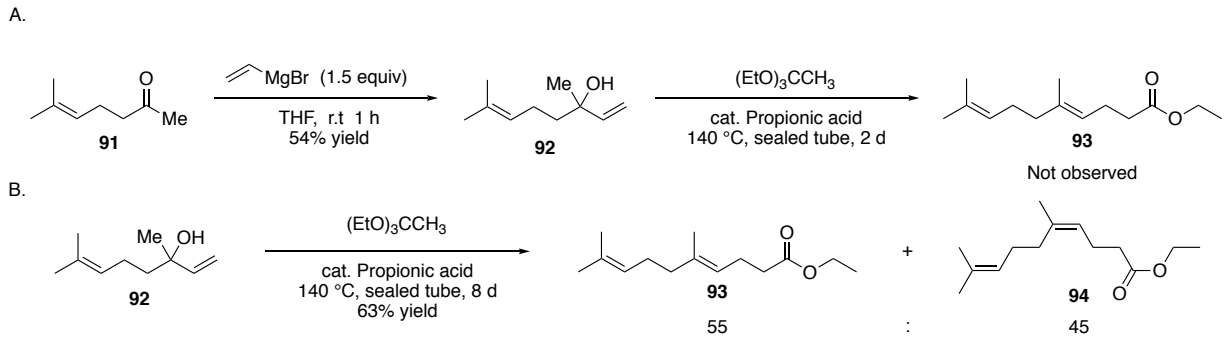

Figure 27: A)Attempted Johnson-Claisen reaction of alcohol **92**. B) Johnson-Claisen reaction of alcohol **92** by Gaydou *et al.*

A 55:45 ratio of products and only modest yields is insufficient for the real system of tertiary alcohol **90**. After this result we decided to explore alternate routes to tetraene products that could result in the DE ring structure of brevenal. We hypothesized that a Kocienski-modified Julia olefination of phenyl tetrazole (PT) sulfone **97** and aldehyde **86** would result in tetraene **98** (Figure 28). Tetraene **98** could then be converted to triepoxide **99** via Sharpless epoxidation of the allylic alcohol followed by Shi epoxidation of the two internal alkenes, and finally protection of the alcohol as the carbonate. Triepoxide **99** would then be set up to form DE ring segment **100** via a Lewis acid activated polyepoxide cascade. PT sulfone **97** could be synthesized from a Mitsunobu reaction of alcohol **96** followed by oxidation of the resultant sulfide. Alcohol **96** could subsequently be formed from geraniol **95**.

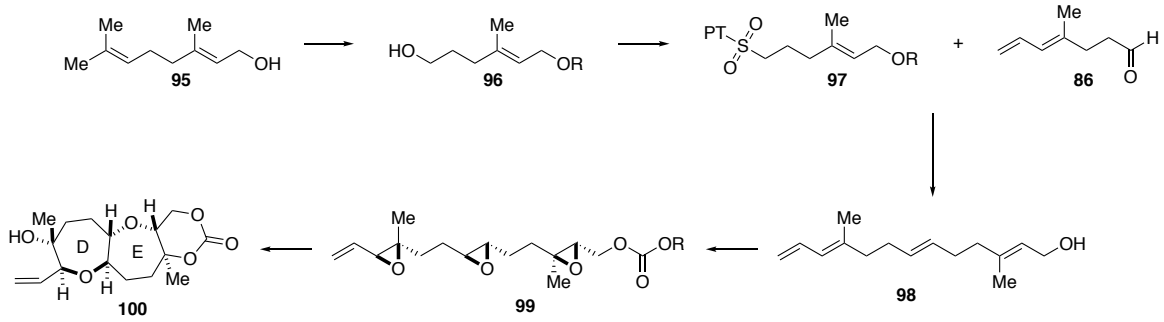

Figure 28: Proposed synthesis of the DE ring system of brevenal via Julia coupling.

Synthesis of sulfone **97** began with TBDPS protection of geraniol (**95**) (Figure 29). TBDPS protected geraniol **101** was then reacted with *m*-CPBA to selectively yield the epoxide at the more electronically rich C6-C7 alkene in moderate yields. The remaining mass balance consisted of diepoxide material, and recovered starting material. To limit the formation of the diepoxide material, the *m*-CPBA was added dropwise via syringe pump over 30 minutes. Epoxide **102** was then cleaved via periodic acid to yield aldehyde **103** in high yields, which was subsequently reduced to alcohol **96**. Mitsunobu reaction of alcohol **96** with phenyltetrazole thiol (PtSH) yielded sulfide **104** in high yields. Oxidation of **104** with ammonium molybdate yielded sulfone **97** in moderate yields. The major byproduct of this reaction was the epoxidation product of alkenyl sulfone **97**. Shorter reaction times led to only partial conversion of starting material.

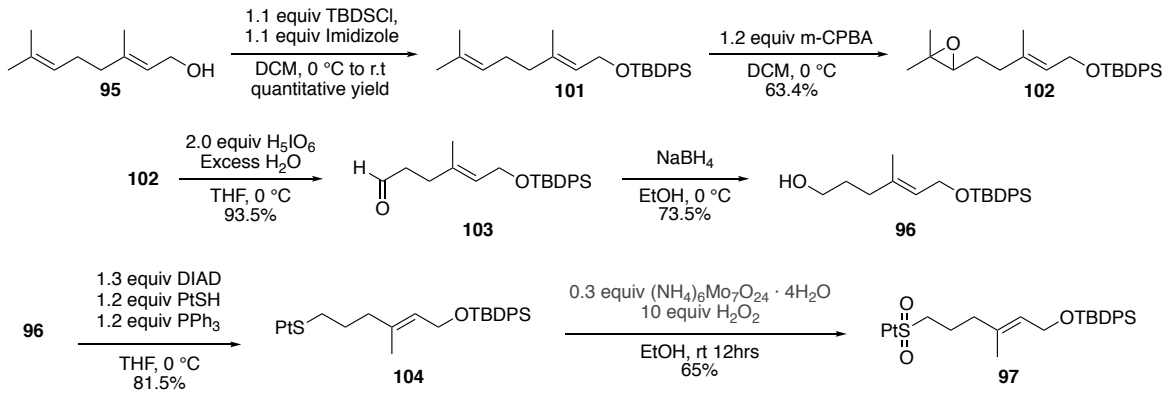

Figure 29: Synthesis of sulfone **97**

For the Julia coupling, KHMDS as the base and dimethoxyethane as the solvent were initially chosen based on literature precedence of high E selectivity and these conditions.[47] The Julia coupling between sulfone **97** and aldehyde **86** yielded tetraene **105** in low yields but with high E/Z selectivity as determined by integration of the newly formed alkene protons ^{1}H NMR data (Figure 30A). The remaining mass balance was recovered sulfone starting material **97**. Aldehyde starting material **86** was present by TLC

of the reaction mixture, however aldehyde **86** was not recovered or observed by ^{1}H NMR after work up and concentration via rotary evaporation. This is likely due to the volatility of low molecular weight aldehyde **86**. Because of the large amount of recovered unreacted sulfone **97** we explored reactions at higher temperatures and base loading to force the reaction. However, reaction of **97** at 0 °C and room temperature yielded similar results. Low yields of tetraene **105** were observed, and large quantities of starting materials recovered.

Because of these results we wanted to insure that deprotonation of the sulfone was occurring. To explore this, 1.25 equivalents of KHMDS were added to sulfone **97**. After stirring for thirty minutes, the reaction mixture was quenched with D_2O. After aqueous work up, the fully deuterated sulfone **106** was observed as the only product via ^{1}H NMR (Figure 30B). With this result, the KHMDS was titrated with menthol and *N*-(4-Phenylbenzylidene)benzylamine as an indicator resulting in a dark blue solution.[48] It was found to be a ~2.5M solution instead of the 1M solution claimed on the label. Unfortunately, attempted reactions with lower base loading resulted in lower yields of desired tetraene product and higher recovery of sulfone starting material. n-Butyllithium was also explored as a base. Attempted Julia couplings of sulfone **97** and aldehyde **86** using n-butyllithium as a base resulted in lower yields and only a 3:1 E:Z selectivity for tetraene **105** (Figure 30C).

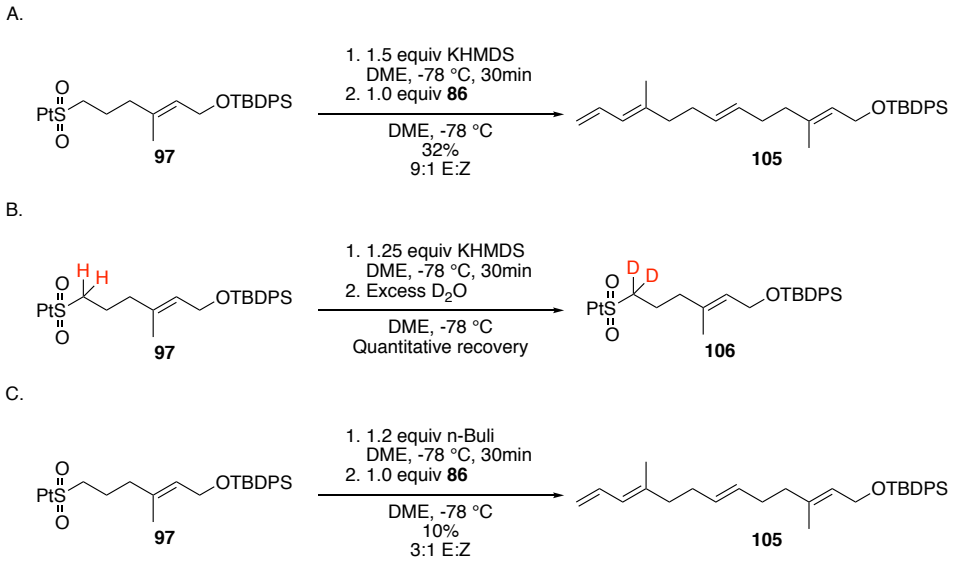

Figure 30: A) Julia coupling of sulfone **97** and aldehyde **86** with KHMDS base.

B) Deprotonation/deuteration of sulfone **97**

C.) Julia coupling of sulfone **97** and aldehyde **86** with n-butyllithium base

Even though **105** was produced in low yields, enough tetraene material was obtained from the Julia coupling to attempt the synthesis of triepoxide **99**. Deprotection of tetraene **105** with tetrabutylammonium fluoride proceeded in moderate yield to alcohol **108** (Figure 31). Alcohol **108** was reacted under Sharpless epoxidation conditions with (+) diethyl tartrate to yield the (R, R) epoxide in low yields. The low yield is potentially due to the small scale. Due to the small amounts of epoxide **108** obtained, Shi epoxidation was not attempted.

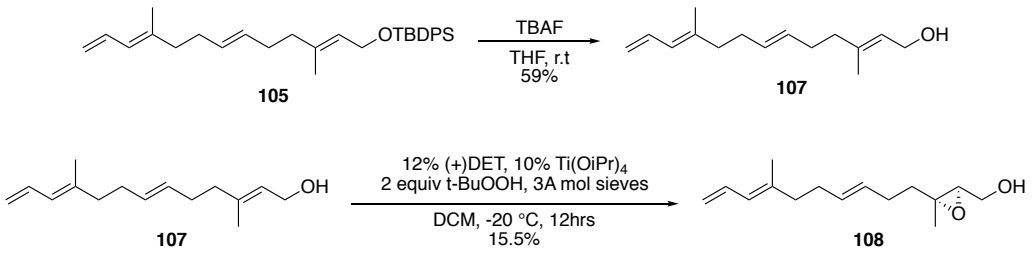

Figure 31: Synthesis of epoxide **108**

Due to the difficulties with the initial route we decided to explore the Julia coupling with the coupling partners swapped. The aldehyde component, **103**, was previously synthesized en route to sulfone **97**. To synthesize the new sulfone coupling partner, alcohol **87** was reacted under Mitsunobu conditions to afford sulfide **109** in good yield (Figure 32A). Oxidation of thio ether **109** with ammonium molybdate proceeded in moderate yields to sulfone **110**. The major byproducts of this reaction were multiple oxidation products of the diene. Julia coupling of sulfone **110** and aldehyde **103** yielded the desired tetraene **105** in low yields but with a 9:1 E:Z ratio (Figure 32B). The remaining mass balance was primarily recovered starting materials sulfone **110** and aldehyde **103**. Due to the lowered reactivity and high recovery of starting materials, no further experiments were done on this reaction.

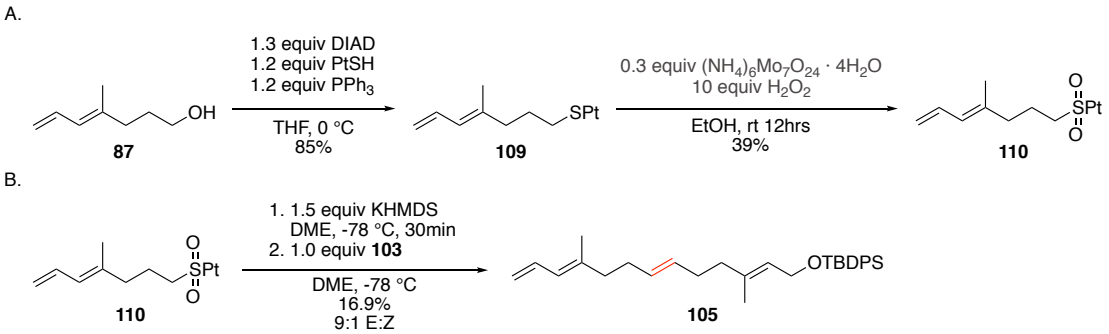

Figure: 32: A) Synthesis of sulfone **110**. B) Julia coupling of sulfone **110** and aldehyde **86**.

To rehearse the Lewis acid catalyzed cyclization chemistry, epoxide **115** was synthesized (Figure 33). The synthesis of epoxide **115** began with Sonogashira coupling of propargyl alcohol and vinyl bromide to yield enynol **112** in good yield. Next **112** was reacted with vinyl magnesium bromide in the presence of copper (I) iodide to yield diene **73** in good yield. Sharpless epoxidation of **113** yielded epoxide **114**, which was

subsequently BOC protected yielding epoxide **115**. When exposed to $BF_3 \cdot THF$, epoxide **115** was expected to cyclize to 6 membered ring **116**. From ^1H NMR and mass spectrometry, we determined that the Boc group had persisted through the reaction for diastereomers obtained and had likely migrated to the free alcohol over the course of the reaction. NOE data showed an interaction of the methyl group on C2 with both diastereotopic protons on C1 for both diastereomers. This suggested that the obtained product was 5 membered ring **117**, because in the 6 membered ring one of the diastereotopic protons would be anti to the methyl group and therefore invisible by NOE. IR of both products showed carbonyl peaks at ~1805 cm^{-1} which was also consistent with 5 membered ring when compared to similar materials.[49-50] The stereochemistry of the quaternary center of **117** has not yet been determined.

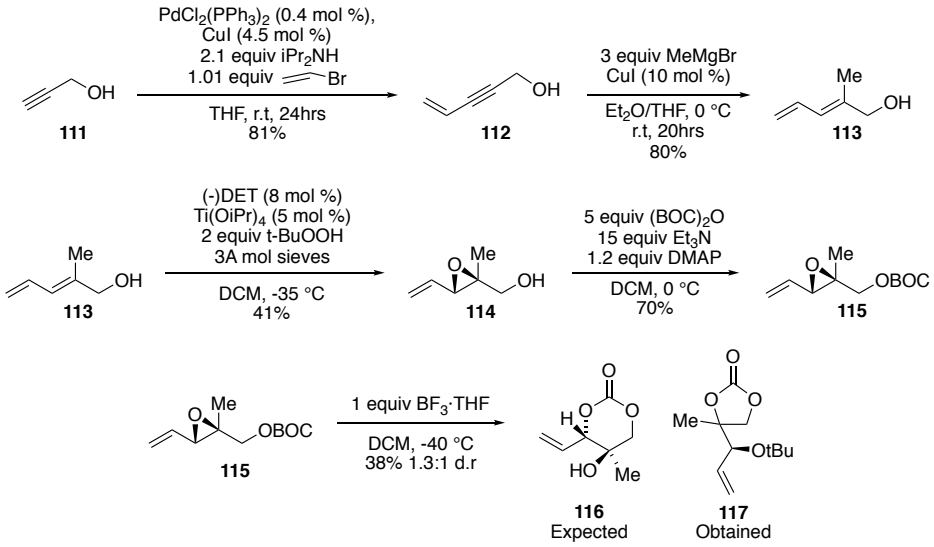

Figure 33: Lewis acid catalyzed cyclization chemistry on model system **115**.

Conclusions and Future directions

Attempts to form tetraene **75** via a Grignard/Claisen protocol proved to be difficult. This was in large part due to E/Z selectivity issues during the final Johnson-Claisen reaction, as well as the stability of the starting materials under the harsh reaction

conditions. Because of these problems, Julia couplings of aldehyde **86** and sulfone **97** to form tetraene **105** were attempted. The Julia coupling was successful in yielding tetraene **105**, however in low yield and high recovery of starting material. Several modifications were made to the Julia coupling including switching the aldehyde and sulfone coupling partner, however no improvements were observed. We believe that these problems are possibly due to the conjugated diene. In the future this may be explored by attempting Julia couplings on alkynyl sulfone **118** and aldehyde **103** to yield diene **119** (Figure 34 A). compound **119** could then be converted to tetraene **105** via carboalumination iodination followed by Stillie coupling. Preliminary results using sulfone **118** and epoxy aldehyde **120** resulted in greater than 50% yields of desired alkene product **121** with decomposition products making up the remaining mass (Figure 34B). Alkene **121** could not be used in further reactions due to incompatibilities of the epoxide during the carboalumination/iodination step.

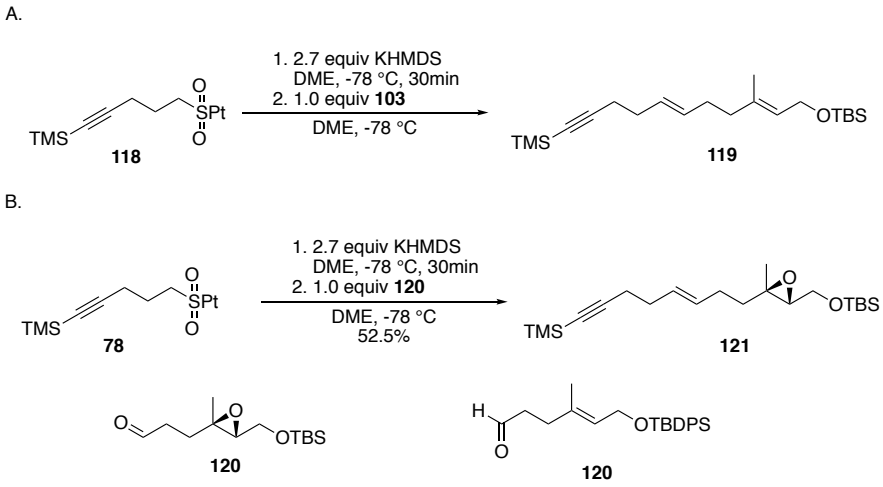

Figure 34: A) Proposed Julia coupling of alkynyl sulfone **118**. B) Preliminary results of Julia coupling between **118** and epoxy aldehyde **120**.

Lewis acid catalyzed cyclization attempts on the model system **115** resulted in exclusively the 5 membered ring exocyclic product as a mixture of diastereomers of **117** instead of the desired endocyclic product **116**. This was confirmed via NOE and IR analysis. To attempt to favor the endocyclic product, future work will focus on metal catalyzed activation of the terminal epoxyalkene.

Experimental

General experimental

^{1}H and ^{13}C nuclear magnetic resonance (NMR) spectra were recorded on a Varian Inova 600 spectrometer (600 MHz ^{1}H, 151 MHz ^{13}C), a Bruker 600 spectrometer (600 MHz ^{1}H, 151 MHz ^{13}C), a Varian Inova 500 spectrometer (500 MHz ^{1}H, 126 MHz ^{13}C), and a Varian Inova 400 spectrometer (400 MHz ^{1}H, 100 MHz ^{13}C) at room temperature in $CDCl_3$ (neutralized and dried over anhydrous K_2CO_3) with internal $CHCl_3$ as the reference (7.26 ppm for ^{1}H, 77.23 ppm ^{13}C), unless otherwise stated. Chemical shifts (δ values) were reported in parts per million (ppm) and coupling constants (*J* values) in Hz. Multiplicity was indicated using the following abbreviations: s = singlet, d = doublet, t = triplet, q = quartet, p = pentet, m = mutiplet, br = broad or a combination thereof. High resolution mass spectra (HRMS) were obtained using a Thermo Electron Corporation Finigan LTQFTMS (at the Mass Spectrometry Facility, Emory University). Analytical thin layer chromatography (TLC) was performed on precoated glass backed Silicycle SiliaPure® 0.25 mm silica gel 60 plates and visualized with UV light, ethanolic *p*-anisaldehyde,. Flash column chromatography was performed using Silicycle SilaFlash® F60 silica gel (40-63 μm). All reactions were carried out with anhydrous solvents in oven dried and argon-charged glassware. All anhydrous solvents were dried with 4 Å molecular sieves purchased form Sigma Aldrich and tested for trace water content with Coulometric KF titrator from Denver instruments. All solvents used in extraction procedures and chromatography were used as received from commercial suppliers without prior purification. Solvents for workup, extraction, and column chromatography were used as received from commercial suppliers without further purification. All other reagents were purchased from Sigma Aldrich, Strem Chemicals, or Oakwood Chemicals and used as received without further purification.

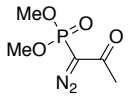

14

Bestmann-Ohira reagent 14

To a 250 mL oven dried round bottom flask equipped with a stir bar, 5.11 g of Dimethyl acetylmethylphosphonate (31 mmol) and THF (60 mL) were added. Next the solution was placed in an ice bath, and 1.33 g of a 60% w/w suspension of NaH in mineral oil (31 mmol) was added over several portions. The solution was allowed to stir for 15 minutes, and 6.74 g of 4-Acetamidobenzenesulfonyl azide (*p*-ABSA) (31 mmol) in THF (15 mL) was added via syringe pump over 30 minutes. The reaction was warmed to room temperature and allowed to react for 6 hours. Next the solution was filtered through a pad of Celite, and washed with Et_2O. The filtrate was then concentrated in vacuo. To the concentrated solution chloroform (25 mL) was added and a precipitate formed. The solution was filtered through Celite again and washed with chloroform, and concentrated

yielding 4.65 g of a yellow oil (24.2 mmol, 78% yield) with no further purification required. **^{1}H NMR** (399 MHz, Chloroform-*d*) δ 3.80 – 3.69 (s, 6H), 2.21 – 2.12 (s, 3H).

Silver dicollidine perchlorate
To a 100 mL round bottom flask 4.72 g of silver nitrate (26.7 mmol) and 5.6 g of sodium perchlorate (44.9 mmol) were added and dissolved in 50 mL of H_2O. Next 10 mL of collidine (75.7 mmol) was added, and a white precipitate immediately formed. The white solid was filtered and washed with water, EtOH, and Et_2O. The solid was then dried over phosphorus pentoxide under vacuum for 2 days yielding 11.5 g (25.6 mmol 96% yield).

Iodine dicollidine perchlorate (IDCP)
To an oven dried 250 mL round bottom flask was added 11.5 g of silver dicollidine perchlorate (25.6 mmol) and 3 mL of collidine (22.7 mmol) was added in 67 mL of chloroform. To the suspension, 6.51 g of elemental iodine (25.6 mmol) was added and stirred. After 15 minutes, a yellow precipitate was formed. The precipitate was removed by filtration through Celite and washed with chloroform. The filtrate was then cooled in an ice bath, and ether added. Upon addition of ether, a white solid precipitated, and was collected by vacuum filtration. The solid was then dried over phosphorus pentoxide under vacuum for 2 days yielding 9.6 g of a white solid (20.5 mmol, 80% yield).

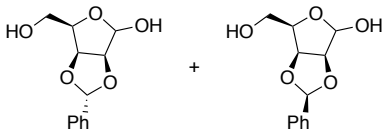

29 **29**

Protected lyxose 29
To a solution of 6.0 g of lyxose **28** (40 mmol) in 15 mL of DMF and 17 mL of distilled benzaldehyde (160 mmol), 4.67 g CSA (20 mmol) was added. The reaction was allowed to proceed for two days under a balloon of argon at which time the reaction was quenched with 13 mL of triethylamine, filtered through Celite, and concentrated in vacuo. The solution was then filtered through silica gel with ethyl acetate, and concentrated again. The solution was then diluted with DCM, washed with water to remove DMF (3X 30mL). The organic layer was separated, dried over Na_2SO_4, filtered, and concentrated. The resulting solid was purified by silica gel flash column chromatography with 1:1→3:1 EtOAc:hexanes as the mobile phase yielding 3.92 g (16.8 mmol, 42% yield) of the desired product as an 1:1 mixture of inseparable diastereomers as a white solid. **^{1}H NMR** (400 MHz, DMSO-d_6) δ 7.42 – 7.36 (m, 10H), 6.49 (d, J = 4.4 Hz, 1H), 6.43 (d, J = 4.4 Hz, 1H), 5.75 (s, 1H), 5.67 (s, 1H), 5.28 (d, J = 4.3 Hz, 1H), 5.24 (d, J = 4.2 Hz, 1H), 4.81 (dd, J = 5.2, 3.9 Hz, 1H), 4.75 (m 3H), 4.55 (dd, J = 5.5,1.1 Hz, 1H), 4.49 (dd, J = 6.2,1.1 Hz, 1H). **^{13}C NMR** (126 MHz, cdcl$_3$) δ 136.2, 135.5, 130.1, 129.8, 128.53, 128.49, 127.0, 126.6, 106.33, 106.31, 105.65, 105.61, 101.2, 100.7, 86.2, 85.3, 80.6, 80.0, 29.7. **FT-IR** ν_{max}/cm^{-1} 3334, 3198 (OH), 2924 (CH) **HRMS** calculated for $C_{12}H_{14}O_5Na$ (mass +23) 261.0734; found: 261.0733 **Melting Point** 98.5-99.4°C

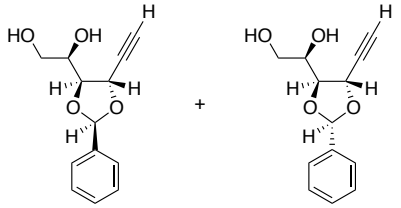

27 **27**

Alkynyl diol 27

To a 250mL 3-neck flask 1.3 g of **29** (5.5 mmol) was added and dissolved in 28 mL of MeOH. Next 1.5 g of K_2CO_3 (10.9 mmol) was added and the mixture stirred under argon. Next a reflux condenser was attached, and the solution was heated to 65 °C. The Bestmann-Ohira reagent, **14**, was then dissolved in 16 mL of MeOH and added *via* syringe pump over 12 hours. After 12 hours the reaction was quenched with 22 mL of 1M acetic acid. The solution was then concentrated in vacuo. The concentrated solution was then extracted with DCM (3 x 30 mL). The organic layer was separated, dried over Na_2SO_4, filtered, and concentrated. The resulting yellow oil was purified by silica gel flash column chromatography with 1:1→3:1 EtOAc:hexanes as the mobile phase yielding 0.558 g (2.37 mmol, 43% yield) of the desired product as a 1:1 mixture of inseparable diastereomers as a clear, colorless oil. **^{1}H NMR** (600 MHz, Chloroform-*d*) δ 7.49 – 7.46 (m, 4H), 7.38-7.35 (m, 6H), 5.99 (s, 1H), 5.98 (s, 1H), 4.84 (d, *J* = 2.1 Hz, 1H), 4.82 (d, *J* = 2.1 Hz, 1H), 4.23 (dd, *J* = 6.0, 4.0 Hz, 1H), 4.10 (d, *J* = 2.64 Hz, 1H), 4.08 (d, *J* = 2.93 Hz, 1H), 3.77-3.80 (m, 3H), 3.73 (q, *J* = 4.66 Hz, 4H), 2.61 (d, *J* = 2.1 Hz, 1H), 2.57 (d, *J* = 2.1 Hz, 1H). **^{13}C NMR** (151 MHz, $CDCl_3$) δ 135.7, 129.9, 128.5, 126.7, 104.0, 83.9, 80.4, 75.7, 70.4, 67.4, 64.1 **FT-IR** ν_{max}/cm^{-1} 3450 (OH), 3284 (CH alkyne), 2889 (CH alkane) **HRMS** calculated for $C_{13}H_{15}O_4$ (mass +1) 235.0963; found: 235.0965

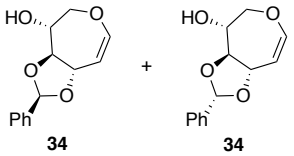

34 **34**

Septanose glycal 34

To a 50 mL schlenk flask 558 mg of **27** (2.37 mmol) was added in 20 mL of toluene along with a stir bar. Next 570 mg of DABCO (4.7 mmol) and 230 mg of tungsten hexacarbonyl (0.5925 mmol) were added and stirred. The flask was then transferred to a photoreactor and exposed to 350 nm light for 12 hours. The solution was then transferred to a 50 mL RBF and concentrated in vacuo. The resulting yellow oil was purified by silica gel flash column chromatography with 1:5→1:1 EtOAc:hexanes as the mobile phase yielding 0.278 g (1.19 mmol, 50% yield) of the desired product as a 1:1 mixture of separable diastereomers as a white solid.

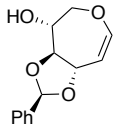

34

^{1}H NMR (399 MHz, Chloroform-*d*) δ 7.47 – 7.45 (m, 2H), 7.38 (td, *J* = 5.0,1.9 Hz, 3H), 6.40 (dd, *J* = 6.4, 1.9 Hz, 1H), 6.10 (s, 1H), 5.18 (dd, *J* = 6.5, 1.6 Hz, 1H), 4.65 (dt, *J* = 9.8, 1.8 Hz, 1H), 4.23 (dt, *J* = 7.5, 2.6 Hz, 1H), 4.16 – 4.13 (m, 1H), 4.12 (t, *J* = 2.2 Hz, 2H), 4.03 (d, *J* = 3.2 Hz, 1H), 4.00 (d, *J* = 3.2 Hz, 1H) 2.44 (t, *J* = 4.6 Hz, 1H). **^{13}C NMR** (126 MHz, cdcl$_3$) δ 149.2, 138.3, 129.4, 128.5, 126.3, 107.1, 104.6, 86.0, 75.4, 73.5, 72.7
HRMS calculated for $C_{13}H_{15}O_4$ (mass +1) 235.0965; found: 235.0964

Crystal Structure

Table 1 Crystal data and structure refinement for AJE-01-199.

Identification code	AJE-01-199
Empirical formula	$C_{26}H_{30}O_9$
Formula weight	486.50
Temperature/K	173(2)
Crystal system	monoclinic
Space group	C2
a/Å	8.7513(2)
b/Å	6.9927(2)
c/Å	19.1912(4)
α/°	90
β/°	91.6770(10)
γ/°	90
Volume/Å^3	1173.91(5)
Z	2
ϱ_{calc}g/cm^3	1.376
μ/mm^{-1}	0.868
F(000)	516.0
Crystal size/mm^3	0.608 × 0.398 × 0.156
Radiation	CuKα (λ = 1.54178)
2Θ range for data collection/°	4.606 to 133.976
Index ranges	-10 ≤ h ≤ 10, -8 ≤ k ≤ 8, -20 ≤ l ≤ 22
Reflections collected	4805
Independent reflections	1938 [R_{int} = 0.0144, R_{sigma} = 0.0156]
Data/restraints/parameters	1938/6/165
Goodness-of-fit on F^2	1.064
Final R indexes [I>=2σ (I)]	R_1 = 0.0310, wR_2 = 0.0819
Final R indexes [all data]	R_1 = 0.0313, wR_2 = 0.0822
Largest diff. peak/hole / e Å^{-3}	0.16/-0.18
Flack parameter	0.14(5)

Table 2 Fractional Atomic Coordinates ($\times 10^4$) and Equivalent Isotropic Displacement Parameters ($Å^2 \times 10^3$) for AJE-01-199. U_{eq} is defined as 1/3 of of the trace of the orthogonalised U_{IJ} tensor.

Atom	*x*	*y*	*z*	U(eq)
O1	2976.6(18)	6258(2)	2793.1(8)	32.2(4)
O2	2783(2)	3698(2)	2045.6(8)	36.6(4)
O3	2093(2)	1508(3)	4112.8(9)	46.3(5)
O4	2771(2)	5709(3)	4364.6(9)	47.4(5)
O1W	5000	2878(5)	5000	61.8(8)
C8	2899(3)	6924(3)	1574.8(12)	30.4(5)
C1	3437(2)	5572(3)	2136.3(12)	30.8(5)
C5	2338(3)	506(4)	3518.0(14)	38.3(6)
C4	2299(2)	1146(4)	2870.3(13)	34.3(5)
C9	3935(3)	7970(4)	1197.3(13)	36.8(6)
C2	2768(3)	4570(3)	3203.2(12)	28.8(5)
C3	2035(2)	3214(3)	2676.0(11)	29.2(5)
C7	1795(3)	4946(4)	3826.0(13)	36.1(6)
C13	1337(3)	7191(4)	1439.4(13)	35.9(5)
C12	834(3)	8458(4)	933.3(14)	41.4(6)
C6	1038(3)	3090(4)	4047.9(15)	45.0(6)
C10	3415(3)	9259(4)	691.1(14)	44.8(7)
C11	1872(3)	9506(4)	557.6(14)	44.5(6)

Table 3 Anisotropic Displacement Parameters ($Å^2 \times 10^3$) for AJE-01-199. The Anisotropic displacement factor exponent takes the form: $-2\pi^2[h^2a^{*2}U_{11}+2hka^*b^*U_{12}+\ldots]$.

Atom	U_{11}	U_{22}	U_{33}	U_{23}	U_{13}	U_{12}
O1	42.3(8)	24.4(8)	30.1(9)	-1.0(7)	1.8(6)	-6.3(7)
O2	47.4(10)	30.4(9)	32.1(9)	-6.2(7)	2.4(7)	-4.2(7)
O3	61.5(11)	35.5(11)	41.8(10)	6.8(8)	0.5(8)	-6.6(9)
O4	70.1(13)	42.5(11)	30.1(10)	-7.7(8)	7.2(8)	-14.6(10)
O1W	87(2)	49.9(18)	48.1(18)	0	-5.5(15)	0
C8	32.2(11)	28.9(12)	30.1(12)	-5.9(9)	1.1(9)	-3.4(9)
C1	28.3(10)	30.9(12)	33.3(13)	-3.6(9)	1.6(9)	-4.6(9)
C5	37.6(12)	28.2(12)	49.0(15)	1.5(11)	-2.9(11)	-4.2(10)
C4	27.9(10)	30.2(13)	44.5(14)	-4.7(10)	-2.2(9)	-0.8(9)
C9	34.2(12)	39.6(14)	36.7(13)	-3.8(11)	3.7(9)	-4.3(10)
C2	28.8(11)	24.4(12)	33.1(12)	-0.5(9)	-1.0(8)	-3.5(9)
C3	28.5(10)	26.2(12)	32.9(12)	-1.7(10)	-0.5(8)	-1.2(9)
C7	38.9(13)	33.1(13)	36.5(14)	-0.8(10)	7.3(10)	-2.9(10)
C13	34.4(12)	32.1(12)	41.3(14)	-0.4(10)	1.6(10)	-3(1)
C12	40.1(13)	37.9(14)	45.8(15)	-1.8(11)	-7.9(10)	3.3(11)
C6	48.4(15)	41.5(15)	46.1(15)	-0.9(12)	17.0(11)	-8.8(12)

C10	54.7(16)	44.6(16)	35.7(14)	3.4(11)	7.6(11)	-14.5(13)
C11	60.4(17)	36.4(15)	36.2(14)	3.9(11)	-5.8(11)	0.0(12)

Table 4 Bond Lengths for AJE-01-199.

Atom	Atom	Length/Å	Atom	Atom	Length/Å
O1	C1	1.418(3)	C5	C4	1.320(4)
O1	C2	1.433(3)	C4	C3	1.509(3)
O2	C1	1.438(3)	C9	C10	1.392(4)
O2	C3	1.433(3)	C2	C3	1.516(3)
O3	C5	1.362(3)	C2	C7	1.511(3)
O3	C6	1.444(4)	C7	C6	1.524(4)
O4	C7	1.425(3)	C13	C12	1.377(4)
C8	C1	1.499(3)	C12	C11	1.386(4)
C8	C9	1.385(3)	C10	C11	1.378(4)
C8	C13	1.397(3)			

Table 5 Bond Angles for AJE-01-199.

Atom	Atom	Atom	Angle/°	Atom	Atom	Atom	Angle/°
C1	O1	C2	104.69(16)	O1	C2	C7	112.04(19)
C3	O2	C1	107.66(17)	C7	C2	C3	113.53(19)
C5	O3	C6	116.0(2)	O2	C3	C4	111.41(19)
C9	C8	C1	120.8(2)	O2	C3	C2	102.74(17)
C9	C8	C13	119.0(2)	C4	C3	C2	112.1(2)
C13	C8	C1	120.2(2)	O4	C7	C2	107.4(2)
O1	C1	O2	107.06(17)	O4	C7	C6	111.9(2)
O1	C1	C8	109.52(18)	C2	C7	C6	109.5(2)
O2	C1	C8	111.85(18)	C12	C13	C8	120.5(2)
C4	C5	O3	127.9(3)	C13	C12	C11	120.4(2)
C5	C4	C3	123.8(2)	O3	C6	C7	113.2(2)
C8	C9	C10	120.1(2)	C11	C10	C9	120.6(2)
O1	C2	C3	101.95(18)	C10	C11	C12	119.4(2)

Table 6 Torsion Angles for AJE-01-199.

A	B	C	D	Angle/°	A	B	C	D	Angle/°
O1	C2	C3	O2	35.9(2)	C9	C8	C1	O2	-128.0(2)
O1	C2	C3	C4	155.62(18)	C9	C8	C13	C12	0.7(4)
O1	C2	C7	O4	-83.2(2)	C9	C10	C11	C12	0.1(4)
O1	C2	C7	C6	155.2(2)	C2	O1	C1	O2	28.3(2)
O3	C5	C4	C3	3.1(4)	C2	O1	C1	C8	149.71(17)

O4	C7	C6	O3	-70.1(3)	C2	C7	C6	O3	48.9(3)
C8	C9	C10	C11	-0.3(4)	C3	O2	C1	O1	-4.6(2)
C8	C13	C12	C11	-0.8(4)	C3	O2	C1	C8	-124.57(19)
C1	O1	C2	C3	-39.4(2)	C3	C2	C7	O4	162.0(2)
C1	O1	C2	C7	-161.08(18)	C3	C2	C7	C6	40.4(3)
C1	O2	C3	C4	-139.49(19)	C7	C2	C3	O2	156.62(19)
C1	O2	C3	C2	-19.3(2)	C7	C2	C3	C4	-83.7(3)
C1	C8	C9	C10	-178.2(2)	C13	C8	C1	O1	-64.6(3)
C1	C8	C13	C12	178.8(2)	C13	C8	C1	O2	53.9(3)
C5	O3	C6	C7	-86.6(3)	C13	C8	C9	C10	-0.1(4)
C5	C4	C3	O2	150.3(2)	C13	C12	C11	C10	0.4(4)
C5	C4	C3	C2	35.8(3)	C6	O3	C5	C4	30.9(3)
C9	C8	C1	O1	113.5(2)					

Table 7 Hydrogen Atom Coordinates (Å×10^4) and Isotropic Displacement Parameters (Å^2×10^3) for AJE-01-199.

Atom	***x***	***y***	***z***	**U(eq)**
H1	4554	5479	2136	37
H5	2560	-786	3575	46
H4A	2442	271	2513	41
H9	4979	7810	1282	44
H2	3766	4069	3360	35
H3	937	3473	2626	35
H7	1004	5887	3700	43
H13	631	6507	1693	43
H12	-209	8612	843	50
H6A	562	3289	4492	54
H6B	238	2762	3708	54
H10	4116	9961	441	54
H11	1530	10367	218	53
H4	2450(30)	6180(50)	4812(10)	53
H1W	4300(20)	3710(40)	4742(13)	53

Experimental

Single crystals of $C_{26}H_{30}O_9$ [AJE-01-199] were [vapor diffusion using THF as the solvent and pentane as the precipitant.]. A suitable crystal was selected and [The crystal was mounted on a loop with paratone oil] on a 'Bruker APEX-II CCD' diffractometer. The crystal was kept at 173(2) K during data collection. Using Olex2 [1], the structure was solved with the XT [2] structure solution program using Intrinsic Phasing and refined with the XL [3] refinement package using Least Squares minimisation.

1. Dolomanov, O.V., Bourhis, L.J., Gildea, R.J, Howard, J.A.K. & Puschmann, H. (2009), J. Appl. Cryst. 42, 339-341.
2. Sheldrick, G.M. (2015). Acta Cryst. A71, 3-8.
3. Sheldrick, G.M. (2008). Acta Cryst. A64, 112-122.

Crystal structure determination of [AJE-01-199]

Crystal Data for $C_{26}H_{30}O_9$ (M =486.50 g/mol): monoclinic, space group C2 (no. 5), a = 8.7513(2) Å, b = 6.9927(2) Å, c = 19.1912(4) Å, β = 91.6770(10)°, V = 1173.91(5) Å^3, Z = 2, T = 173(2) K, μ(CuKα) = 0.868 mm^{-1}, *Dcalc* = 1.376 g/cm^3, 4805 reflections measured (4.606° ≤ 2Θ ≤ 133.976°), 1938 unique (R_{int} = 0.0144, R_{sigma} = 0.0156) which were used in all calculations. The final R_1 was 0.0310 (I > 2σ(I)) and wR_2 was 0.0822 (all data).

Refinement model description

Number of restraints - 6, number of constraints - unknown.

Details:

```
1. Fixed Uiso
 At 1.2 times of:
  All C(H) groups, All C(H,H) groups, All C(H,H,H) groups
2. Restrained distances
 O1W-H1W
 0.982 with sigma of 0.02
 O4-H4
 0.982 with sigma of 0.02
 H4-O3_$1
 2 with sigma of 0.02
 H1W-O4
 2 with sigma of 0.02
 H1W_$2-H1W
 1.55 with sigma of 0.02
3.a Ternary CH refined with riding coordinates:
 C1(H1), C2(H2), C3(H3), C7(H7)
3.b Secondary CH2 refined with riding coordinates:
 C6(H6A,H6B)
3.c Aromatic/amide H refined with riding coordinates:
 C5(H5), C4(H4A), C9(H9), C13(H13), C12(H12), C10(H10), C11(H11)
```

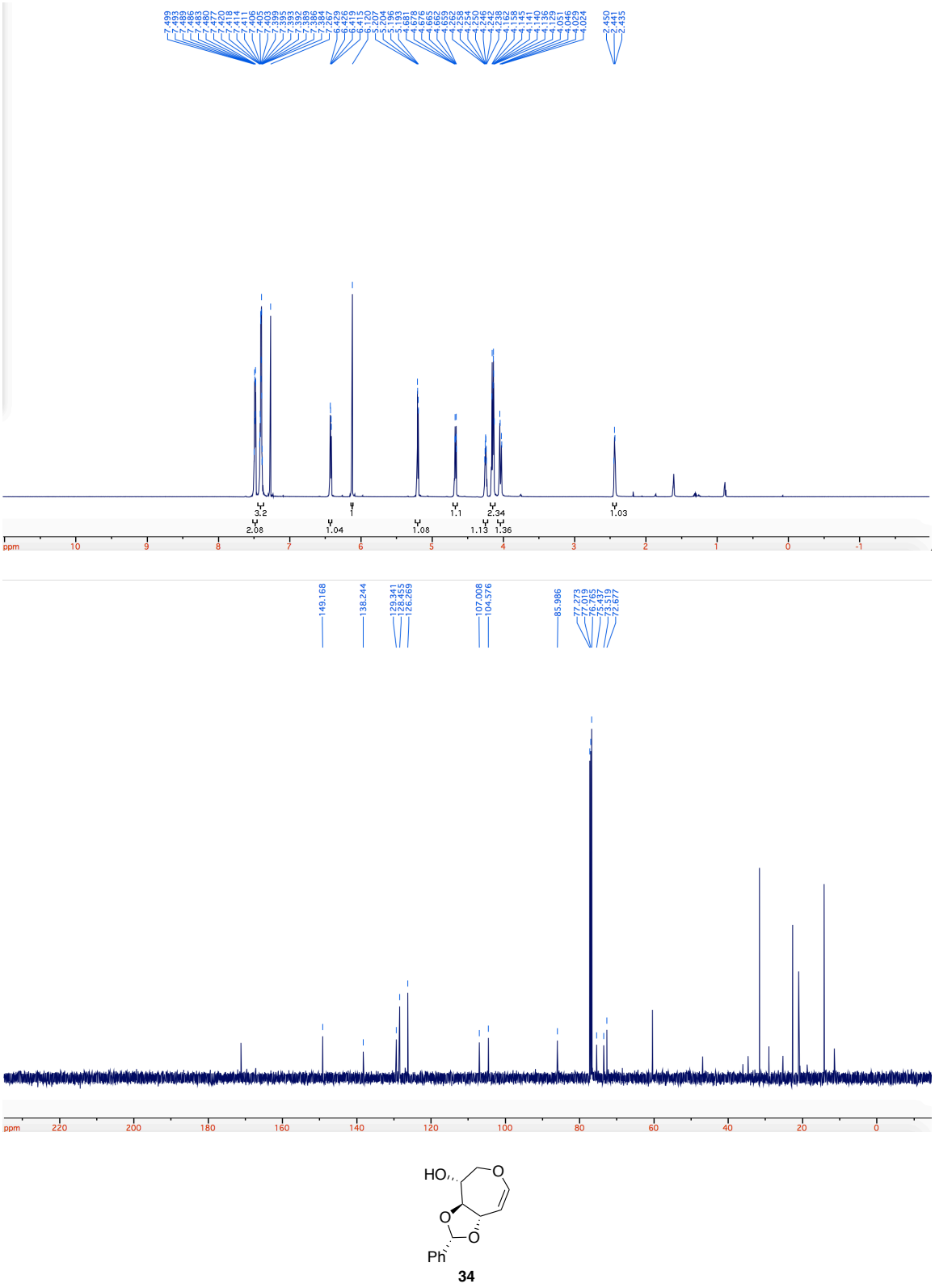

34

^{1}H NMR (399 MHz, Chloroform-*d*) δ 7.49-7.47 (m, 2H), 7.40-7.38 (m, 3H), 6.45 (dd, *J* = 6.5, 2.0 Hz, 1H) 6.08 (s, 1H), 5.25 (dd *J* = 6.5, 1.3 Hz, 1H) 4.72 (d, *J* = 9.8 1H) 4.18-

4.16 (m, 1H) 4.14-4.11 (m, 1H) 4.09-4.04 (m, 2H) **^{13}C NMR** (126 MHz, cdcl$_3$) δ 149.7, 129.4, 128.4, 126.6, 106.1, 104.4, 84.0, 75.6, 74.9, 73.3 **FT-IR** ν_{max}/cm^{-1} 3536 (OH), 2911 (CH) **HRMS** calculated for $C_{13}H_{15}O_4$ (mass +1) 235.0965; found: 235.0965 **melting point** 80.8-81.3 °C **optical rotation** α_D^{20} +30.0

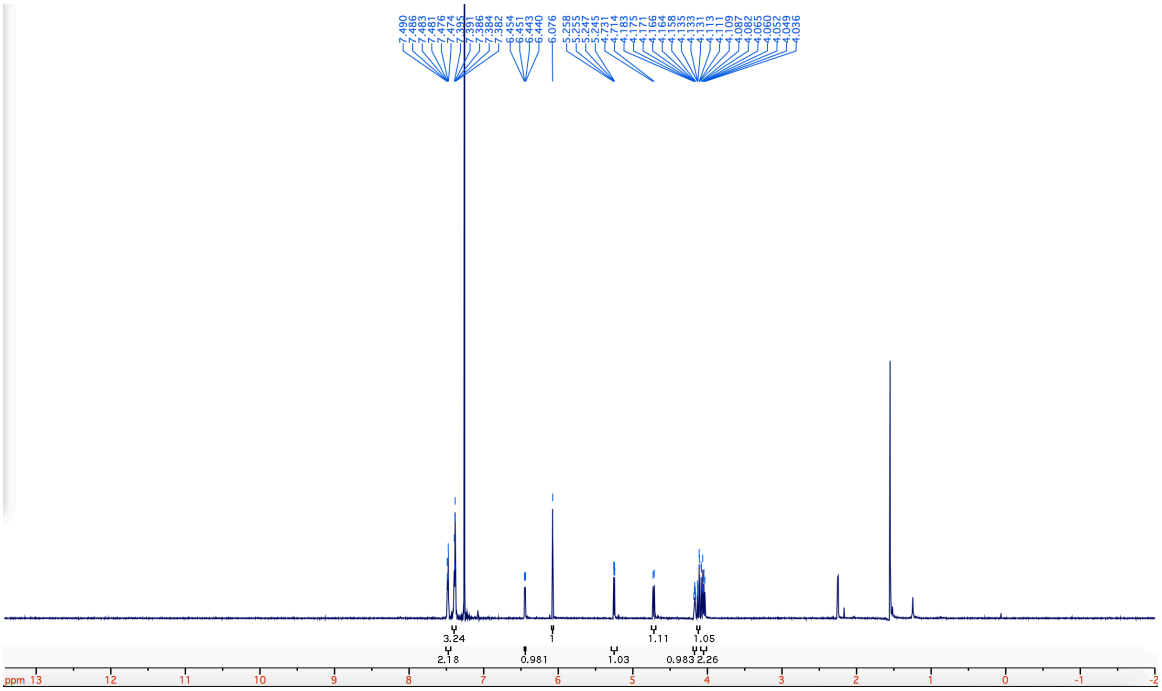

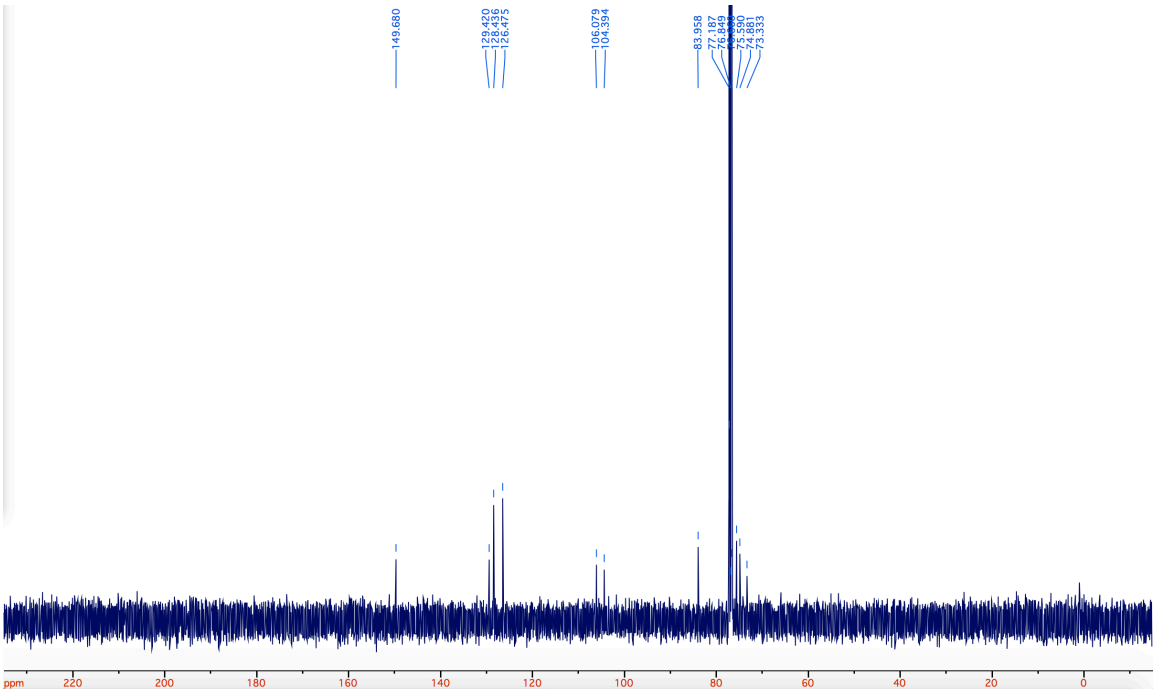

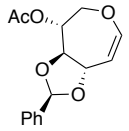

36

Acetate protected septanose glycal 36

To a 20 mL vial containing 50 mg of **34** (0.213 mmol) and a stir bar, 0.88 mL of acetic anhydride (8.7 mmol) and 0.32 mL of pyridine (4.05 mmol) were added. The solution was then allowed to react for 12 hours. After 12 hours the reaction was concentrated in vacuo with no further purification required. **^{1}H NMR** (400 MHz, Chloroform-*d*) δ 7.48 – 7.41 (m, 2H), 7.38 – 7.33 (m, 3H), 6.39 (dd, *J* = 6.6, 1.9 Hz, 1H), 6.10 (s, 1H), 5.31 (dd, *J* = 7.8, 2.5 Hz, 1H), 5.14 (dd, *J* = 6.5, 1.4 Hz, 1H), 4.71 (dt, *J* = 10.0, 1.7 Hz, 1H), 4.35 (dd, *J* = 9.9, 7.8 Hz, 1H), 4.27 (dd, *J* = 14.1, 1.1 Hz, 1H), 4.02 (dd, *J* = 14.1, 3.0 Hz, 1H), 2.15 (s, 3H). **^{13}C NMR** (126 MHz, cdcl$_3$) δ 170.1, 148.3, 139.1, 129.1, 128.3, 126.1, 111.6, 104.2, 80.1, 72.0, 70.5, 67.4, 20.9

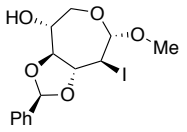

38

1-methoxy, 2-iodo septanose 38

To a solution of **34** (53 mg, 0.21 mmol) in 1.2 mL of methanol IDCP (100 mg, 0.21 mmol) was added and stirred. Next the reaction was allowed to proceed for 1 hour. After 1 hour the solution was concentrated in vacuo. The resulting solid was purified by silica gel flash column chromatography with 2:1 EtOAc:hexanes as the mobile phase yielding 60 mg (0.15 mmol, 72% yield) of the desired product as a white solid. **^{1}H NMR** (600 MHz, Acetone-d_6) δ 7.52 – 7.46 (m, 2H), 7.39 (dd, *J* = 5.2, 2.1 Hz, 3H), 6.03 (s, 1H), 4.71 (d, *J* = 7.9 Hz, 1H), 4.14 (dd, *J* = 10.9, 7.9 Hz, 1H), 4.06 (dd, *J* = 11.1, 8.2 Hz, 1H), 4.04 – 3.96 (m, 2H), 3.93 (dd, *J* = 13.4, 3.6 Hz, 1H), 3.89 (dd, *J* = 13.5, 4.4 Hz, 1H), 3.43 – 3.34 (s, 3H).

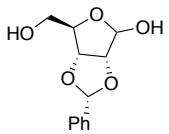

28

Protected ribose 31

To a solution of 20.4 g of ribose 30 (133 mmol) in 45 mL of DMF, 58 mL of distilled benzaldehyde (532 mmol), and 15.68 g of CSA (67 mmol) was added. The reaction was allowed to proceed for two days under a balloon of argon at which time the reaction was quenched with 40 mL of triethylamine, filtered through Celite, and concentrated in vacuo. The solution was then filtered through silica gel with ethyl acetate, and

concentrated again. The solution was then diluted with DCM, washed with water to remove DMF (3 x 100 mL). The organic layer was separated, dried over Na_2SO_4, filtered, and concentrated. The resulting solid was purified by silica gel flash column chromatography with 1:1→3:1 EtOAc:hexanes as the mobile phase yielding 10.97 g (46.1 mmol, 35% yield) of the desired product as a white solid. **^{1}H NMR** (400 MHz, $CDCl_3$) δ 7.49 (dd, *J* = 6.7, 3.0 Hz, 2H), 7.39-7.37 (m, 3H) 5.97 (s, 1H), 5.56 (d, *J* = 6.3 Hz, 1H), 5.00 (d, *J* = 5.7 Hz, 1H), 4.69 (d, *J* = 5.5 Hz, 1H), 4.58 (t, *J* = 2.4 Hz, 1H), 3.78 (m, 2H) **^{13}C NMR** (126 MHz, cdcl$_3$) δ 136.1, 130.0, 128.7, 126.9, 105.8, 102.5, 87.5, 82.6, 63.6 **FT-IR** ν_{max}/cm^{-1} 3391 (OH), 2939 (CH) **HRMS** calculated for $C_{12}H_{14}O_5Na$ (mass +23) 261.0734; found: 261.0733 **melting point** 102.6-104.3°C **optical rotation** α_D^{20} -23.1° (c 0.31, $CHCl_3$)

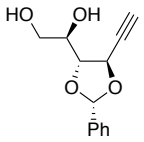

32

Alkynyl diol 32

To a 1 L 3-neck flask **31** (9 g, 41 mmol) was added and dissolved in MeOH (250 mL). Next K_2CO_3 (11 g, 82 mmol) was added and the mixture stirred under argon. Next a reflux condenser was attached, and the solution was heated to 65 °C. The Bestmann-Ohira reagent **14** was then dissolved in MeOH (120 mL) and added *via* syringe pump over 12 hours. After 12 hours the reaction was quenched with 82ml of 1M acetic acid. The solution was then concentrated in vacuo. The concentrated solution was then extracted with DCM (3 x 100 mL). The organic layer was separated, dried over Na_2SO_4, filtered, and concentrated. The resulting solid was purified by silica gel flash column chromatography with 1:1→3:1 EtOAc:hexanes as the mobile phase yielding 4.58 g (20.6 mmol, 51% yield) of the desired product as an oil. **^{1}H NMR** (400 MHz, Chloroform-*d*) δ 7.58 – 7.55 (m, 2H), 7.49 – 7.47 (m, 3H), 6.10 (s, 1H), 4.96 (dd, *J* = 6.0, 2.1 Hz, 1H), 4.38 (dd, *J* = 6.0, 3.7 Hz, 1H) 3.92 (dd, *J* = 9.0, 4.5 Hz, 1H) 3.87 (d, *J* = 4.5 Hz, 1H), 2.70 (d, *J* = 2.1 Hz, 1H). **^{13}C NMR** (151MHz, $CDCl_3$) δ 138.0, 130.0, 128.7, 126.8, 103.8, 83.3, 81.2, 75.5, 71.8, 67.5, 63.3 **FT-IR** ν_{max}/cm^{-1} 3279 (OH), 2926 (CH) **HRMS** calculated for $C_{13}H_{14}O_4Na$ (mass +23) 257.0785; found: 235.0784 **Optical rotation** α_D^{20} -19.3° (c 0.33, $CHCl_3$)

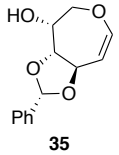

35

Septanose glycal 35

To a 500 mL schlenk flask 4.58 g of **32** (20.6 mmol) was added in 200 mL of toluene along with a stir bar. Next 4.62 g of DABCO (41.2 mmol) and 1.81 g of tungsten hexacarbonyl (5.15 mmol) were added and stirred. Next the flask was transferred to a photoreactor and exposed to 350 nm light for 12 hours. The solution was then transferred to a 500 mL RBF and concentrated in vacuo. The resulting yellow oil was purified by silica gel flash column chromatography with 1:3→1:1 EtOAc:hexanes as the mobile phase yielding 1.43 g (6.43 mmol, 31.2% yield) of the desired product as a white solid. **^{1}H NMR** (500 MHz, Chloroform-*d*) δ 7.51-7.48 (m, 2H), 7.44 – 7.39 (m, 3H), 6.41 (dd, *J* = 6.3, 2.1 Hz, 1H), 6.15 (s, 1H), 5.30 (dd, *J* = 6.3, 1.8 Hz, 1H), 5.02 (dt, *J* = 9.7, 1.8 Hz, 1H), 4.58 (dddd, *J* = 7.8, 5.8, 3.9, 1.9 Hz, 1H), 4.28 (dd, *J* = 12.5, 5.3 Hz, 1H), 4.06 (dd, *J* = 9.7, 3.9 Hz, 1H), 3.79 (dd, *J* = 12.5, 8.0 Hz, 1H) 2.42 (d, *J* = 2.0 Hz, 1H) **^{13}C NMR** (126 MHz, cdcl$_3$) δ 148.6, 138.7, 129.4, 128.6, 126.3, 109.2, 104.4, 82.0, 72.9, 71.7, 66.0 **FT-IR** ν_{max}/cm^{-1} 3444 (OH), 2884 (CH) **HRMS** calculated for $C_{13}H_{15}O_4$ (mass +1) 235.0965; found: 235.0964 **melting point** 87.5-88.6 °C **optical rotation** α_D^{20} -46.0

Crystal Structure

Table 1 Crystal data and structure refinement for AJE-01-190.

Identification code	AJE-01-190
Empirical formula	$C_{13}H_{14}O_4$
Formula weight	234.24
Temperature/K	100(2)
Crystal system	monoclinic
Space group	$P2_1$
a/Å	9.8776(16)
b/Å	11.2114(17)
c/Å	10.4484(16)
α/°	90
β/°	94.542(2)
γ/°	90
Volume/Å^3	1153.4(3)
Z	4
ϱ_{calc}g/cm^3	1.349
μ/mm^{-1}	0.100
F(000)	496.0
Crystal size/mm^3	0.600 × 0.587 × 0.170
Radiation	MoKα (λ = 0.71073)
2Θ range for data collection/°	3.91 to 61.462
Index ranges	-14 ≤ h ≤ 14, -15 ≤ k ≤ 14, -14 ≤ l ≤ 14
Reflections collected	11534
Independent reflections	5811 [R_{int} = 0.0300, R_{sigma} = 0.0434]
Data/restraints/parameters	5811/1/309
Goodness-of-fit on F^2	1.031
Final R indexes [I>=2σ (I)]	R_1 = 0.0435, wR_2 = 0.1043
Final R indexes [all data]	R_1 = 0.0509, wR_2 = 0.1102
Largest diff. peak/hole / e Å^{-3}	0.40/-0.22
Flack parameter	0.13(6)

Table 2 Fractional Atomic Coordinates ($\times 10^4$) and Equivalent Isotropic Displacement Parameters ($Å^2 \times 10^3$) for AJE-01-190. U_{eq} is defined as 1/3 of of the trace of the orthogonalised U_{IJ} tensor.

Atom	*x*	*y*	*z*	U(eq)
O4'	9416.1(14)	6991.8(14)	5017.9(14)	14.5(3)
O4	4169.0(14)	4466.3(15)	5592.9(14)	15.8(3)
O1'	11860.5(14)	7981.7(15)	5927.7(15)	18.2(3)
O1	6586.0(15)	5576.5(15)	6347.8(15)	20.2(3)
O3'	9748.4(15)	4990.7(14)	4698.7(14)	16.6(3)
O3	4529.5(15)	2461.7(15)	5300.8(15)	18.1(3)
O2	6582.8(17)	3424.4(17)	8941.6(15)	23.3(4)
O2'	11524.7(16)	5849.6(16)	8512.6(15)	22.1(4)
C9	3648.9(19)	3677(2)	3488(2)	14.4(4)
C2'	11082.7(19)	7396(2)	6818.9(19)	13.7(4)
C9'	8804(2)	6211.6(19)	2921.0(19)	14.1(4)
C6	5603.8(18)	2919(2)	6195.0(19)	14.0(4)
C14'	9982(2)	6455(2)	2322(2)	19.5(5)
C7'	10068.2(19)	6517.7(19)	6175.5(19)	12.1(4)
C10	2432.1(19)	3972(2)	2792(2)	17.3(4)
C2	5920(2)	4944(2)	7286(2)	16.4(4)
C7	4929.8(18)	4017(2)	6708.8(19)	14.0(4)
C11	2412(2)	4216(2)	1488(2)	21.6(5)
C12	3602(2)	4156(2)	866(2)	21.7(5)
C8'	8862.5(19)	5984(2)	4336.1(19)	13.9(4)
C8	3658.6(19)	3449(2)	4902(2)	15.3(4)
C6'	10725.1(19)	5390(2)	5712.9(19)	13.3(4)
C4'	11231(2)	4744(2)	7985(2)	19.7(4)
C10'	7559(2)	6210(2)	2204(2)	21.1(5)
C5'	10918(2)	4482(2)	6757(2)	17.3(4)
C3	7061(2)	4320(2)	8102(2)	19.7(4)
C4	6371(2)	2303(2)	8429(2)	20.4(5)
C14	4850(2)	3633(2)	2869(2)	18.2(4)
C3'	12119(2)	6715(2)	7711(2)	19.2(4)
C12'	8671(3)	6683(2)	305(2)	24.5(5)
C5	5983(2)	2021(2)	7221(2)	18.2(4)
C13	4821(2)	3874(2)	1562(2)	20.6(5)
C13'	9918(2)	6688(2)	1016(2)	22.9(5)
C11'	7491(3)	6456(3)	891(2)	26.9(5)

Table 3 Anisotropic Displacement Parameters ($Å^2×10^3$) for AJE-01-190. The Anisotropic displacement factor exponent takes the form: $-2\pi^2[h^2a^{*2}U_{11}+2hka^*b^*U_{12}+\ldots]$.

Atom	U_{11}	U_{22}	U_{33}	U_{23}	U_{13}	U_{12}
O4'	16.9(6)	11.1(8)	14.7(6)	-0.7(6)	-3.0(5)	1.7(5)
O4	17.8(6)	12.0(8)	17.2(7)	-0.2(6)	-1.9(5)	1.3(6)
O1'	15.7(6)	15.0(9)	23.9(8)	5.1(7)	-0.1(6)	-1.3(6)
O1	20.5(7)	16.0(9)	24.3(8)	4.5(7)	2.1(6)	-4.5(6)
O3'	22.8(7)	9.4(8)	16.9(7)	-1.3(6)	-3.4(6)	1.4(6)
O3	21.0(7)	10.8(8)	21.3(7)	-1.5(6)	-5.3(6)	-0.1(6)
O2	33.7(8)	19.7(9)	16.4(7)	0.9(7)	0.6(6)	-1.6(7)
O2'	31.5(8)	18.2(9)	15.9(7)	1.7(7)	-1.9(6)	-1.0(7)
C9	16.1(8)	9.6(10)	17.0(9)	-1.5(8)	-0.9(7)	0.0(7)
C2'	13.2(8)	12.5(10)	15.5(9)	-1.7(8)	0.5(7)	0.1(7)
C9'	17.6(9)	10.2(11)	14.3(9)	-1.3(8)	-0.1(7)	2.5(7)
C6	12.7(8)	13.0(11)	16.3(9)	-2.0(8)	0.8(7)	-0.1(7)
C14'	19.0(9)	20.8(12)	18.9(10)	0.6(9)	2.6(8)	1.9(8)
C7'	12.0(8)	11.8(10)	12.4(8)	-0.7(8)	0.4(7)	0.9(7)
C10	13.2(8)	16.6(12)	21.6(10)	-3.8(9)	-2.5(7)	0.2(7)
C2	18.9(9)	14.3(11)	16.3(9)	-1.6(8)	2.7(8)	-1.2(8)
C7	12.9(8)	12.4(10)	16.7(9)	0.9(8)	2.5(7)	0.1(7)
C11	19.8(9)	21.2(13)	22.5(10)	-5.2(9)	-6.7(8)	2.7(9)
C12	27.5(10)	19.2(13)	17.8(10)	-3.5(9)	-2.1(8)	1.6(9)
C8'	13.5(8)	11.8(10)	16.1(9)	-0.6(8)	0.2(7)	1.7(7)
C8	14.1(8)	11.9(11)	19.8(9)	-0.9(9)	0.6(7)	-0.3(7)
C6'	13.9(8)	10.8(10)	14.8(9)	-0.8(8)	-0.6(7)	1.7(7)
C4'	25(1)	14.7(12)	19.1(10)	3.8(9)	0.6(8)	2.4(8)
C10'	17.9(9)	22.6(14)	22.2(11)	-1.9(9)	-2.9(8)	-2.1(8)
C5'	20.0(9)	11.4(11)	20.5(10)	2.1(8)	1.4(8)	3.2(8)
C3	20.4(9)	19.6(12)	18.3(9)	-0.4(9)	-2.4(8)	-3.8(8)
C4	22.7(10)	16.3(12)	22(1)	5.0(9)	0.7(8)	1.4(8)
C14	15.7(8)	18.7(12)	19.9(10)	0.8(9)	-0.8(7)	2.6(8)
C3'	20.7(10)	16.7(12)	19.3(10)	0.8(9)	-3.7(8)	-1.4(8)
C12'	41.2(13)	16.6(12)	15.2(10)	-0.6(9)	-0.9(9)	2.4(10)
C5	17.0(9)	13.6(11)	23.9(10)	1.0(9)	1.4(8)	1.4(8)
C13	21.1(9)	21.0(13)	20.2(10)	-0.6(9)	4.8(8)	3.1(9)
C13'	29.4(11)	20.8(13)	19.3(10)	0(1)	6.9(9)	1.8(10)
C11'	29.8(12)	26.6(15)	22.2(11)	-1.3(10)	-11.6(9)	-0.2(10)

Table 4 Bond Lengths for AJE-01-190.

Atom	Atom	Length/Å	Atom	Atom	Length/Å
O4'	C7'	1.427(2)	C9'	C14'	1.392(3)
O4'	C8'	1.422(3)	C9'	C8'	1.497(3)

O4	C7	1.428(2)	C9'	C10'	1.388(3)
O4	C8	1.421(3)	C6	C7	1.518(3)
O1'	C2'	1.415(2)	C6	C5	1.496(3)
O1	C2	1.414(2)	C14'	C13'	1.386(3)
O3'	C8'	1.448(3)	C7'	C6'	1.518(3)
O3'	C6'	1.446(2)	C10	C11	1.388(3)
O3	C6	1.451(3)	C2	C7	1.519(3)
O3	C8	1.443(3)	C2	C3	1.528(3)
O2	C3	1.437(3)	C11	C12	1.389(3)
O2	C4	1.376(3)	C12	C13	1.392(3)
O2'	C4'	1.378(3)	C6'	C5'	1.494(3)
O2'	C3'	1.437(3)	C4'	C5'	1.328(3)
C9	C10	1.395(3)	C10'	C11'	1.396(3)
C9	C8	1.499(3)	C4	C5	1.328(3)
C9	C14	1.396(3)	C14	C13	1.391(3)
C2'	C7'	1.523(3)	C12'	C13'	1.387(3)
C2'	C3'	1.532(3)	C12'	C11'	1.383(4)

Table 5 Bond Angles for AJE-01-190.

Atom	**Atom**	**Atom**	**Angle/°**	**Atom**	**Atom**	**Atom**	**Angle/°**
C8'	O4'	C7'	104.97(16)	O4	C7	C6	102.40(16)
C8	O4	C7	105.91(16)	O4	C7	C2	111.31(18)
C6'	O3'	C8'	107.94(16)	C6	C7	C2	114.11(16)
C8	O3	C6	107.70(16)	C10	C11	C12	120.2(2)
C4	O2	C3	116.57(17)	C11	C12	C13	119.7(2)
C4'	O2'	C3'	117.16(17)	O4'	C8'	O3'	106.24(15)
C10	C9	C8	119.51(17)	O4'	C8'	C9'	110.01(17)
C10	C9	C14	119.73(19)	O3'	C8'	C9'	111.41(16)
C14	C9	C8	120.73(18)	O4	C8	O3	106.83(15)
O1'	C2'	C7'	112.47(16)	O4	C8	C9	109.78(18)
O1'	C2'	C3'	105.09(16)	O3	C8	C9	111.88(17)
C7'	C2'	C3'	109.33(18)	O3'	C6'	C7'	102.35(15)
C14'	C9'	C8'	120.63(18)	O3'	C6'	C5'	111.32(18)
C10'	C9'	C14'	119.61(19)	C5'	C6'	C7'	111.60(16)
C10'	C9'	C8'	119.74(18)	C5'	C4'	O2'	127.7(2)
O3	C6	C7	101.27(15)	C9'	C10'	C11'	120.1(2)
O3	C6	C5	110.64(18)	C4'	C5'	C6'	124.2(2)
C5	C6	C7	112.61(17)	O2	C3	C2	113.36(17)
C13'	C14'	C9'	120.4(2)	C5	C4	O2	127.7(2)
O4'	C7'	C2'	111.74(17)	C13	C14	C9	119.69(19)
O4'	C7'	C6'	102.48(15)	O2'	C3'	C2'	114.02(17)
C6'	C7'	C2'	113.34(16)	C11'	C12'	C13'	120.5(2)

C11	C10	C9	120.21(18)	C4	C5	C6	123.9(2)
O1	C2	C7	112.86(17)	C14	C13	C12	120.48(19)
O1	C2	C3	104.69(16)	C14'	C13'	C12'	119.7(2)
C7	C2	C3	109.37(19)	C12'	C11'	C10'	119.7(2)

Table 6 Torsion Angles for AJE-01-190.

A	**B**	**C**	**D**	**Angle/°**	**A**	**B**	**C**	**D**	**Angle/°**
O4'	C7'	C6'	O3'	-34.93(18)	C7	C6	C5	C4	-33.1(3)
O4'	C7'	C6'	C5'	-154.08(16)	C7	C2	C3	O2	-46.2(2)
O1'	C2'	C7'	O4'	-41.8(2)	C11	C12	C13	C14	1.1(4)
O1'	C2'	C7'	C6'	73.4(2)	C8'	O4'	C7'	C2'	161.88(15)
O1'	C2'	C3'	O2'	-166.95(18)	C8'	O4'	C7'	C6'	40.20(17)
O1	C2	C7	O4	-41.7(2)	C8'	O3'	C6'	C7'	17.15(19)
O1	C2	C7	C6	73.6(2)	C8'	O3'	C6'	C5'	136.49(16)
O1	C2	C3	O2	-167.38(18)	C8'	C9'	C14'	C13'	-178.8(2)
O3'	C6'	C5'	C4'	-149.27(19)	C8'	C9'	C10'	C11'	178.2(2)
O3	C6	C7	O4	-38.09(18)	C8	O4	C7	C6	37.83(17)
O3	C6	C7	C2	-158.49(16)	C8	O4	C7	C2	160.16(15)
O3	C6	C5	C4	-145.6(2)	C8	O3	C6	C7	24.89(19)
O2	C4	C5	C6	-4.6(3)	C8	O3	C6	C5	144.48(16)
O2'	C4'	C5'	C6'	-4.8(3)	C8	C9	C10	C11	178.4(2)
C9	C10	C11	C12	0.6(4)	C8	C9	C14	C13	-178.5(2)
C9	C14	C13	C12	-0.2(4)	C6'	O3'	C8'	O4'	6.92(19)
C2'	C7'	C6'	O3'	-155.51(16)	C6'	O3'	C8'	C9'	126.73(17)
C2'	C7'	C6'	C5'	85.3(2)	C4'	O2'	C3'	C2'	83.6(2)
C9'	C14'	C13'	C12'	0.3(4)	C10'	C9'	C14'	C13'	-0.4(4)
C9'	C10'	C11'	C12'	0.9(4)	C10'	C9'	C8'	O4'	-118.6(2)
C6	O3	C8	O4	-2.64(19)	C10'	C9'	C8'	O3'	123.9(2)
C6	O3	C8	C9	117.53(18)	C3	O2	C4	C5	-31.5(3)
C14'	C9'	C8'	O4'	59.8(3)	C3	C2	C7	O4	-157.83(15)
C14'	C9'	C8'	O3'	-57.8(3)	C3	C2	C7	C6	-42.5(2)
C14'	C9'	C10'	C11'	-0.2(4)	C4	O2	C3	C2	85.9(2)
C7'	O4'	C8'	O3'	-30.00(17)	C14	C9	C10	C11	0.3(4)
C7'	O4'	C8'	C9'	-150.72(15)	C14	C9	C8	O4	76.5(3)
C7'	C2'	C3'	O2'	-46.0(2)	C14	C9	C8	O3	-42.0(3)
C7'	C6'	C5'	C4'	-35.6(3)	C3'	O2'	C4'	C5'	-28.7(3)
C10	C9	C8	O4	-101.6(2)	C3'	C2'	C7'	O4'	-158.11(16)
C10	C9	C8	O3	140.0(2)	C3'	C2'	C7'	C6'	-42.9(2)
C10	C9	C14	C13	-0.5(4)	C5	C6	C7	O4	-156.27(16)
C10	C11	C12	C13	-1.3(4)	C5	C6	C7	C2	83.3(2)
C7	O4	C8	O3	-22.71(18)	C13'	C12'	C11'	C10'	-1.0(4)
C7	O4	C8	C9	-144.22(15)	C11'	C12'	C13'	C14'	0.4(4)

Table 7 Hydrogen Atom Coordinates (Å×10^4) and Isotropic Displacement Parameters (Å^2×10^3) for AJE-01-190.

Atom	*x*	*y*	*z*	U(eq)
H1'	11374	8488	5515	27
H1	6015	5982	5896	30
H2'	10597	7997	7322	16
H6	6414	3147	5734	17
H14'	10835	6462	2811	23
H7'	9371	6306	6781	15
H10	1614	4007	3212	21
H2	5437	5514	7828	20
H7	4295	3773	7361	17
H11	1582	4423	1019	26
H12	3585	4307	-30	26
H8'	7929	5818	4598	17
H8	2713	3280	5128	18
H6'	11612	5580	5360	16
H4'	11256	4093	8568	24
H10'	6752	6042	2608	25
H5'	10810	3665	6530	21
H3A	7686	3943	7526	24
H3B	7584	4924	8625	24
H4	6519	1654	9007	24
H14	5684	3438	3339	22
H3'A	12764	6303	7182	23
H3'B	12643	7296	8265	23
H12'	8627	6837	-591	29
H5	5944	1200	6994	22
H13	5638	3847	1140	25
H13'	10725	6850	609	28
H11'	6638	6467	402	32

Experimental

Single crystals of $C_{13}H_{14}O_4$ [AJE-01-190] were [THF:Pentane vapor diffusion]. A suitable crystal was selected and [The crystal was mounted on a loop with paratone oil] on a 'Bruker APEX-II CCD' diffractometer. The crystal was kept at 100(2) K during data collection. Using Olex2 [1], the structure was solved with the XT [2] structure solution program using Intrinsic Phasing and refined with the XL [3] refinement package using Least Squares minimisation.

1. Dolomanov, O.V., Bourhis, L.J., Gildea, R.J, Howard, J.A.K. & Puschmann, H. (2009), J. Appl. Cryst. 42, 339-341.
2. Sheldrick, G.M. (2015). Acta Cryst. A71, 3-8.
3. Sheldrick, G.M. (2008). Acta Cryst. A64, 112-122.

Crystal structure determination of [AJE-01-190]

Crystal Data for $C_{13}H_{14}O_4$ (M =234.24 g/mol): monoclinic, space group $P2_1$ (no. 4), a = 9.8776(16) Å, b = 11.2114(17) Å, c = 10.4484(16) Å, β = 94.542(2)°, V = 1153.4(3) Å^3, Z = 4, T = 100(2) K, μ(MoKα) = 0.100 mm^{-1}, *Dcalc* = 1.349 g/cm^3, 11534 reflections measured (3.91° ≤ 2Θ ≤ 61.462°), 5811 unique (R_{int} = 0.0300, R_{sigma} = 0.0434) which were used in all calculations. The final R_1 was 0.0435 (I > 2σ(I)) and wR_2 was 0.1102 (all data).

Refinement model description

Number of restraints - 1, number of constraints - unknown.

Details:

```
1. Fixed Uiso
 At 1.2 times of:
  All C(H) groups, All C(H,H) groups
 At 1.5 times of:
  All O(H) groups
2.a Ternary CH refined with riding coordinates:
 C2'(H2'), C6(H6), C7'(H7'), C2(H2), C7(H7), C8'(H8'), C8(H8), C6'(H6')
2.b Secondary CH2 refined with riding coordinates:
 C3(H3A,H3B), C3'(H3'A,H3'B)
2.c Aromatic/amide H refined with riding coordinates:
 C14'(H14'), C10(H10), C11(H11), C12(H12), C4'(H4'), C10'(H10'),
C5'(H5'),
 C4(H4), C14(H14), C12'(H12'), C5(H5), C13(H13), C13'(H13'), C11'(H11')
2.d Idealised tetrahedral OH refined as rotating group:
 O1'(H1'), O1(H1)
```

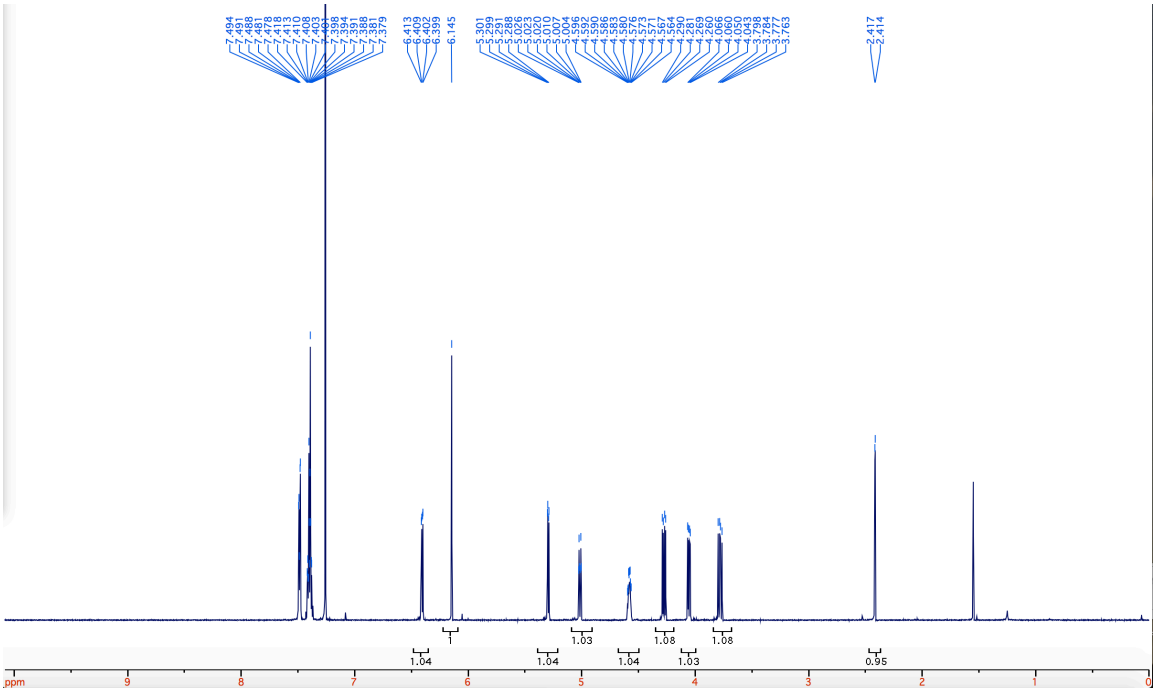

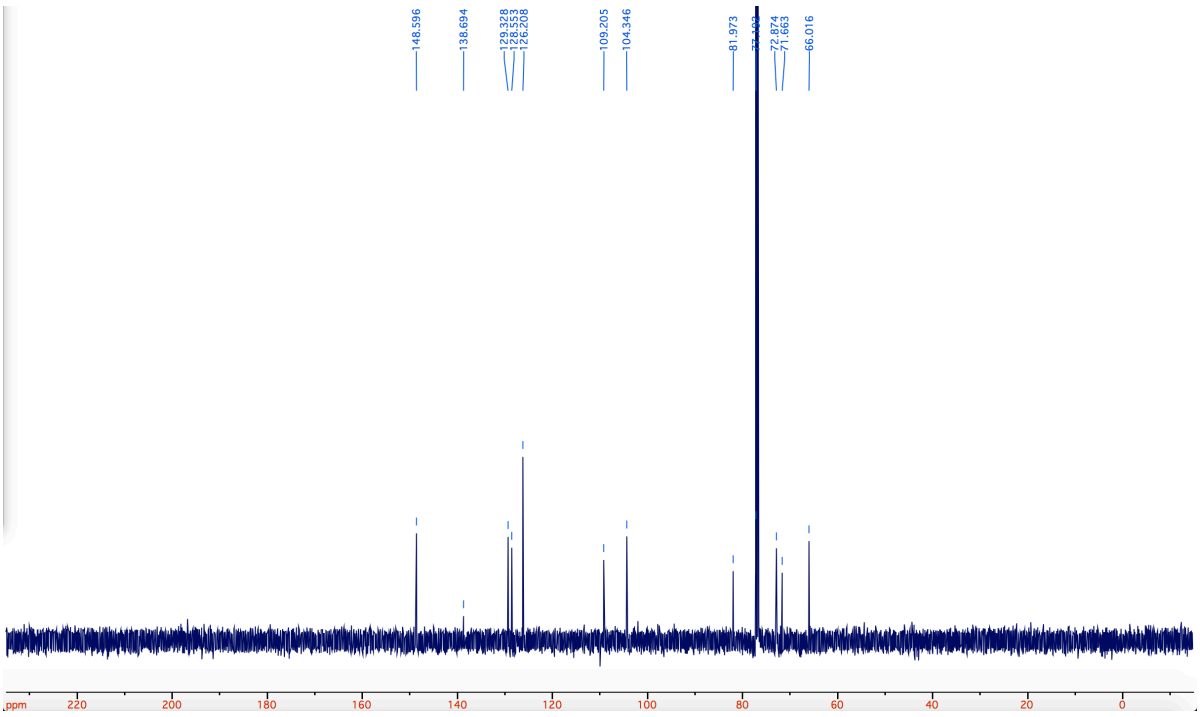

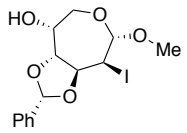

39

1-methoxy, 2-iodo septanose 39

To a solution of 28 mg of **35** (0.10 mmol) in 0.6 mL of methanol 58.3 mg of IDCP (0.10 mmol) was added and stirred. The reaction was allowed to proceed for 5 hours. After 5 hours the solution was concentrated in vacuo. The resulting solid was purified by silica gel flash column chromatography with 2:1 EtOAc:hexanes as the mobile phase yielding 31 mg (0.82 mmol, 82% yield) of the desired as a white solid. **^{1}H NMR** (600 MHz, Chloroform-*d*) δ 7.46 (dd, *J* = 4.3, 1.8 Hz, 2H), 7.43 – 7.27 (m, 3H), 6.16 (s, 1H), 4.75 (d, *J* = 6.7 Hz, 1H), 4.69 (dd, *J* = 6.7, 5.4 Hz, 1H), 4.30 (dd, *J* = 13.7, 1.7 Hz, 1H), 4.27 (d, *J* = 2.1 Hz, 1H), 4.18 (dd, *J* = 8.6, 2.2 Hz, 1H), 4.13 – 4.06 (m, 2H), 3.69 (dd, *J* = 13.6, 2.5 Hz, 1H), 3.41 (s, 3H).

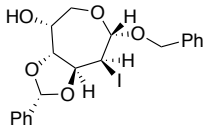

40

1-benzyl, 2-iodo septanose 40

To a solution of 42.4 mg of **39** (0.181 mmol) in 1 mL of MeCN 60 µL of benzyl alcohol (0.543 mmol) was added and stirred. Next the solution was placed in an ice bath under argon, and 61 mg of NIS (0.272mmol) was added. The solution was then warmed to room temperature, and allowed to react for 4 hours. The solution was then concentrated in vacuo, redisolved in 5 mL of DCM and washed with sodium thiosulfate (3 x 5 mL). The organic layer was separated, dried over Na_2SO_4, filtered, and concentrated. The resulting solid was purified by silica gel flash column chromatography with 3:1 EtOAc:hexanes as the mobile phase yielding 47.4 mg (0.101 mmol, 56% yield) of a white solid. **^{1}H NMR** (600 MHz, Chloroform-*d*) δ 7.47 (ddd, *J* = 5.3, 3.1, 1.8 Hz, 2H), 7.41 – 7.35 (m, 7H), 6.16 (s, 1H), 4.85 – 4.79 (m, 2H), 4.79 – 4.75 (m, 1H), 4.52 (d, *J* = 11.9 Hz, 1H), 4.35 – 4.29 (m, 1H), 4.26 (t, *J* = 2.1 Hz, 1H), 4.18 – 4.12 (m, 2H), 3.59 (dt, *J* = 13.7, 2.3 Hz, 1H). **^{13}C NMR** (126 MHz, cdcl$_3$) δ 136.9, 136.2, 129.8, 128.6, 128.5, 128.4, 128.2, 126.6, 110.0, 104.7, 104.7, 81.2, 72.1, 71.5, 70.1, 67.9, 36.5. **HRMS** calculated for $C_{20}H_{22}IO_5Na$ (mass +Na) 491.0326; found: 491.0328

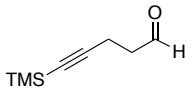

78

Aldehyde 78

To a solution of **79** (312.6 mg, 2.0 mmol) in 10 mL of MeCN in a 50 mL round bottomed flask (RBF) was added 5 mol% (0.1 mmol) of [Cu(MeCN)$_4$], TEMPO, and 2,2'-bipyridyl, along with 10 mol% (0.2 mmol) N-methylimidazole sequentially turning the solution dark red in color. The reaction mixture was then stirred open to air for 8 hours during which time the solution turned green. The reaction was then quenched via addition of 50 mL of H_2O. The reaction mixture was then transferred to a 250 mL separatory funnel and washed 2 times with 50 mL of pentane. The pentane extracts were then washed with brine, transferred to a flask, and dried over $MgSO_4$. The solution was then filtered, transferred to a 250 mL RBF, and concentrated in vacuo resulting in 258.2mg (1.62 mmol, 80.9%) of the desired products as a light red oil requiring no further purification. **^{1}H NMR** (600 MHz, Chloroform-*d*) δ 9.91 (s, 1H) 2.80 (t, J = 6.9 Hz, 2H) 2.66 (t, J = 6.9 Hz, 2H) 0,257 (s, 9H)

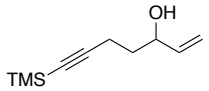

80

Allylic alcohol 80

To a 10 mL oven dried RBF equipped with a stir bar under argon, was added 258.2 mg (1.62 mmol) of **78** in 3 mL of THF. The solution was then cooled to -78 °C via dry ice bath, and 2.6 mL (2.6 mmol) of 1M vinyl magnesium bromide solution in THF was added dropwise. The solution was then stirred at -78 °C for 1 hr. The solution was then quenched with 3 mL of concentrated NH_4^+, transferred to a separatory funnel, and extracted 3X with 10 mL of Et_2O. The combined organics were then dried over $MgSO_4$, filtered, and concentrated in vacuo. The resulting yellow oil was then purified via silica gel column chromatography affording 154 mg (0.872 mmol, 52.2%) of the desired product as a clear, colorless oil. **^{1}H NMR** (600 MHz, Chloroform-*d*) δ 5.92 (ddd, *J* = 17.0, 10.6, 6.2 Hz, 1H) 5.32 (dt, *J* = 17.2, 1.4 Hz, 1H) 5.18 (dt, *J* = 10.4, 1.3 Hz, 1H) 4.31 (t, *J* = 11.0 Hz, 1H) 2.39 (q, *J* = 6.9 Hz, 2H) 1.80 (t, *J* = 7.0 Hz, 2H) 0.198 (s, 9H)

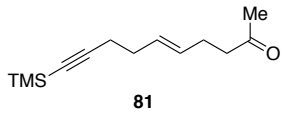

81

Methyl ketone 81

To a 20 mL sealed tube equipped with a stir bar was added 400 mg (2.2 mmol) of **80** in 2 mL (20.8 mmol) of 2-methoxypropene with 5 drops of propionic acid under a flow of argon. Next the tube was sealed, placed behind a blast shield, and the reaction heated to 150 °C via an oil bath. The reaction was allowed to proceed for 6hrs, cooled to room temperature, and diluted with pentane. The reaction mixture was then transferred to a separatory funnel, and washed once with $NaHCO_3$ and once with H_2O.The combined organics were then dried over $MgSO_4$, and concentrated in vacuo. The oil was then purified via silica gel column chromatography affording 167.8 mg (0.755 mmol, 34.3%) of the desired product as a clear, colorless oil. **^{1}H NMR** (600 MHz, Chloroform-*d*) δ 5.42-5.40 (m, 2H) 2.44 (t, *J* = 7.4 Hz, 2H) 2.23-2.20 (m, 2H) 2.18 (d, *J* = 6.4 Hz, 2H) 2.13 (t, *J* = 5.5 Hz, 2H) 2.08 (s, 3H), 0.083 (s, 9H)

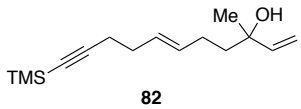

82

Tertiary alcohol 82

To a 10 mL oven dried RBF equipped with a stir bar under argon, was added 316.1 mg (1.42 mmol) of **81** in 3 mL of THF. The solution was then cooled to -78 °C via a dry ice bath, and 2.2 mL (2.2mmol) of 1M vinylmagnesium bromide solution in THF was added dropwise. The solution was then stirred at -78 °C for 1 hr. the solution was then quenched with 3 mL of concentrated NH_4^+, transferred to a separatory funnel, and extracted 3X with 10 mL of Et_2O. The combined organics were then dried over $MgSO_4$, filtered, and concentrated in vacuo. The resulting oil was then purified via silica gel column chromatography affording 109 mg (0.438 mmol, 30.8%) of the desired product as a clear, colorless oil. **^{1}H NMR** (600 MHz, Chloroform-*d*) δ 5.88 (dd, *J* = 17.3, 10.8, Hz, 1H) 5.47-5.44 (m, 2H) 5.19 (d, *J* = 17.3 Hz, 1H) 5.03 (d, *J* = 10.8 Hz, 1H) 2.23 (t, *J* = 7.0 Hz,

2H) 2.17 (t, *J* = 6.0 Hz, 2H) 2.05-2.02 (m, 2H) 1.60-1.56 (m, 2H) 1.26 (s, 3H), 0.110 (s, 9H)

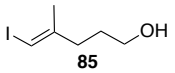

85

Vinyl iodide 85

To a flame dried 500 ml RBF equipped with a stir bar was added 3.47 g (11.9 mmol) of cp_2ZrCl_2 under argon. Next 60 mL of dry DCM was added and stirred. To the suspension was added 37 mL (71.3 mmol) of 2M Me_3Al in heptane dropwise at room temperature evolving a white gas. The solution was then cooled to 0 °C via ice bath and 2 g (23.76 mmol) of **84** was added dropwise evolving more white gas. The ice bath was then removed, and the reaction was allowed to proceed over night. After 16 hours the reaction mixture was cooled to 0 °C and 7.24g (28.52 mmol) of I_2 dissolved in 36 ml of dry THF was added. After 30 minutes the reaction was quenched via addition of 80 mL of H_2O dropwise evolving more white gas. Next the solution was transferred to a separatory funnel, and the aqueous layer extracted 3X with 100 mL of EtOAc. The combined organics were then washed with brine, and dried over $MgSO_4$. The solution was then filtered, concentrated in vacuo, and purified via silica gel column chromatography. The desired product was obtained as 4.57 g (20.20 mmol, 85.0%) as a clear colorless oil. The material must be used immediately because upon standing for greater than 24 hrs the oil turns dark black due to decomposition. **^{1}H NMR** (600 MHz, Chloroform-*d*) δ 5.87 (s, 1H) 3.56 (t, *J* = 6.4 Hz, 2H) 2.26-2.23 (m, 2H) 1.80 (s, 3H) 1.66-1.62 (m, 2H)

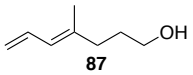

87

Diene 87

To an oven dried 250 mL RBF equipped with a stir bar under argon was added 411.4 mg (0.356 mmol) of $Pd(PPh_3)_4$. Next 1.60 g (7.12 mmol) of **85** was added at 0 °C and stirred for 20 minutes. Next, 21.5 mL (21.5 mmol) of vinyl magnesium bromide was added dropwise and stirred for an additional 30 minutes. The reaction was then quenched with NH_4^+ solution and diluted with 60 mL of H_2O. The solution was then extracted 3X with 50 mL of Et_2O, dried over $MgSO_4$, and concentrated in vacuo. The resulting solution was then filtered through a plug of silica and washed with hexanes to 20% Et_2O:hexanes. The filtrate was then concentrated in vacuo and purified by silica gel column chromatography yielding 470 mg (3.70 mmol, 52%) of the desired product as a clear colorless oil. **^{1}H NMR** (600 MHz, Chloroform-*d*) δ 6.57 (dt, *J* = 16.8, 10.5 Hz, 1H) 5.89 (d, *J* = 10.7 Hz, 1H) 5.10 (d, *J* = 16.8 Hz, 1H) 5.00 (d, *J* = 10.2 Hz, 1H) 3.64 (t, *J* = 5.8 Hz, 2H) 2.14 (t, *J* = 7.6 Hz, 2H) 1.77 (s, 3H) 1.72 (dt, *J* = 14.7, 7.2 Hz, 2H)

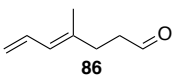

86

Aldehyde 86

To a solution of **87** (470 mg, 3.72 mmol) in 20 mL of MeCN in a 100 mL RBF was added 5 mol% (0.19 mmol) of $[Cu(MeCN)_4]$, TEMPO, and 2,2'-bipyridyl, along with 10 mol% (0.37 mmol) N-methylimidazole sequentially, turning the solution dark red in color. The reaction mixture was then stirred open to air for 8 hours during which time the solution turned green. The reaction was then quenched via addition of 50 mL of H_2O. The reaction mixture was then transferred to a 250 mL separatory funnel and washed 2 times with 50 mL of Et_2O. The Et_2O extracts were then washed with brine, transferred to a flask, and dried over $MgSO_4$. The solution was then filtered, transferred to a 250 mL RBF, and carefully concentrated in vacuo yielding 799.0 mg (3.72 mmol, 100%) of the desired product as a 45:55 solution in Et_2O as a light orange oil. The product was not concentrated further due to its high volatility. **^{1}H NMR** (600 MHz, Chloroform-*d*) δ 9.81 (s, 1H) 6.58 (dt, *J* = 16.8, 10.5 Hz, 1H) 5.89 (d, *J* = 10.8 Hz, 1H) 5.15 (d, *J* = 16.8 Hz, 1H) 5.05 (d, *J* = 10.1 Hz, 1H) 2.61 (t, *J* = 7.4 Hz, 2H) 2.42 (t, *J* = 7.5 Hz, 2H) 1.79 (s 3H)

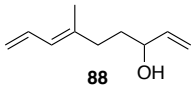

88

Allylic alcohol 88

To an oven dried 50 mL RBF equipped with a stir bar under argon was added 558.5 mg (2.6 mmol) of a 45:55 solution of **86**:Et_2O in 5 mL of THF. Next the solution was cooled to 0 °C and 4.0 mL (4.0 mmol) of 1M vinylmagnesium bromide in THF was added dropwise over 5 minutes. The reaction was allowed to proceed for 1 hour and quenched with 10 mL of concentrated NH_4^+. The reaction mixture was then transferred to a separatory funnel, and extracted 3X with 10 mL of Et_2O. The combined organics were then dried over $MgSO_4$, filtered, and concentrated in vacuo. The crude product was then purified via silica gel column chromatography in 4:1 hex:EtOAc yielding 173.8 mg (1.14 mmol,43.8%) of the desired product as a clear, colorless oil. **^{1}H NMR** (600 MHz, Chloroform-*d*) δ 6.55 (dt, *J* = 16.8, 10.5 Hz, 1H) 5.85 (ddd, *J* = 17.1, 10.9, 6.3 Hz, 2H) 5.21 (dt, *J* = 17.2, 1.4 Hz, 1H) 5.09 (dt, *J* = 8.9, 1.5 Hz, 1H) 5.07 (dd, *J* = 13.7, 1.6 Hz, 1H) 4.96 (dd, *J* = 10.2, 1.7 Hz, 1H) 2.19-2.08 (m, 2H) 1.85-1.81 (m, 1H) 1.75 (s 3H) 1.69-1.62 (m, 2H)

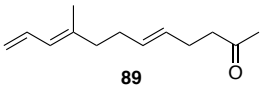

89

Methyl ketone 89

To an oven dried 20 mL sealed tube equipped with a stir bar was added 84.9 mg (0.558 mmol) of **88** in 1 mL (10.4 mmol) of 2-methoxypropene with 3 drops of propionic acid under a flow of argon. Next the tube was sealed, placed behind a blast shield, and the reaction heated to 150 °C via oil bath. The reaction was allowed to proceed for 3 hours, cooled to room temperature, and diluted with pentane. The reaction mixture was then transferred to a separatory funnel, and washed with once $NaHCO_3$ and once with H_2O. The combined organics were then dried over $MgSO_4$, and concentrated in vacuo yielding 61.2 mg (0.367 mmol, 62.4%) of the desired product as a light yellow oil with no further purification required. **^{1}H NMR** (600 MHz, Chloroform-*d*) δ 6.55 (dt, *J* = 16.8, 10.5 Hz, 1H) 5.82 (d, *J* = 10.9 Hz, 1H) 5.40 (q, *J* = 4.8, Hz, 2H) 5.07 (dd, *J* = 16.8, 1.8 Hz, 1H)

4.97 (d, *J* = 10.0, 1.5 Hz, 1H) 2.46 (d, *J* = 7.4 Hz, 2H) 2.26-2.22 (m, 2H) 2.11 (s, 3H) 2.08 (dt, *J* = 7.8, 3.8 Hz, 4H) 1.73 (s, 3H)

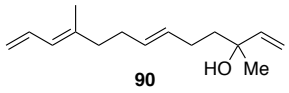

90

Tertiary alcohol 90

To an oven dried 10 mL RBF equipped with a stir bar under argon was added 56.5 mg (0.294 mmol) of **89** in 1 mL of THF. Next the solution was cooled to 0 °C and 0.441 mL (0.441mmol) of 1M vinylmagnesium bromide in THF was added dropwise over 5 minutes. The reaction was allowed to proceed for 1 hour and quenched with 2 mL of concentrated NH_4^+. The reaction mixture was then transferred to a separatory funnel, and extracted 3X with 5 mL of Et_2O. The combined organics were then dried over $MgSO_4$, filtered, and concentrated in vacuo. The crude product was then purified via silica gel column chromatography in 4:1 hex:EtOAc yielding 28.7 mg (0.13 mmol, 44.3%) of the desired product as a clear, colorless oil. **^{1}H NMR** (600 MHz, Chloroform-*d*) δ 6.56 (dt, *J* = 16.9, 10.5 Hz, 1H) 5.89 (dd, *J* = 17.4, 10.8 Hz, 1H) 5.42 (d, *J* = 4.4, Hz, 2H) 5.20 (d, *J* = 17.3 Hz, 1H) 5.09 (d, *J* = 16.9, Hz, 1H) 5.05 (d, *J* = 10.7) 4.97 (d, *J* = 10.2 Hz, 1H) 2.12-2.07 (m, 4H) 2.04-2.01 (m, 2H) 1.74 (s, 3H) 1.59 (dtd, *J* = 13.5, 6.8, 3.1 Hz, 2H) 1.26 (s, 3H)

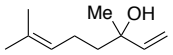

92

Tertiary alcohol 92

To an oven dried 100 mL RBF equipped with a stir bar under argon was added 0.54 mL (631 mg, 5 mmol) of **91** in 20 mL of THF. Next 7.5 mL (7.5 mmol) of 1M vinylmagnesium bromide in THF was added dropwise over 5 minutes. The reaction was allowed to proceed for 1 hour and quenched with 40 mL of concentrated NH_4^+. The reaction mixture was then transferred to a separatory funnel, and extracted 3X with 100 mL of Et_2O. The combined organics were then dried over $MgSO_4$, filtered, and concentrated in vacuo. The crude product was then purified via silica gel column chromatography in 3:1 hex:EtOAc yielding 414 mg (2.69 mmol, 53.7%) of the desired product as a clear, colorless oil. **^{1}H NMR** (600 MHz, Chloroform-*d*) δ 5.96 (dd, *J* = 17.3, 10.7 Hz, 1H) 5.26 (dd, *J* = 17.3, 1.3 Hz, 1H) 5.17 (tt, *J* = 7.2, 1.4 Hz, 1H) 5.10 (dd, *J* = 10.7, 1.3 Hz, 1H) 2.07 (dt, *J* = 16.4, 8.2 Hz, 2H) 1.72 (s, 3H) 1.65 (s, 3H) 1.61 (dt, *J* = 9.9, 6.4 Hz, 2H) 1.32 (s, 3H)

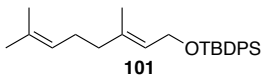

101

TBDPS protected geraniol 101

To a solution of 10 g (11.3 mL, 64.83 mmol) geraniol **95** in 130 mL THF in a 500 mL RBF was added 5.3 g (77.8 mmol) imidazole and 21.4 g (77.8 mmol) TBDPS chloride at 0 °C. the solution was then stirred for 3 hours at room temperature. The reaction was then quenched with 200 mL of H_2O, transferred to a sepratory funnel, and extracted 3X with 100 mL Et_2O. The combined organics were then dried over $MgSO_4$, filtered, and concentrated in vacuo yielding 25.45 g (64.83 mmol, 100%) of the desired product as a clear colorless oil with no further purification required. **^{1}H NMR** (600 MHz, Chloroform-*d*) δ 7.73-7.69 (m, 4H) 7.42-7.35 (m, 6H) 5.39 (td, *J* = 6.3, 1.2 Hz, 1H) 5.12-5.08 (m, 1H) 4.23 (d, *J* = 6.3 Hz, 2H) 3.74 (t, *J* = 6.5 Hz, 2H) 2.06 (t, *J* = 7.6 Hz, 2H) 1.98 (t, *J* = 7.5 Hz, 2H) 1.69 (s, 3H) 1.61 (s, 3H) 1.44 (s, 3H) 1.05 (s, 9H)

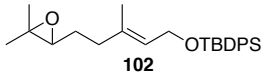

102

Epoxide 102

To a solution of 10 g (25.47 mmol) **101** in 90 mL of DCM in a 500 mL RBF was added 5.27 g (30.56 mmol) m-CPBA in 90 mL of DCM with stirring under argon. The reaction was allowed to proceed for 1 hour. The reaction was then filtered, and 7.5 g of calcium hydroxide was added to the solution. The reaction mixture was then allowed to stir for an additional hour and was then filtered and concentrated in vacuo. The oil was then purified via silica gel column chromatography in 7:1 hex:EtOAc yielding 5.44 g (13.3 mmol, 52.3%) of the desired product as a clear, colorless oil. **^{1}H NMR** (600 MHz, Chloroform-*d*) δ 7.74-7.71 (m, 4H) 7.45-7.37 (m, 6H) 5.43 (t, *J* = 5.7 Hz, 1H) 4.24 (d, *J* = 6.2 Hz, 2H) 2.72 (t, *J* = 6.3 Hz, 1H) 2.40 (d, *J* = 6.2 Hz, 2H) 2.15 (dt, *J* = 14.1, 7.3 Hz, 1H) 2.09 (q, *J* = 7.3 Hz, 1H) 1.47 (s, 3H) 1.31 (s, 3H) 1.26 (s, 3H) 1.06 (s, 9H)

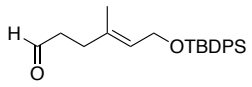

103

Aldehyde 103

To a solution of 2.0 g (4.89 mmol) of **102** in 18 mL of THF in a 100 mL RBF equipped with a stir bar was added 2.11 g (9.80 mmol) of H_5IO_6 in 11 mL of H_2O at 0 °C and stirred. After 30 minutes 27 mL of concentrated $NaHCO_3$ solution was added. The solution was then transferred to a sepratory funnel and extracted 2X with 50 mL of Et_2O. The combined organics were then dried over $MgSO_4$, filtered, and concentrated in vacuo yielding 1.50 g (4.08 mmol, 83.5%) of the desired product as a clear, colorless oil. **^{1}H NMR** (600 MHz, Chloroform-*d*) δ 9.73 (t, *J* = 1.7 Hz, 1H) 7.72-7.66 (m, 5H) 7.42-7.38 (m, 5H) 5.38 (td, *J* = 6.2, 1.3 Hz, 1H) 4.21 (d, *J* = 6.2 Hz, 2H) 2.49 (td, *J* = 7.5, 1.7 Hz, 2H) 2.28 (t, *J* = 7.5 Hz, 2H) 1.44 (s, 3H) 1.03 (s, 9H)

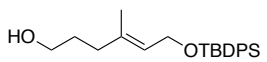

96

Alcohol 96

To a solution of 1.50 g (4.08 mmol) of **103** in 75 mL of EtOH in a 250 mL RBF equipped with a stir bar at 0 °C was added 323 mg (8.20 mmol) of $NaBH_4$ and stirred. After 1 hour, the solution was concentrated, and 90 mL of $NaHCO_3$ was added. The mixture was then transferred to a sepratory funnel and extracted 2X with 100 mL of EtOAc. The combined organics were then dried over $MgSO_4$ and concentrated in vacuo. The crude oil was then purified via silica gel column chromatography in 3:1 hex:EtOAc yielding 943 mg (2.57 mmol 63.0%) of the desired product as a clear colorless oil. **^{1}H NMR** (600 MHz, Chloroform-*d*) δ 7.67-7.65 (m, 5H) 7.41-7.35 (m, 5H) 5.40 (td, *J* = 6.3, 1.1 Hz, 1H) 4.20 (d, *J* = 6.3 Hz, 2H) 3.60 (t, *J* = 7.6 Hz, 2H) 2.03 (t, *J* = 7.6 Hz, 2H) 1.64 (dt, *J* = 14.4, 7.0 Hz, 2H) 1.44 (s, 3H) 1.03 (s, 9H)

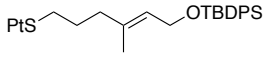

104

Sulfide 104

To a solution of 943 mg (2.57 mmol) of **96** in 23 mL of THF in a 100 mL RBF equipped with a stir bar under argon at 0 °C was added 882 mg (4.70 mmol) of phenyl tetrazol thiol (PtSH) and 1.26 g (4.67 mmol) of PPH_3 were added. Next 1.0 mL (1.01 g, 5.02 mmol) DIAD was added dropwise over 5 minutes and the reaction was allowed to warm to room temperature over 1 hour. After 1 hour, the reaction mixture was diluted with 20 mL of Et_2O and quenched with 15 mL of $NaHCO_3$. The mixture was then transferred to a sepratory funnel and the aqueous layer extracted 2X with 50 mL of Et_2O. The combined organics were then dried over $MgSO_4$, filtered, and concentrated in vacuo. The resultant crude oil was then purified via silica gel column chromatography in 9:1 hex:EtOAc yielding 1.10 g (2.10 mmol, 81.5%) of the desired product as a clear, colorless oil. **^{1}H NMR** (600 MHz, Chloroform-*d*) δ 7.73-7.67 (m, 5H) 7.60-7.54 (d, *J* = 7.5 Hz, 3H) 7.41-7.37 (m, 7H) 5.40 (td, *J* = 6.2, 1.2 Hz, 1H) 4.22 (d, *J* = 6.2 Hz, 2H) 3.3 (t, *J* = 7.3 Hz, 2H) 2.12 (t, *J* = 7.2 Hz, 2H) 1.92 (quin, *J* = 7.3 Hz, 2H) 1.44 (s, 3H) 1.04 (s, 9H)

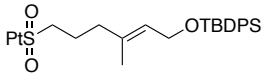

97

Sulfone 97

To a solution of 1.10 g (2.10 mmol) of **104** in 21 mL of EtOH in a 100 mL RBF equipped with a stir bar was added 773 mg (0.626 mmol) of ammonium molybdate at 0 °C. Next 2.14 mL (20.9 mmol) of 30% H_2O_2 was added dropwise. The mixture was then warmed to room temperature and allowed to react for 16 hours. The reaction was then quenched with 50 mL of H_2O. The reaction mixture was then transferred to a sepratory funnel and extracted 2X with 50 mL of Et_2O. The combined organics were then dried over $MgSO_4$, filtered, and concentrated in vacuo. The crude product was then purified via silica gel column chromatography in 4:1 hex:EtOAc yielding 527 mg (0.86 mmol, 41.1%) of the desired product as a clear, colorless oil. **^{1}H NMR** (600 MHz, Chloroform-*d*) δ 7.67-7.65 (m, 5H) 7.60 (d, *J* = 7.5 Hz, 3H) 7.40-7.36 (m, 7H) 5.40 (td, *J* = 6.2, 1.0 Hz, 1H) 4.20 (d, *J* = 6.2 Hz, 2H) 3.65-3.61 (m, 2H) 2.15 (t, *J* = 7.24 Hz, 2H) 2.04 (dt, *J* = 15.1, 7.5 Hz,

2H) 1.43 (s, 3H) 1.02 (s, 9H) **HRMS** calculated for $C_{30}H_{37}O_3N_4SSi$ (mass +1) 561.23501; found: 561.23550

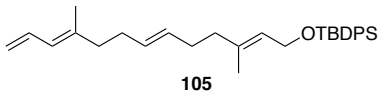

105

Tetraene 105

To a solution of 527 mg (0.94 mmol) of sulfone **97** in 6.3 mL dimethoxy ethane (DME) in a 50 mL RBF equipped with a stir bar under argon was added 1.41 mL (3.53 mmol) of 2.5M KHMDS in THF at -78 °C. The reaction was allowed to run for 30 minutes and then 201 mg (0.939 mmol) of a 45:55 solution of **86**:Et_2O was added dropwise. The reaction was then stirred for 2 hours and quenched with concentrated NH_4Cl solution. The reaction mixture was then transferred to a sepratory funnel and extracted 3X with EtOAc. The combined organics were then dried over $MgSO_4$, filtered, and concentrated in vacuo. The crude oil was then purified via silica gel column chromatography in 2% EtOAc in hexanes affording 137.8 mg (0.30 mmol, 32.0%) of the desired product as a clear colorless oil. **^{1}H NMR** (600 MHz, Chloroform-*d*) δ 7.71 (dd, *J* = 7.8, 1.3 Hz, 4H) 7.44-7,37 (m, 6H) 6.58 (dt, *J* = 16.8, 10.5 Hz, 1H) 5.86 (d, *J* = 10.9 Hz, 1H) 5.42 (dt, *J* = 4.6, 2.3 Hz, 2H) 5.39 (td, *J* = 6.2, 1.0 Hz, 1H) 5.10 (dd, *J* = 16.8, 1.9 Hz, 1H) 4.99 (dd, *J* = 10.1, 1.7 Hz, 1H) 4.23 (d, *J* = 6.3 Hz, 2H) 2.11 (td, *J* = 7.5, 3.8 Hz, 4H) 2.08 (dt, *J* = 8.5, 4.0 Hz, 2H) 2.02 (t, *J* = 7.4 Hz, 2H) 1.76 (s, 3H) 1.44 (s, 3H), 1.06 (s, 9H) **HRMS** calculated for $C_{31}H_{41}OSi$ (mass +1) 457.29212; found: 457.29209

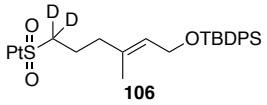

106

Deuterated sulfone 106

To a solution of 60 mg (0.11 mmol) of **97** in 1 mL of DME at -78 °C in a 10 mL RBF equipped with a stir bar under argon was added 0.1 mL (0.25 mmol) of 2.5M KHMDS. After 30 minutes the solution was quenched with D_2O and transferred to a sepratory funnel. The reaction mixture was extracted with EtOAC. The combined organics were then dried over $MgSO_4$, filtered, and concentrated in vacuo with no further purification. ^{1}H NMR showed the doubly deuterated product. **^{1}H NMR** (600 MHz, Chloroform-*d*) δ 7.67-7.65 (m, 5H) 7.60 (d, *J* = 7.5 Hz, 3H) 7.40-7.36 (m, 7H) 5.43 (td, *J* = 6.2, 1.0 Hz, 1H) 4.24 (d, *J* = 6.1 Hz, 2H) 2.16 (t, *J* = 7.2 Hz, 2H) 2.04 (dt, *J* = 15.1, 7.5 Hz, 2H) 1.43 (s, 3H) 1.02 (s, 9H)

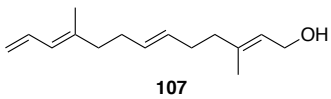

107

Alcohol 107

To a solution of 137.8 mg (.300 mmol) of **105** in 2.6 mL THF in a 25 mL RBF under argon equipped with a stir bar was added 0.45 mL (0.45 mmol) 1M TBAF solution in THF at room temperature. After 2 hours, the solution was quenched with 2 mL concentrated ammonium chloride solution. The solution was then transferred to a sepratory funnel and the aqueous layer was extracted 3X with Et_2O. The combined organics were then dried over $MgSO_4$, filtered, and concentrated in vacuo. The crude oil was then purified via silica gel column chromatography in 4:1 hex:EtOAc to afford 32.4 mg (0.147, 49%) of the desired product as a clear colorless oil. **^{1}H NMR** (600 MHz, Chloroform-*d*) δ 6.57 (dt, *J* = 16.9, 10.5 Hz, 1H) 5.84 (d, *J* = 10.9 Hz, 1H) 5.42-5.39 (m, 3H) 5.09 (dd, *J* = 16.8, 2.0 Hz, 1H) 4.98 (dd, *J* = 10.2, 1.9 Hz, 1H) 4.15 (d, *J* = 6.9 Hz, 2H) 2.11-2.04 (m, 8H) 1.75 (s, 3H) 1.66 (s, 3H)

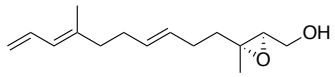

108

Epoxide 108

To a 10 mL vial equipped with a stir bar under argon was added 10 mg of 4A mol sieves, 4.1 mg (0.02 mmol) of (+) DET, and 4.7 mg (0.016 mmol) of $Ti(OiPr)_4$. The solution was then cooled to -20 °C and 53.5 µL (.294 mmol) of 5.5M tert butanol was added dropwise and stirred for 30 minutes. Next 36.2 mg (0.164 mmol) of **107** in 0.5 mL of DCM was added dropwise and the reaction allowed to stir over night at -20 °C. The reaction was then quenched via addition of 0.1 mL H_2O and 3 drops of concentrated NaOH solution in brine at 0 °C. After 15 minutes 2 layers formed and the aqueous phase was extracted 3X with 3 ml of DCM. The combined organic were then dried over $MgSO_4$, filtered, and concentrated in vacuo. The crude material was then purified via pipet column chromatography in 4:1 hex:EtOAC yielding 6.0 mg (0.025 mmol, 15.5%) of the desired product. **^{1}H NMR** (600 MHz, Chloroform-*d*) δ 6.57 (dt, *J* = 16.8, 10.5 Hz, 1H) 5.84 (d, *J* = 10.4 Hz, 1H) 5.42-5.40 (m, 2H) 5.08 (dd, *J* = 16.8, 2.0 Hz, 1H) 4.98 (dd, *J* = 10.12, 1.7 Hz, 1H) 3.82 (dd, *J* = 12.1, 4.1 Hz, 1H) 3.68 (dd, *J* = 12.1, 6.7 Hz, 2H) 2.96 (dd, *J* = 6.7, 4.3 Hz, 1H) 2.13-2.08 (m, 9H) 1.74 (s, 3H) 1.29 (s, 3H)

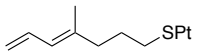

109

Sulfide 109

To a solution of 1.08g (8.57 mmol) of **87** in 51.2 mL of THF in a 250 mL RBF equipped with a stir bar under argon at 0 °C was added 1.83 g (10.28 mmol) of PtSH and 2.70 g (10.28 mmol) of PPH_3 were added. Next 2.3 mL (2.3g, 5.02 mmol) of DIAD was added dropwise over 5 minutes and the reaction was allowed to warm to room temperature over 1 hour. After 1 hour, the reaction mixture was diluted with 40 mL of Et_2O and quenched with 30 mL of $NaHCO_3$. The mixture was then transferred to a sepratory funnel and the aqueous layer extracted 2X with 100 mL of Et_2O. The combined organics were then dried over $MgSO_4$, filtered, and concentrated in vacuo. The resultant crude oil was then purified via silica gel column chromatography in 9:1 hex:EtOAc yielding 2.09 g (7.28 mmol, 85.0%) of the desired product as a clear, colorless oil. **^{1}H NMR** (600 MHz,

Chloroform-*d*) δ 7.59-7.54 (m, 5H) 6.55 (dt, *J* = 16.8, 10.5 Hz, 1H) 5.87 (d, *J* = 10.9 Hz, 1H) 5.10 (dd, *J* = 16.9, 1.4 Hz, 1H) 5.03 (dd, *J* = 10.2, 1.0 Hz, 1H) 3.36 (t, *J* = 7.3 Hz, 2H) 2.21 (t, *J* = 7.4 Hz, 2H) 2.21 (t, *J* = 7.4 Hz, 2H) 1.99 (quin, *J* = 7.4 Hz, 2H) 1.76 (s, 3H)

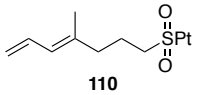

110

Sulfone 110

To a solution of 2.09 g (7.28 mmol) of **109** in 74 mL of EtOH in a 250 mL RBF equipped with a stir bar was added 2.70 g (2.19 mmol) of ammonium molybdate at 0 °C. Next 7.47 mL (72.8 mmol) of 30% H_2O_2 was added dropwise. The mixture was then warmed to room temperature and allowed to react for 16 hours. The reaction was then quenched with 100 mL of H_2O. The reaction mixture was then transferred to a sepratory funnel and extracted 2X with 100 mL of Et_2O. The combined organics were then dried over $MgSO_4$, filtered, and concentrated in vacuo. The crude product was then purified via silica gel column chromatography in 4:1 hex:EtOAc yielding 814 mg (2.21 mmol, 30.3%) of the desired product as a clear, colorless oil. **^{1}H NMR** (600 MHz, Chloroform-*d*) δ 7.67 (dd, *J* = 7.8, 1.8 Hz, 2H) 7.59, (td, *J* = 5.7, 2.3 Hz, 3H) 6.53 (dt, *J* = 16.8, 10.5 Hz, 1H) 5.87 (d, *J* = 10.9 Hz, 1H) 5.13 (dd, *J* = 16.8, 1.6 Hz, 2H) 5.03 (dd, *J* = 10.2, 1.4 Hz, 1H) 3.67 (m, 2H) 2.24 (t, *J* = 7.2 Hz, 2H) 2.10 (dt, *J* = 15.2, 7.6 Hz, 2H) 1.75 (s, 3H)

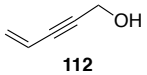

112

Alkene 112

To a 10.5 ml (10.5 mmol) 1M solution of vinyl bromide in THF in a 100 mL RBF equipped with a stir bar under argon was added 88 mg (0.45 mmol) of CuI, 30 mg (0.4 mmol) of $PdCl_2(PPH_3)_2$, and 2.96 mL (21 mmol) of iPr_2NH. The solution was then cooled to 0 °C and 0.58 mL (10 mmol) of **111** was added dropwise. The reaction was then allowed to warm to room temperature, and react for 24 hours. The reaction was then poured into 20 mL of a 2:1 mixture of saturated NH_4Cl:Et_2O. The mixture was then transferred to a sepratory funnel and the aqueous phase extracted 3X with 50 mL of Et_2O. The organics were then dried over $MgSO_4$, filtered, and concentrated in vacuo yielding 665.5 mg (8.1 mmol, 81%) of the desired product requiring no further purification. **^{1}H NMR** (600 MHz, Chloroform-*d*) δ 5.82 (dtd, *J* = 11.0, 1.9, 1.0 Hz, 1H) 5.64 (ddd, *J* = 17.6, 2.2, 0.57 Hz, 1H) 5.50-5.49 (ddt, *J* = 11.0, 2.2, 0.52 Hz, 1H) 4.37 (s, 2H)

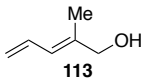

113

Diene 113

To a suspension of CuI in 3 mL THF in a 50 ml RBF equipped with a stir bar under argon was added 8.1 ml (24.3 mmol) of a 3M methyl magnesium bromide solution in Et_2O at 0 °C. To the suspension was added 665 mg (8.1 mmol) of **112** in 3 mL of THF over 10 minutes. The reaction mixture was then allowed to react overnight and quenched via dropwise addition of 13 mL of saturated NH_4Cl solution at 0 °C. The reaction mixture was then diluted with H_2O and the mixture transferred to a sepratory funnel. The aqueous layer was then extracted 3X with 25 mL of Et_2O. The organics were then dried over $MgSO_4$, filtered, and concentrated in vacuo yielding 631.7 mg (6.44 mmol, 79.5%) of the desired product requiring no further purification. **^{1}H NMR** (600 MHz, Chloroform-*d*) δ 6.58 (dt, *J* = 16.9, 10.6 Hz, 1H) 6.07 (ddt, *J* = 10.8, 1.7, 0.86 Hz, 1H) 5.20 (dd, *J* = 16.9 1.5 Hz, 1H) 5.10 (dt, *J* = 10.2, 0.65 Hz, 1H) 4.07 (d, *J* = 4.3 Hz, 2H) 1.78 (s, 3H)

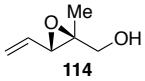

114

Epoxide 114

To 250 mL RBF equipped with a stir bar under argon was added 400 mg of 4Å mol sieves, 0.08 (0.48 mmol) of (-) DET, and 0.09 mL (0.30 mmol) of $Ti(OiPr)_4$. The solution was then cooled to -20 °C and 2.3 mL (12.6 mmol) of 5.5M tert butanol was added dropwise and stirred for 30 minutes. Next 631.7 mg (6.44 mmol) **113** in 20 mL of DCM was added dropwise and the reaction allowed to stir over night at -20 °C. The reaction was then quenched via addition of 4 mL H_2O and 2 mL of concentrated NaOH solution in brine at 0 °C. After 15 minutes 2 layers formed and the aqueous phase was extracted 3X with 60ml of DCM. The combined organic were then dried over $MgSO_4$, filtered, and concentrated in vacuo. The crude material was then purified via silica gel column chromatography in 4:1 hex:EtOAC yielding 282.6 mg (2.47mmol, 41.1%) of the desired product. **^{1}H NMR** (600 MHz, Chloroform-*d*) δ 5.76 (ddd, *J* = 17.4, 10.4, 7.2 Hz, 1H) 5.50 (dt, *J* = 17.2, 1.1 Hz, 1H) 5.39 (dt, *J* = 10.5, 0.65 Hz, 1H) 3.74 (dd, *J* = 12.3, 2.8 Hz, 1H) 3.65 (dd, *J* = 12.3, 8.5 Hz, 1H) 3.56 (d, *J* = 7.3 Hz, 1H) 1.29 (s, 3H)

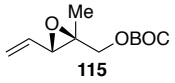

115

Boc protected alcohol 115

To a solution of 200 mg (1.75 mmol) **114** in 75 ml of DCM in a 250 mL RBF equipped with a stir bar under argon was added 3.66 mL (26.3 mmol) of Et_3N, and256.6 mg (2.1 mmol) of DMAP and cooled to 0 °C. Next 1.90 g (8.75 mmol) of BOC_2O was added dropwise. The reaction was allowed to proceed for 16 hours and then quenched with 50 mL of H_2O. The mixture was then transferred to a sepratory funnel and the aqueous phase extracted 3X with 50 mL of DCM. The organics were then dried over $MgSO_4$, filtered, and concentrated in vacuo. The crude material was then purified via silica gel column chromatography in 6:1 hex:EtOAC yielding 262.7 mg (1.22mmol, 70.0%) of the desired product. . **^{1}H NMR** (600 MHz, Chloroform-*d*) δ 5.71 (ddd, *J* = 17.3, 10.4, 7.0 Hz, 1H) 5.48 (dt, *J* = 17.2, 1.5 Hz, 1H) 5.38 (dt, *J* = 10.5, 1.50 Hz, 1H) 4.07 (app q, *J* = 10.8 Hz, 2H) 3.39 (d, *J* = 6.9 Hz, 1H) 1.54 (s, 3H) 1.47 (s, 9H)

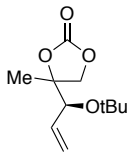

117

Carbonate ester 117

To a solution of **115** in 10ml of DCM in a 50 mL RBF equipped with a stir bar under argon at -40 °C was added $BF_3 \cdot THF$ dropwise. The reaction mixture was then stirred at -40 °C for 30 minutes and quenched with o.4 mL H_2O. Next the reaction mixture was warmed to room temperature, and transferred to a sepratory funnel. The aqueous layer was then extracted 3X with 25 mL of DCM. The organics were then dried over $MgSO_4$, filtered, and concentrated in vacuo. The crude material was purified via pipet column chromatography yielding 49.6 mg (0.232mmol, 38%) of the desired product as a 1.3:1 mixture of separable diastereomers.

Major diastereomer:

^{1}H NMR (600 MHz, Chloroform-*d*) δ 5.78 (ddd, *J* = 17.0, 10.8, 6.0 Hz, 1H) 5.50 (d, *J* = 17.2 Hz, 1H) 5.33 (d, *J* = 10.5 Hz, 1H) 4.54 (d, *J* = 8.1 Hz, 1H) 4.12 (d, *J* = 5.4 Hz, 1H) 3.86 (d, *J* = 8.2 Hz, 1H) 1.45 (s, 3H), 1.21 (s, 9H) **^{13}C NMR** (126 MHz, Chloroform-*d*) δ 155.0, 135.2, 119.4, 83.7, 75.7, 75.4, 70.1, 28.4, 22.5 **FT-IR** ν_{max}/cm^{-1} 2977 (CH), 1806 (CO) **HRMS** calculated for $C_{11}H_{19}O_4$ (mass +1) 215.1278; found: 215.1277

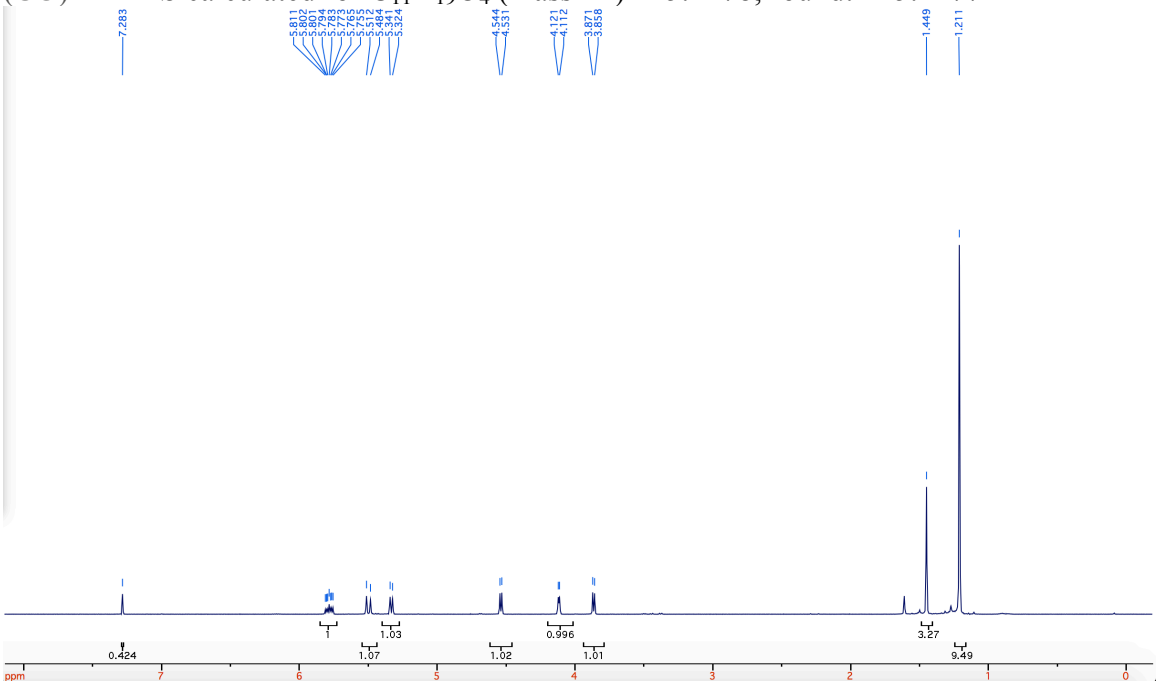

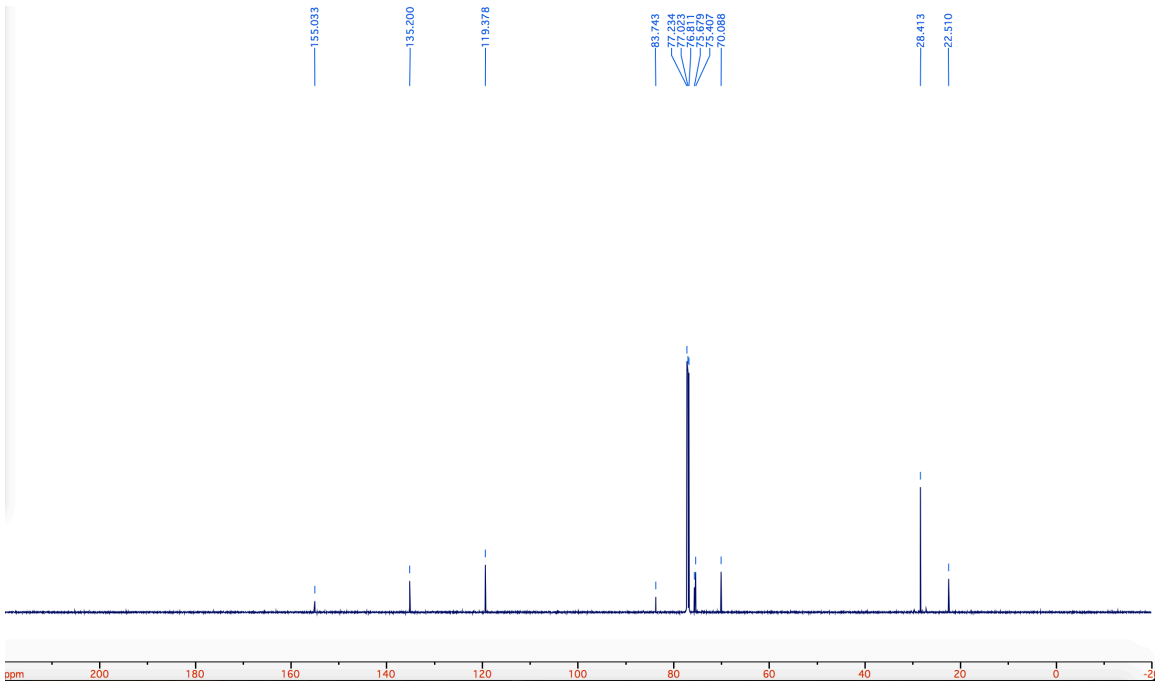
155.033
135.200
119.378
83.743
77.234
77.023
76.811
75.679
75.407
70.088
28.413
22.510
ppm
200
180
160
140
120
100
80
60
40
20
0

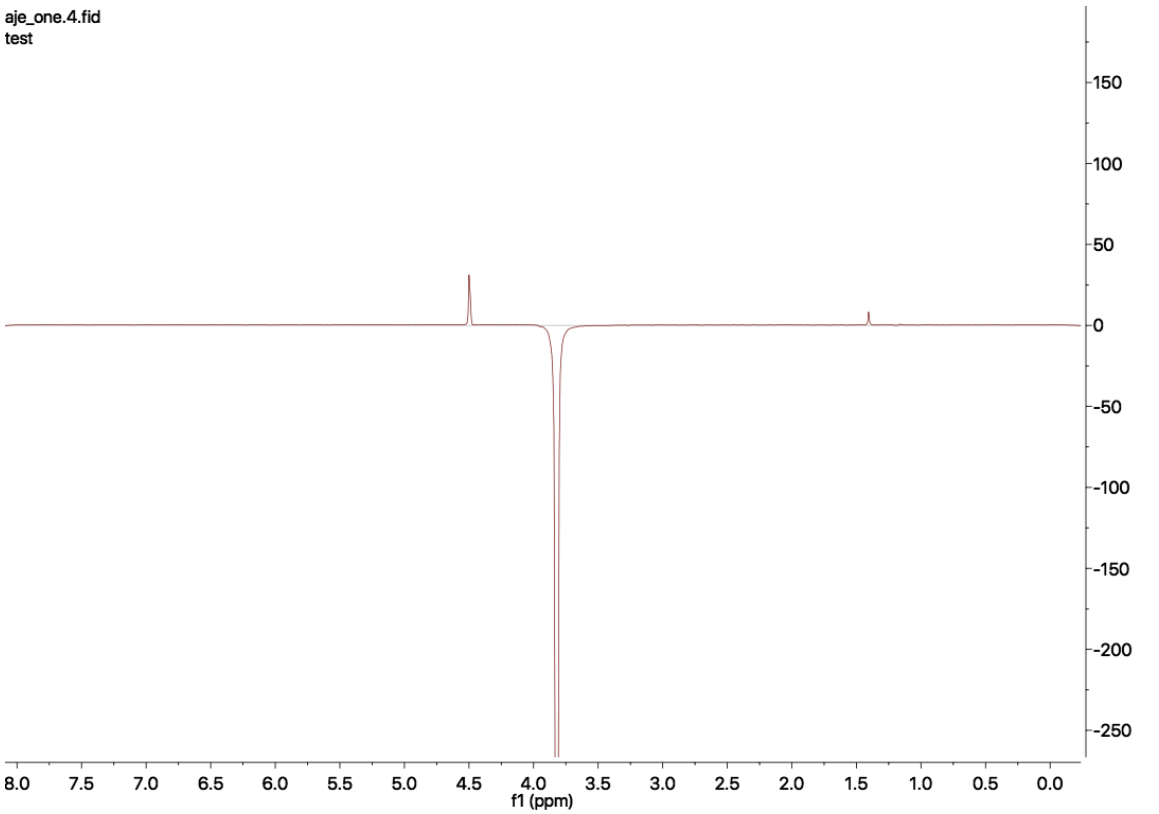
aje_one.4.fid
test
150
100
50
0
-50
-100
-150
-200
-250
8.0
7.5
7.0
6.5
6.0
5.5
5.0
4.5
4.0
3.5
3.0
2.5
2.0
1.5
1.0
0.5
0.0
f1 (ppm)

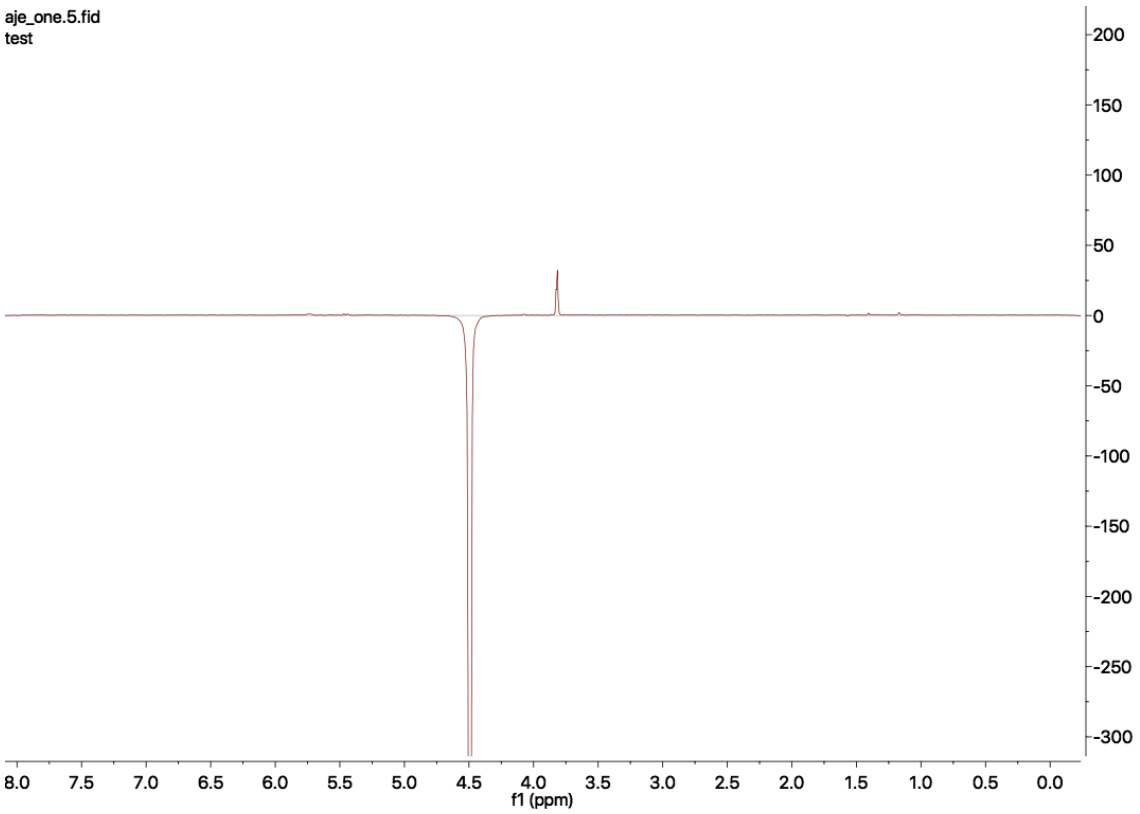
aje_one.5.fid
test
200
150
100
50
0
-50
-100
-150
-200
-250
-300
8.0
7.5
7.0
6.5
6.0
5.5
5.0
4.5
4.0
3.5
3.0
2.5
2.0
1.5
1.0
0.5
0.0
f1 (ppm)

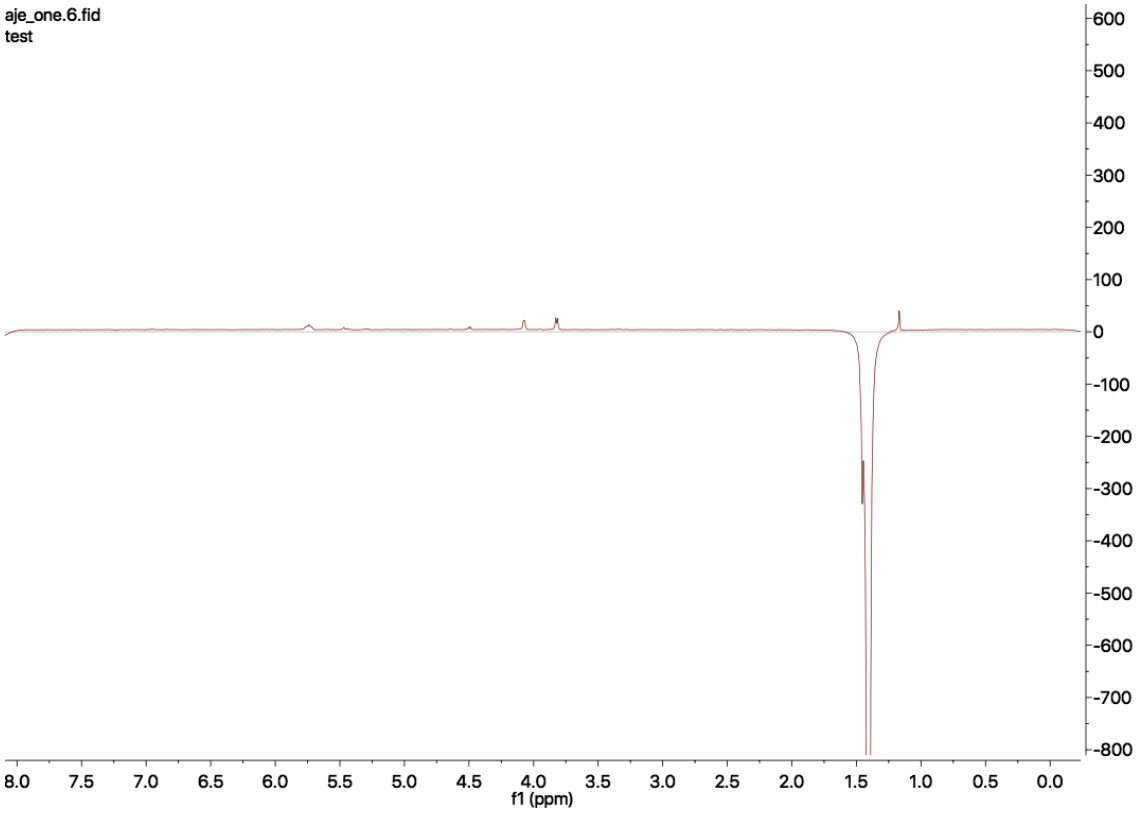
aje_one.6.fid
test
600
500
400
300
200
100
0
-100
-200
-300
-400
-500
-600
-700
-800
8.0
7.5
7.0
6.5
6.0
5.5
5.0
4.5
4.0
3.5
3.0
2.5
2.0
1.5
1.0
0.5
0.0
f1 (ppm)

Minor diastereomer:
^{1}H NMR (600 MHz, Chloroform-*d*) δ 5.95 (ddd, *J* = 17.3, 10.2, 7.3 Hz, 1H) 5.57 (d, *J* = 17.1 Hz, 1H) 5.50 (d, *J* = 10.5 Hz, 1H) 4.80 (d, *J* = 7.2 Hz, 1H) 4.19 (d, *J* = 12.0 Hz, 1H) 4.09 (d, *J* = 12.0 Hz, 1H) 1.56 (s, 4H), 1.50 (s, 10H) **^{13}C NMR** (126 MHz, Chloroform-*d*) δ 152.69, 128.64, 122.34, 85.34, 83.24, 83.15, 66.93, 27.65, 21.34 **FT-IR** ν_{max}/cm^{-1} 2977 (CH), 1807 (CO) **HRMS** calculated for $C_{11}H_{19}O_4$ (mass +1) 215.12779; found: 215.12785

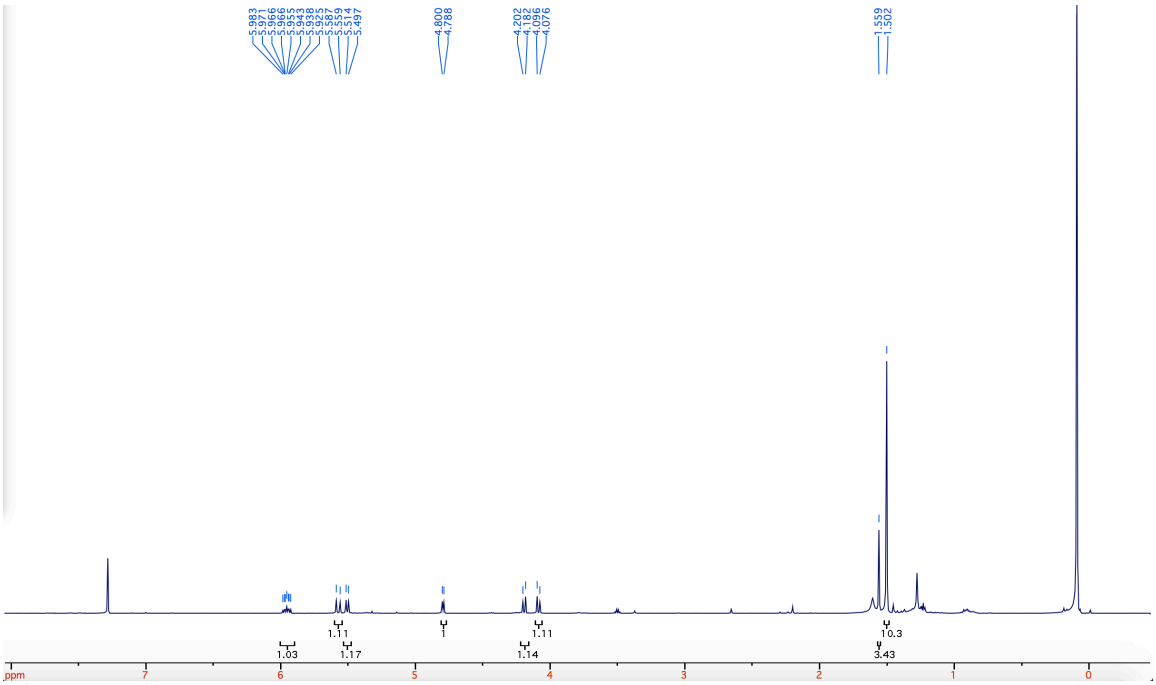

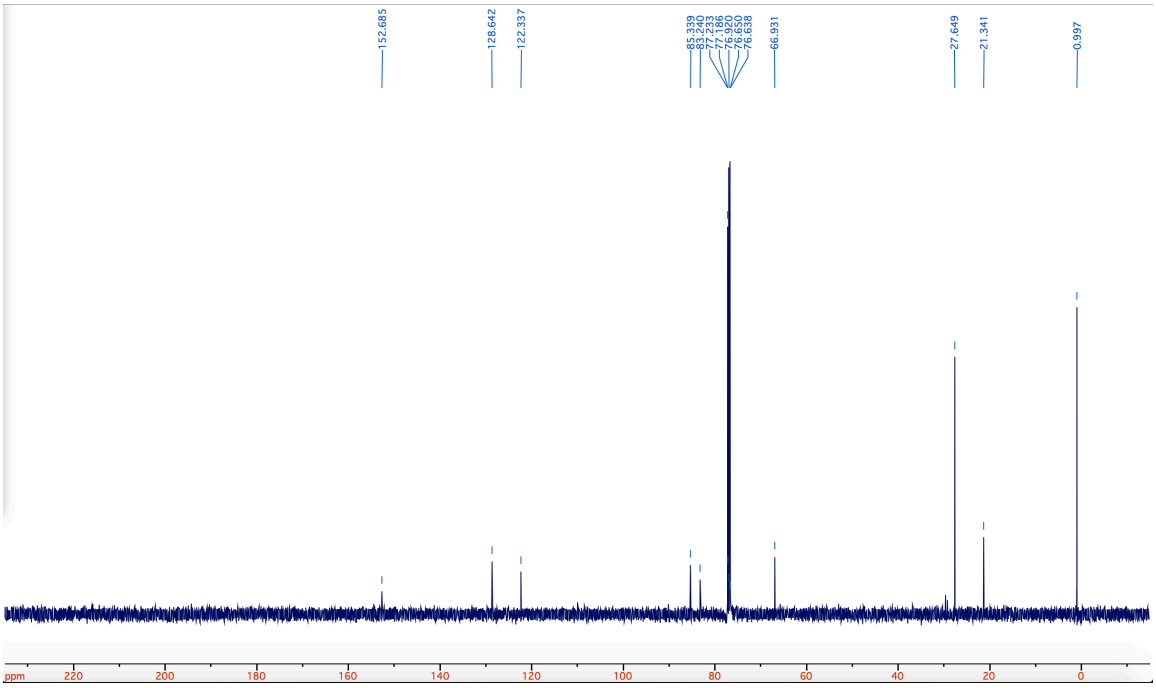

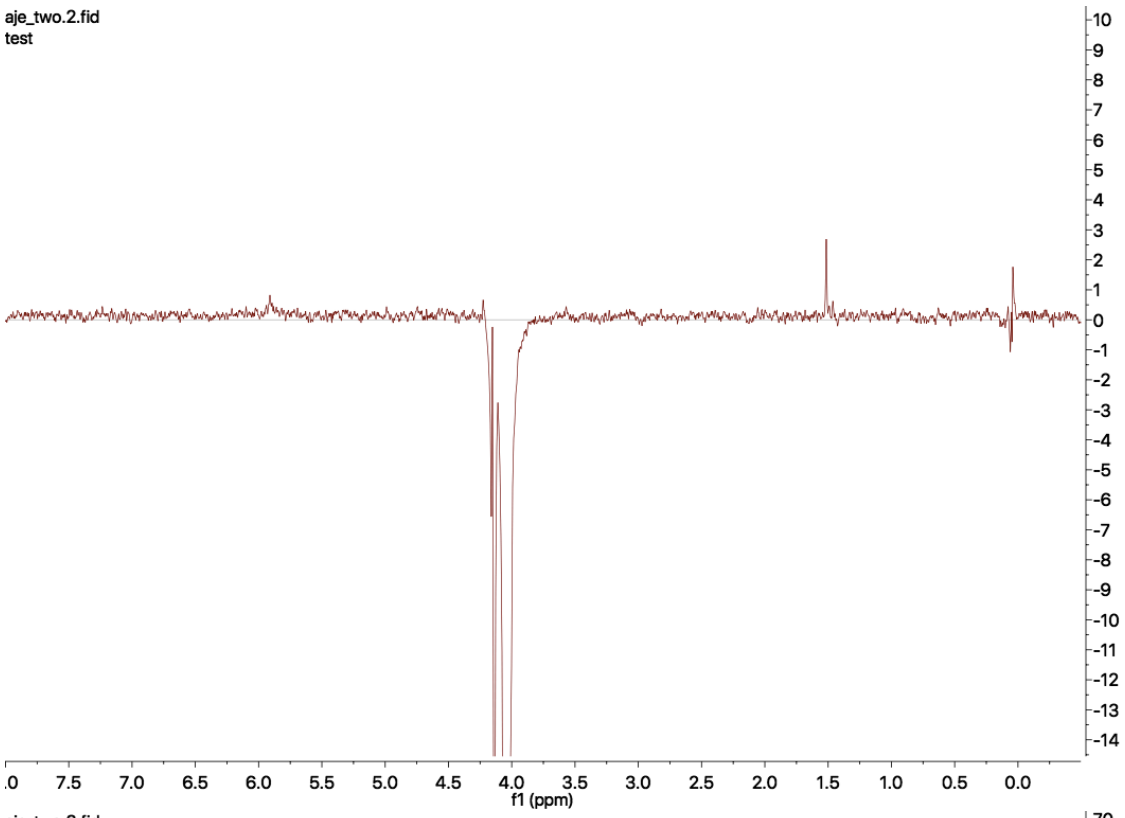
aje_two.2.fid
test
10
9
8
7
6
5
4
3
2
1
0
-1
-2
-3
-4
-5
-6
-7
-8
-9
-10
-11
-12
-13
-14
.0 7.5 7.0 6.5 6.0 5.5 5.0 4.5 4.0 3.5 3.0 2.5 2.0 1.5 1.0 0.5 0.0
f1 (ppm)

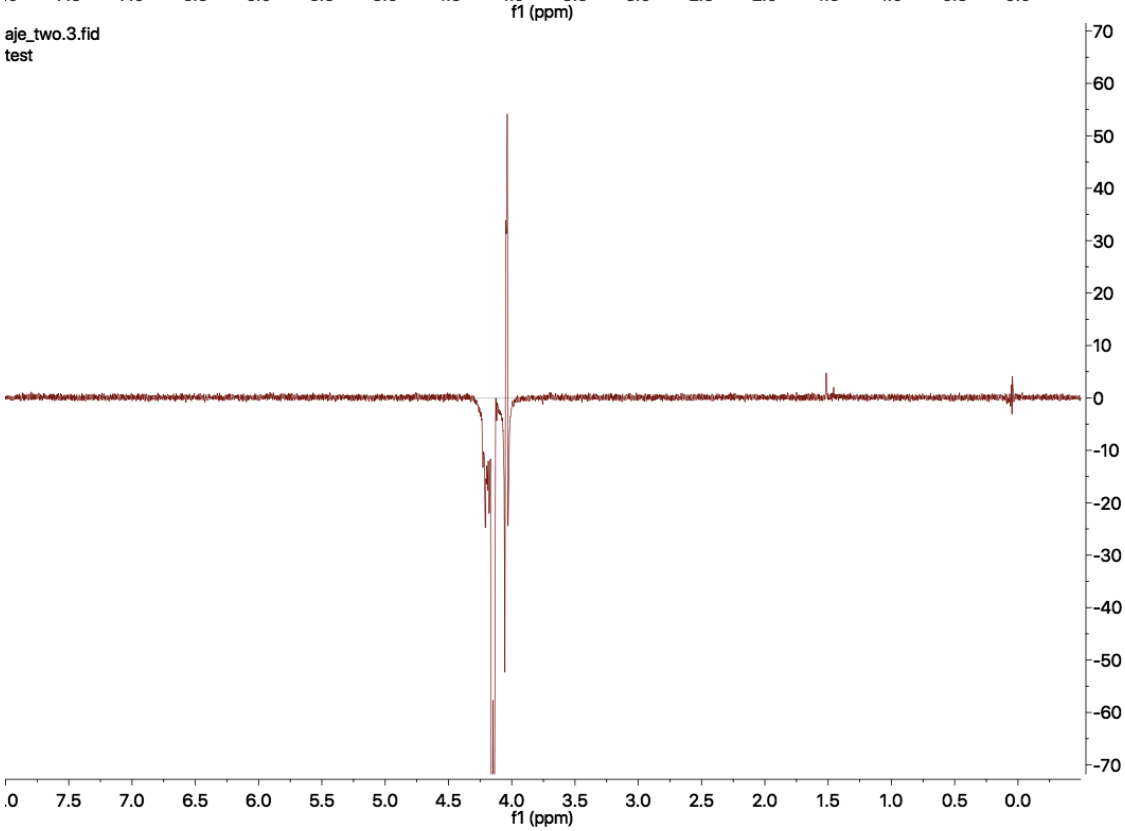
aje_two.3.fid
test
70
60
50
40
30
20
10
0
-10
-20
-30
-40
-50
-60
-70
.0 7.5 7.0 6.5 6.0 5.5 5.0 4.5 4.0 3.5 3.0 2.5 2.0 1.5 1.0 0.5 0.0
f1 (ppm)

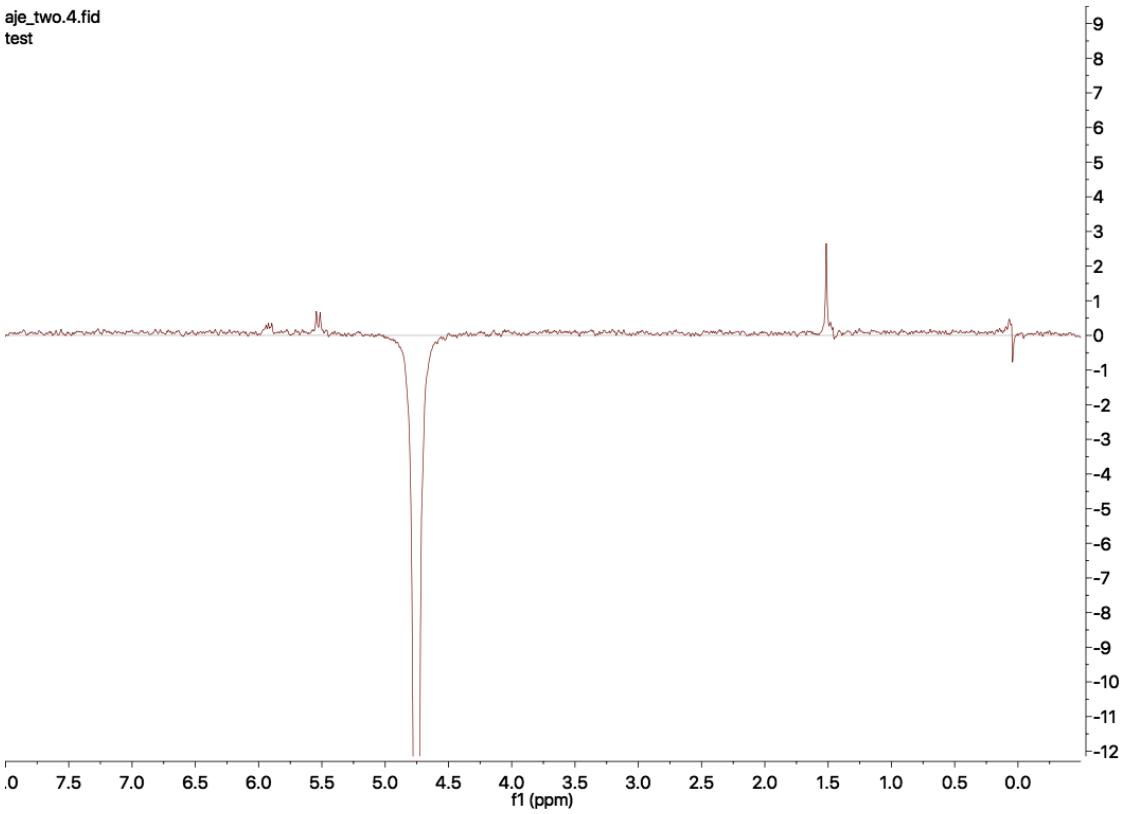

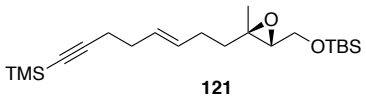

121

Alkene 121

To a solution of 697 mg (2.0 mmol) of sulfone **118** in 12.6 mL DME in a 100 mL RBF equipped with a stir bar under argon was added 2.0 mL (5.0 mmol) of 2.5M KHMDS in THF at -78 °C. The reaction was allowed to run for 30 minutes and then 516.9 mg (2.0 mmol) of **120** was added dropwise. The reaction was then stirred for 2 hours and quenched with concentrated NH_4Cl solution. The reaction mixture was then transferred to a sepratory funnel and extracted 3X with EtOAc. The combined organics were then dried over $MgSO_4$, filtered, and concentrated in vacuo. The crude oil was then purified via silica gel column chromatography in 2% EtOAc in hexanes affording 400 mg (1.05 mmol, 52.5%) of the desired product as a clear colorless oil. **^{1}H NMR** (600 MHz, Chloroform-*d*) δ 5.45 (td, *J* = 3.3, 1.3 Hz, 2H) 3.71 (ddd, *J* = 5.3, 2.4, 1.1 Hz, 2H) 2.87 (t, *J* = 5.36 Hz, 1H) 2.26-2.22 (m, 2H) 2.11-2.07 (m, 2H) 1.67 (ddd, *J* = 13.68, 9.08, 6.25 Hz, 1H) 1.483 (ddd, *J* = 13.63, 9.56, 6.94 Hz, 1H) 1.24 (s, 3H) 0.879 (s, 9H) 0.125 (s, 9H) 0.069 (s, 3H) 0.058 (s, 3H)

References

1. Checco, J. W.; Lee, E. F.; Evangelista, M.; Sleebs, N. J.; Rogers, K.; Pettikiriarachchi, A.; Kershaw, N. J.; Eddinger, G. A.; Belair, D. G.; Wilson, J. L.; Eller, C. H.; Raines, R. T.; Murphy, W. L.; Smith, B. J.; Gellman, S. H.; Fairlie, W. D., *J. Am. Chem. Soc.* **2015,** *137* (35), 11365-75.

2. Eschenmoser, A., *Science* **1999,** *284* (5423), 2118-24.

3. Sabatino, D.; Damha, M. J., *J. Am. Chem. Soc.* **2007,** *129* (26), 8259-8270.

4. Choi, K. Y.; Chung, H.; Min, K. H.; Yoon, H. Y.; Kim, K.; Park, J. H.; Kwon, I. C.; Jeong, S. Y., *Biomaterials* **2010,** *31* (1), 106-114.

5. Li, L.; Xu, Y.; Milligan, I.; Fu, L.; Franckowiak, E. A.; Du, W., S *Angew. Chem. Int. Ed. Engl.* **2013,** *52* (51), 13699-702.

6. Turner, N. J.; Kielty, C. M.; Walker, M. G.; Canfield, A. E., *Biomaterials* **2004,** *25* (28), 5955-5964.

7. Castro, S.; Duff, M.; Snyder, N. L.; Morton, M.; Kumar, C. V.; Peczuh, M. W., *Org. Biomol. Chem.* **2005,** *3* (21), 3869-3872.

8. Grindley, T. B.; Gulasekharam, V., *J. Chem. Soc. Chem. Commun.* **1978,** (23), 1073-1074.

9. Vannam, R.; Peczuh, M. W., *Eur. J. Org. Chem.* **2016,** *2016* (10), 1800-1812.

10. Sridhar, P. R.; Venukumar, P., *Org. Lett.* **2012,** *14* (21), 5558-5561.

11. Vannam, R.; Peczuh, M. W., *Org. Biomol. Chem.* **2016,** *14* (16), 3989-3996.

12. Somsák, L., *Chem. Rev.* **2001,** *101* (1), 81-136.

13. Alcázar, E.; Pletcher, J. M.; McDonald, F. E., *Org. Lett.* **2004,** *6* (21), 3877-3880.

14. Boone, M. A.; McDonald, F. E.; Lichter, J.; Lutz, S.; Cao, R.; Hardcastle, K. I., *Org. Lett.* **2009,** *11* (4), 851-4.

15. Nicolaou, K. C.; Mitchell, H. J., *Angew. Chem. Int. Ed. Engl.* **2001,** *40* (9), 1576-1624.

16. Balmond, E. I.; Coe, D. M.; Galan, M. C.; McGarrigle, E. M., *Angew. Chem. Int. Ed.* **2012,** *51* (36), 9152-9155.

17. Kimura, T.; Eto, T.; Takahashi, D.; Toshima, K., *Org. Lett.* **2016,** *18* (13), 3190-3193.

18. Laval, C.; Just, G., *Tetrahedron* **1990,** *46* (1), 151-162.

19. Kotke, M.; Schreiner, P. R., *Synthesis* **2007,** *2007* (05), 779-790.

20. Bolitt, V.; Mioskowski, C.; Lee, S. G.; Falck, J. R., *J. Org. Chem.* **1990,** *55* (23), 5812-5813.

21. Friesen, R. W.; Danishefsky, S. J., *J. Am. Chem. Soc.* **1989,** *111* (17), 6656-6660.

22. Thiem, J.; Karl, H.; Schwentner, J., *Synthesis* **1978,** *1978* (09), 696-698.

23. Lin, Y.-Y.; Risk, M.; Ray, S. M.; Van Engen, D.; Clardy, J.; Golik, J.; James, J. C.; Nakanishi, K., *J. Am. Chem. Soc.* **1981,** *103* (22), 6773-6775.

24. Murata, M.; Yasumoto, T., *Nat. prod. rep.* **2000,** *17* (3), 293-314.

25. Prasad, A. V. K.; Shimizu, Y., *J. Am. Chem. Soc.* **1989,** *111* (16), 6476-6477.

26. Bourdelais, A. J.; Jacocks, H. M.; Wright, J. L. C.; Bigwarfe, P. M.; Baden, D. G., *J. Nat. Prod.* **2005,** *68* (1), 2-6.

27. Potera, C., F *Science* **2007,** *316* (5831), 1561-1562.

28. Fuwa, H.; Ebine, M.; Sasaki, M., *J. Am. Chem. Soc.* **2006,** *128* (30), 9648-9650.

29. Ebine, M.; Fuwa, H.; Sasaki, M., *Chem. Eur. J.* **2011,** *17* (49), 13754-13761.

30. Ebine, M.; Fuwa, H.; Sasaki, M., *Org. Lett.* **2008,** *10* (11), 2275-2278.

31. Takamura, H.; Kikuchi, S.; Nakamura, Y.; Yamagami, Y.; Kishi, T.; Kadota, I.; *Org. Lett.* **2009,** *11* (12), 2531-2534.

32. Zhang, Y.; Rohanna, J.; Zhou, J.; Iyer, K.; Rainier, J. D., *J. Am. Chem. Soc.* **2011,** *133* (9), 3208-3216.

33. Lee, M. S.; Qin, G.; Nakanishi, K.; Zagorski, M. G., *J. Am. Chem. Soc.* **1989,** *111* (16), 6234-6241.

34. Mori, Y.; Furuta, H.; Takase, T.; Mitsuoka, S.; Furukawa, H., *Tet. Lett.* **1999,** *40* (45), 8019-8022.

35. Tetsuo, T.; Kenshu, F.; Akio, M., *Chem. Lett.* **2000,** *29* (3), 272-273.

36. Kenshu, F.; Akio, M., *Bull. Chem. Soc. Jpn.* **2004,** *77* (12), 2129-2146.

37. McDonald, F. E.; Tong, R. B.; Valentine, J. C.; Bravo, F., *Pure. Appl. Chem.* **2007,** *79* (2), 281-291.

38. Morten, C. J.; Byers, J. A.; Van Dyke, A. R.; Vilotijevic, I.; Jamison, T. F., *Chem. Soc. Rev.* **2009,** *38* (11), 3175-3192.

39. Iimori, T.; Still, W. C.; Rheingold, A. L.; Staley, D. L., *J. Am. Chem. Soc.* **1989,** *111* (9), 3439-3440.

40. Van Dyke, A. R.; Jamison, T. F., *Angew. Chem. Int. Ed.* **2009,** *48* (24), 4430-4432.

41. Vilotijevic, I.; Jamison, T. F., *Science* **2007,** *317* (5842), 1189-1192.

42. Armbrust, K. W.; Beaver, M. G.; Jamison, T. F., *J. Am. Chem. Soc.* **2015,** *137* (21), 6941-6946.

43. Bravo, F.; McDonald, F. E.; Neiwert, W. A.; Hardcastle, K. I., *Org. Lett.* **2004,** *6* (24), 4487-4489.

44. Bravo, F.; McDonald, F. E.; Neiwert, W. A.; Do, B.; Hardcastle, K. I., *Org. Lett.* **2003,** *5* (12), 2123-2126.

45. Hurtak, J. A.; McDonald, F. E., *Org. Lett.* **2017,** *19* (22), 6036-6039.

46. Wong, O. A.; Shi, Y., Organocatalytic Oxidation. *Chem. Rev.* **2008,** *108* (9), 3958-3987.

47. Blakemore, P. R., *J. Chem. Soc.* **2002,** (23), 2563-2585.

48. Duhamel, L.; Plaquevent, J.-C., *J. Organomet. Chem.* **1993,** *448* (1), 1-3.

49. Yang, J.; Hao, Q.; Liu, X.; Ba, C.; Cao, A., *Biomacromolecules* **2004,** *5* (1), 209-218.

50. Mizuno, T.; Nakai, T.; Mihara, M., *Heteroat. Chem.* **2010,** *21* (7), 541-545.